INITIAL CHARACTERIZATION OF TWO NOVEL SPINDLE PROTEINS, CHICA AND HURP:

Focus on the role of the Ran-importin β-regulated HURP protein in kinetochore-fiber stabilization.

Dissertation zur Erlangung des
naturwissenschaftlichen Doktorgrades
der Fakultät für Biologie der
Ludwig-Maximilians Universität München

vorgelegt von
Susanna Nagel

Martinsried / München 2008

Initial Characterization of two novel spindle proteins, CHICA and HURP:

Focus on the role of the Ran-importin β-regulated HURP protein in kinetochore-fiber stabilization.

Dissertation zur Erlangung des

naturwissenschaftlichen Doktorgrades

der Fakultät für Biologie

der Ludwig-Maximilians Universität München

vorgelegt von

Susanna Nagel

Martinsried /München 2008

Eingereicht am:

Tag des Promotionskolloquiums: 19. Juni 2008

Gutachter

Erstgutachter: Prof. Dr. Erich A. Nigg

Zweitgutachter: Prof. Dr. Peter B. Becker

Hiermit erkläre ich, dass ich die vorliegende Dissertation selbständig angefertigt habe und keine anderen als die von mir angegebenen Quellen und Hilfsmittel benutzt habe. Sämtliche Experimente sind von mir selbständig durchgeführt worden, falls nicht explizit auf Dritte verwiesen wird. Ich versichere, dass ich weder versucht habe diese Dissertation oder Teile davon an einer anderen Stelle einzureichen, noch eine Doktorprüfung durchzuführen.

Susanna Nagel   Martinsried, den 14. 03. 2008

Table of contents

TABLE OF CONTENTS

Summary

During mitotic spindle assembly, the sister chromatids have to be captured by kinetochore (K) -fibers (bundles of kinetochore microtubules; KMTs) to ensure stable attachment of the chromosomes. This is a prerequisite for chromosome congression at the metaphase plate, and the subsequent segregation of separated sister chromatids to the spindle poles. Although, this is a critical step during mitosis, the identity and regulation of the proteins that mediate the formation and stabilization of K-fibers are still largely unknown. This thesis describes a functional characterization of HURP (hepatoma upregulated protein) and CHICA (C20Orf129), two proteins recently identified in a proteomic survey of the human spindle apparatus (Sauer et al., 2005). The spindle association of both proteins was analyzed with polyclonal antibodies, showing that that of HURP and CHICA were mutually exclusive. While HURP decorated the KMT plus ends, CHICA localized to the spindle pole caps and had no major influence on K-fiber stability. The description of the CHICA project will be brief, as this work was primarily continued by Dr. Anna Santamaria. Her investigations demonstrated that CHICA is important for the spindle recruitment of the chromokinesin Kid, which is required for polar ejection forces.

Our studies showed that HURP binds to, and bundles microtubules (MTs) *in vitro*. *In vivo*, HURP localizes predominantly to K-fibers in the vicinity of chromosomes and is required for K-fiber stabilization. Moreover, we revealed that importin β binds to the N-terminus of HURP and demonstrated that the nucleotide state of the small GTPase Ran controls HURP localization and function. We conclude that the spindle assembly pathway centered on RanGTP contributes to K-fiber stabilization and that HURP is a critical target of this pathway. To better understand the mechanism of HURP recruitment to the K-fibers we subsequently carried out a structure-function analysis of the different HURP domains. This study revealed that the N-terminus, which contains two coiled coil domains binds to, and bundles MTs and is essential for the initial loading of HURP onto the spindle, whereas the C-terminus (including a Guanylate kinase-associated protein domain; GKAP) is involved in the specific KMT plus end targeting. Furthermore, we identified a conserved mitosis-specific Cdk1 phosphorylation site in the GKAP domain of HURP, indicating that in addition to the RanGTP gradient, Cdk1 phosphorylation may also play a role in HURP recruitment to the K-fibers.

1

Zusammenfassung

Während der Bildung der Mitosespindel müssen die Schwesterchromatiden von Kinetochor (K)-Fasern (Bündel von Kinetochor Mikrotubuli; KMTs) erfasst werden, um eine stabile Anhaftung der Chromosomen zu gewährleisten. Dies ist die Voraussetzung für die Ausrichtung der Chromosomen in der Metaphaseebene und die anschließende Verteilung der Schwesterchromatiden auf die Spindelpole. Obwohl dies während der Mitose ein wichtiger Schritt ist sind die Identität und die Regulation der Proteine, die den Aufbau und die Stabilisierung der K-Fasern bewirken noch weitestgehend unbekannt. Diese Doktorarbeit beschreibt die funktionelle Charakterisierung von HURP (hepatoma upregulated protein) und CHICA (C20Orf129), zwei Proteinen, die vor Kurzem in einer Bestandsaufnahme der Proteinkomponenten des humanen Spindelapparates gefunden wurden (Sauer et al., 2005). Die Spindel Assoziation von beiden Proteinen wurde mittels polyklonalen Antikörpern analysiert. Diese Analyse verdeutlichte, dass HURP und CHICA sich gegenseitig ausschließen. Während HURP die KMT Plus Enden bedeckte, lokalisierte CHICA an den Spindelpolkappen und hatte keinen wesentlichen Einfluss auf die K-Faser Stabilität. Das CHICA Projekt wird hier nur kurz beschrieben, da diese Arbeit primär von Dr. Anna Santamaria fortgeführt wurde. Ihre Untersuchungen zeigten, dass CHICA wichtig für die Spindel Rekrutierung von Kid ist, eines Chromokinesins, dass für die polaren Abstoßungskräfte notwendig ist.

Unsere Studien zeigten, dass HURP *in vitro* Mikrotubuli (MTs) bindet und bündelt. *In vivo* lokalisiert HURP vorwiegend an den K-Fasern in der Nähe der Chromosomen und ist für die Stabilisierung der K-Faser erforderlich. Zudem haben wir herausgefunden, dass Importin β an den N-Terminus von HURP bindet und haben gezeigt, dass der Nukleotid Zustand der kleinen GTPase Ran die Lokalisation und Funktion von HURP bestimmt. Daraus folgern wir, dass der auf RanGTP bezogene Spindel Aufbauweg an der K-Faser Stabilisierung beteiligt ist und dass HURP ein entscheidendes Target dieses Weges darstellt. Um den Mechanismus der HURP Rekrutierung zu den K-Fasern besser zu verstehen, führten wir anschließend eine funktionelle Strukturanalyse der verschiedenen HURP Domänen durch. Diese Untersuchung zeigte, dass der N-Terminus, der die beiden Coiled Coil Domänen beinhaltet, Mikrotubuli bindet und bündelt und essentiell für die Beladung der

Spindel mit HURP ist. Wohingegen der C-Terminus (inklusive einer Guanylat Kinase-assoziierten Protein Domäne; GKAP) in das spezifische Targeting zum KMT Plus Ende involviert ist. Darüber hinaus haben wir eine konservierte Mitose-spezifische Cdk1 Phosphorylierungsstelle in der GKAP Domäne von HURP identifiziert. Dies deutet darauf hin, dass auch Cdk1 Phosphorylierung zusätzlich zum RanGTP Gradienten, eine Rolle in der HURP Rekrutierung zu den K-Fasern spielen kann.

1 Introduction

1.1 Mitosis

A key event in the cell cycle is the accurate separation of previously duplicated chromatids during mitosis. Once the DNA has been replicated properly, the chromatin condenses into distinct morphological structures (chromosomes) at the beginning of mitosis. The chromosomes each comprise two sister chromatids that are connected by intertwined (catenated) DNA and held together by a multiprotein complex called cohesin. During mitosis, cohesin is removed at anaphase onset, allowing the separation of the paired sister chromatids and their equal distribution to the two daughter cells. The movement of the sister chromatids to the opposite spindle poles, called sister chromatid segregation, is carried out by the microtubule-based spindle apparatus, that forms at early prophase and is involved in metaphase plate formation.
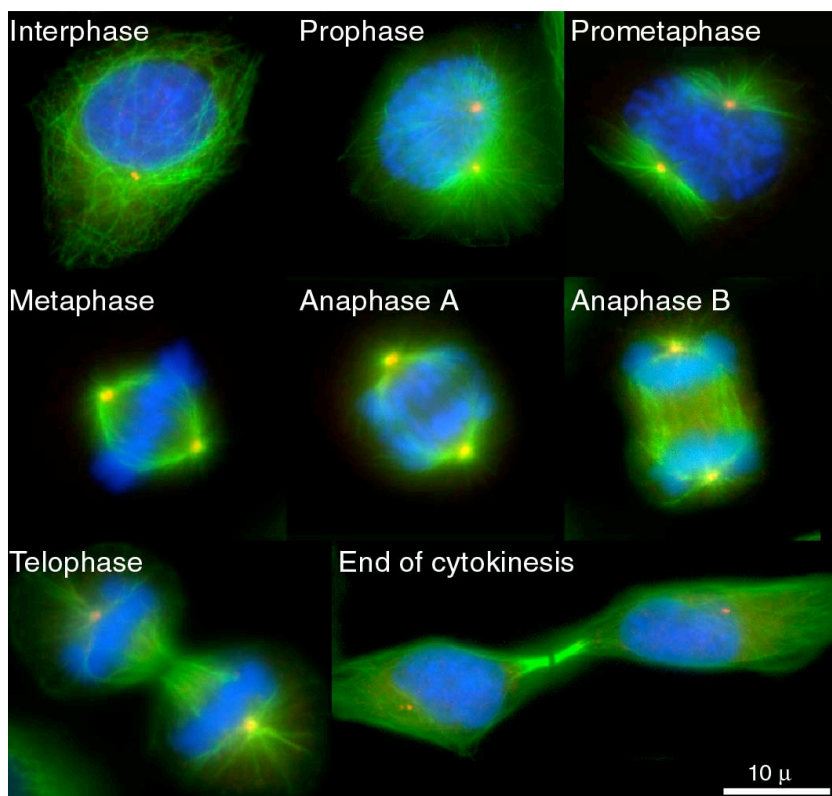
Figure 1. Events of mitosis and cytokinesis (M-phase)
Immunofluorescence (IF) images of mitotic cells, showing tubulin in green, DNA in blue and pericentrin, a centrosome marker in red. M-phase comprises nuclear division (= mitosis) and cell division (= cytokinesis). Mitosis can be subdivided in five stages: prophase, prometaphase, metaphase, anaphase and telophase. During metaphase, chromosomes that have attached to the mitotic spindle align at the metaphase plate and subsequently segregate to the spindle poles. Cell division is complete, when the nascent daughter cells are separated from each other by abscission.

The different events of mitosis were originally distinguished into five stages; namely prophase, prometaphase, metaphase, anaphase and telophase (Figure 1). During prometaphase the sister chromatids are captured at kinetochores (specialized protein rich structures assembled upon centromeric DNA) by nascent spindle microtubules that emanate from separated centrosomes at the spindle poles. Bipolar attached chromosomes are then moved towards the center of the cell in a process known as chromosome congression, leading to metaphase. Once all chromosomes have been properly aligned at the metaphase plate, tension is thought to be created between the sister chromatids by a balance of forces. As a consequence, the spindle assembly checkpoint (SAC), is satisfied which in turn leads to anaphase-promoting complex (APC/Cdc20) mediated ubiquitin-dependent degradation of the separase inhibitor securin, thereby inducing the removal of cohesin from sister chromatids. This results in anaphase onset. In anaphase A the sister chromatids are separated simultaneously and subsequently pulled apart to the opposite poles by shortening of KMTs. In anaphase B chromosome segregation is accelerated by spindle pole separation. The cell division plane is determined by spindle-cortex interactions, which results in the formation of a contractile actin-myosin ring at the position of the cleavage furrow. During telophase, the spindle is disassembled and the nuclear envelope is reformed around the decondensing chromosomes, resulting in the formation of two daughter nuclei. Following chromosome segregation, the cell is ingressed at the furrow, dividing it in two. Finally, cytokinesis is completed by abscission of the cleavage furrow, resulting in two nascent daughter cells (Pines and Rieder, 2001).

1.2 The mitotic spindle – a dynamic assembly of microtubules and motors

The mitotic spindle, a highly dynamic microtubule-based structure, ensures the faithful segregation of the genetic material during mitosis. The spindle apparatus is composed of a bipolar array of MTs, the main function of which is the accurate segregation of the sister chromatids to the opposite spindle poles (Figure 2). This process is driven by a balance of forces (see below) and the coordinated activity of microtubule-associated proteins (MAPs) and kinesin-related motors (KRMs).

The primary structural element of the spindle are two halves of radial MTs, with their minus ends tethered at the poles and their plus ends attached to the

chromosomes. The overlap of spindle MT plus ends from opposite poles at the spindle midzone, results in an antiparallel microtubule array. In most vertebrate cells, the spindle pole is formed by the centrosome that serves as a MT-organizing center (MTOC). The centrosome is structurally composed of a pair of centrioles, surrounded by the pericentriolar matrix (PCM), including the γ-tubulin ring complex (γTuRC) that induces MT nucleation. Higher plants and many vertebrate oocytes do not have centrosomes, and the generation of the spindle poles in these cells depends on the self-organizing capability of MTs, with the help of MAPs (see below) (adapted from Morgan, 2006).
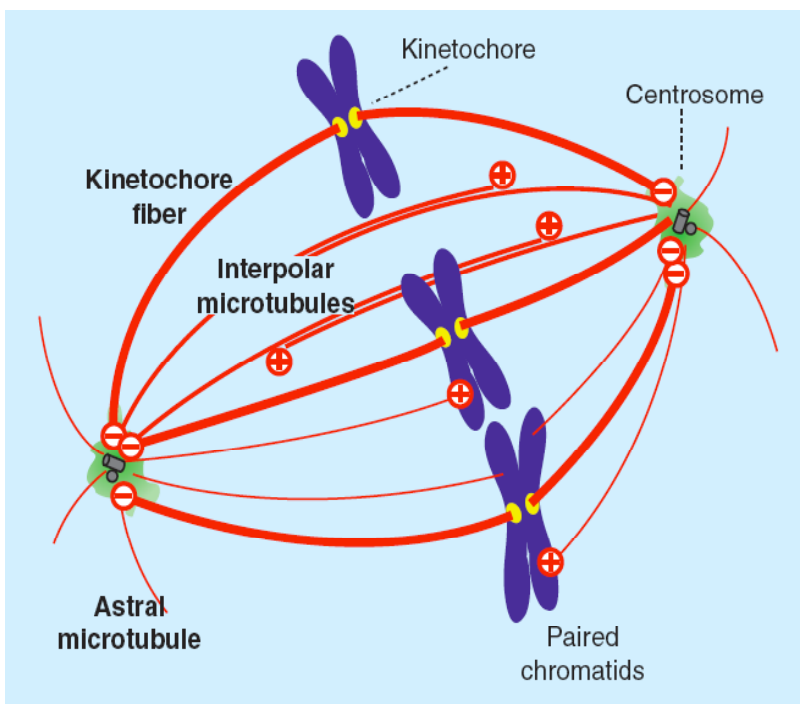
Figure 2. The mitotic spindle, a bipolar array of MTs
The mitotic spindle is a highly dynamic bipolar array of MTs, formed around the chromosomes. The most important function of the spindle is the stable attachment of the sister chromatids to the opposite spindle poles. Three morphological different MT-populations assist in this function: kinetochore MTs (KMTs), astral MTs (AMTs) and interpolar MTs (IMTs) (adapted from Gadde and Heald, 2004).

The mitotic spindle contains three morphologically different populations of MTs. KMTs connect the sister chromatids to the spindle poles by end-on attachments at the kinetochore, which provides a high affinity binding site for spindle microtubules on the chromosomes. In animal cells, several KMTs bundle together to form stable kinetochore-fibers (K-fibers) (see below). Interpolar microtubules (IMTs) that originate from opposite spindle poles stabilize the spindle bipolarity and interact in an antiparallel manner in the spindle midzone. Finally, except in acentrosomal cells, the orientation and positioning of the spindle is maintained by astral microtubules (AMTs) that extend away from the centrosomes to the cell cortex (Gadde and Heald, 2004). Altogether, these different MTs form a lattice that forms the foundation of the mitotic spindle (Figure 2). Proper spindle

assembly relies on two key features of MTs; their dynamic instability (Mitchison and Kirschner, 1984) and their ability to recruit mechanochemical motors, such as dynein, and members of the kinesin family, which are required for MT cross-linking and spindle organization (see further sections).

1.2.1 MT dynamics

Microtubules are polar polymers, formed by around 13 protofilaments of $\alpha\beta$-tubulin dimers that create a hollow tube with α-tubulin at the minus end and β-tubulin at the plus end. MT polymerization is driven by GTP hydrolysis through the GTPase activity of β-tubulin, upon binding of GTP-tubulin-dimers. As α-tubulin has low GTPase activity, it remains GTP-bound in the polymer, which results in a slow-growing minus end and a fast-growing plus end. GTP-tubulin has a higher affinity for the growing microtubule than GDP-tubulin. The different binding affinities of GTP- and GDP-tubulin therefore result in the dynamic instability of microtubules, an intriguing property discovered in 1984 by Mitchison and Kirschner. At high tubulin concentrations, a "GTP-cap" is formed, when addition of new GTP-tubulin is faster than GTP hydrolysis, which results in rapid MT growth (Figure 3, top). In contrast, when the rate of GTP hydrolysis is faster than that of tubulin addition, GDP-tubulin dimers tend to dissociate and the microtubule switches from fast growth to shrinkage (catastrophe) (Figure 3, bottom). The addition of GTP-tubulin in turn, can induce shrinking microtubules to grow once again, a phenomenon known as rescue (Desai and Mitchison, 1997).
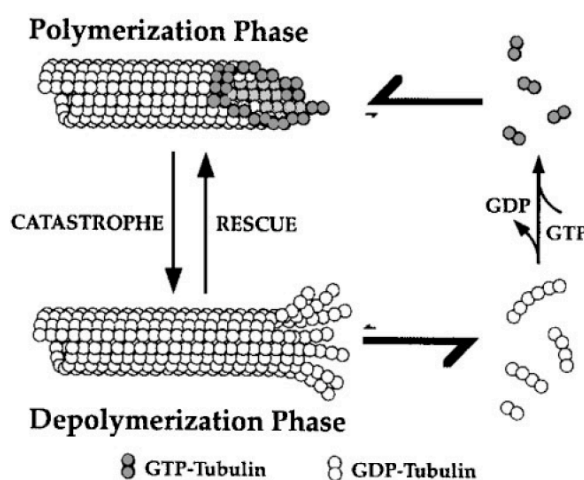
Figure 3. Dynamic instability of MTs
MTs are highly dynamic polymers of $\alpha\beta$-tubulin dimers that can rapidly change from growth to shrinkage (catastrophe), depending on the concentration of free tubulin dimers. MT polymerization and depolymerization are driven by the equilibrium between GTP-tubulin addition and -hydrolysis:
GTP-tubulin addition > GTP hydrolysis = growth;
GTP-tubulin addition < GTP hydrolysis = shrinkage / catastrophe;
GTP-tubulin addition = GTP hydrolysis = rescue.
(Adapted from Desai and Mitchison, 1997)

As a consequence of the different MT binding affinities of α- and β-tubulin, the association of tubulin is higher at the plus end than at the minus end, which results in the movement of tubulin subunits towards the minus end. In a "treadmilling" model, this flux of tubulin dimers towards the microtubule minus end was proposed to influence spindle organization. The model proposed that at metaphase tubulin polymerizes at the kinetochores and depolymerizes at the poles (Margolis and Wilson, 1981; Mitchison and Salmon, 2001). Later, the phenomenon of poleward flux of tubulin dimers, could be directly demonstrated by fluorescence speckle microscopy (FSM) (Desai et al., 1998; Maddox et al., 2003). Poleward flux derives from the active transport of the MT-associated tubulin towards the pole, although, the MT itself persists. The poleward movement of tubulin occurs due to simultaneous MT depolymerization at the minus end (the spindle pole) and MT polymerization at the kinetochore-attached plus end (Figure 8A). However, this intrinsic property of microtubules is not sufficient to explain the flux rates observed by FSM (Desai et al., 1998; Maddox et al., 2003). Rather, motors and other proteins that change MT dynamics have been reported to contribute to microtubule flux, as well (see further paragraphs) (Mitchison and Salmon, 2001).

During chromosome oscillation in metaphase, MT depolymerization also occurs at the kinetochore. However, the rates of MT polymerization and poleward flux are in equilibrium, thereby promoting chromosome congression. Upon anaphase onset, poleward flux exceeds MT polymerization, which results in slow kinetochore movement towards the pole (anaphase A). Upon recruitment of catastrophe factors, such as kinesin-13 (see further paragraphs) (Howard and Hyman, 2003), microtubules finally switch to depolymerization at the plus end and, in cooperation with poleward flux, this accelerates the chromatid segregation at late anaphase (anaphase B) (Maddox et al., 2003).

1.2.2   K-fiber formation

One of the most important requirements for successful cell division is the capture of all chromosomes by the mitotic spindle apparatus. This complex process requires the formation of K-fibers, which consist of 20-30 MTs each (McEwen et al., 1997). K-fibers are important for chromosome congression and biorientation at a metaphase plate, as well as chromosome separation during anaphase A and B. During mitosis,

an increase in the frequency of MT shrinkage and growth called "catastrophe" (Gadde and Heald, 2004) contributes to the capture of sister chromatids at the kinetochores by KMTs from the nearest pole. The chromatid is then moved towards the pole by minus end-directed motors (dynein and kinesin-14) (Sharp et al., 2000), where the lateral connection is converted into an end-on attachment (Rieder and Alexander, 1990; Savoian et al., 2000; Tanaka et al., 2005). As the MT density increases towards the poles, the chromatid is captured by additional microtubules, resulting in the generation of stable microtubule bundles, the K-fibers. Following attachment of the unoccupied kinetochore from the other spindle pole the sister chromatid pair is pulled in the opposite direction. In some cases monooriented chromosomes are transported along the KMTs of already bioriented sister-chromatid pairs by CENP-E, a plus end-directed kinesin-7 motor and encounter microtubules from the opposite spindle pole (Kapoor et al., 2006). The resulting bipolar attachments lead to continuous oscillation of the chromosomes between the spindle poles and eventual chromosome alignment in the metaphase plate.

Recent live-cell imaging studies have revealed that MT assembly at kinetochores also contributes to K-fiber formation (Khodjakov et al., 2003; Maiato et al., 2004). The kinetochore-mediated MT bundles are ultimately captured by microtubules generated by the centrosome and incorporated into the spindle. These observations suggest that two partially redundant pathways cooperate in the formation of K-fibers in somatic cells.

1.3 Spindle assembly pathways

Spindle assembly is thought to involve two pathways, one dependent on centrosomes (Kirschner and Mitchison, 1986), the other on RanGTP and chromatin (Dasso, 2002; Gruss and Vernos, 2004; Heald et al., 1996; Heald et al., 1997; Heald and Weis, 2000). How these mechanisms cooperate to form K-fibers, is only just beginning to emerge (Figure 4C) (Rieder, 2005).

1.3.1 Centrosome-mediated "search-and-capture" hypothesis

In cells containing centrosomes, these organelles function as the primary microtubule organizing centers by promoting the formation of radial arrays of dynamically unstable MTs (see above). These centrosomal microtubules explore the cytoplasm, until they are captured by kinetochores in a "search-and-capture"

mechanism (Figure 4A) (Kirschner and Mitchison, 1986). The selective stabilization of kinetochore-bound MTs then favors the formation of mature K-fibers, which turn over more slowly than other spindle MTs (Hayden et al., 1990). Motor proteins and spindle assembly factors, like dynein and NuMA focus the microtubule minus ends at the centrosome, while other motors, like Eg5, cross-link the antiparallel MT lattice (Wittmann et al., 2001). In this classical model, the chromosomes have a relatively passive role, waiting to be incorporated into the developing spindle, as they are randomly captured one by one (O'Connell and Khodjakov, 2007). However, this rather unbiased mechanism does not explain the rates of chromosome capture that have been observed experimentally (Wollman et al., 2005). Furthermore, animal cells can still assemble a spindle when their centrosomes have been inactivated (Hinchcliffe et al., 2001; Khodjakov et al., 2000) (Figure 4B), suggesting additional mechanisms of K-fiber formation. Nevertheless, centrosomes facilitate the organization of microtubules through integration of preassembled spindle components into a functional spindle apparatus, and by insuring the correct positioning of the spindle in the cell through AMTs (Figure 4C) (Wadsworth and Khodjakov, 2004). In general, centrosomes increase the fidelity of mitosis in animal cells and cooperate with the chromatin induced spindle assembly pathway (see below) in preventing chromosome missegregation and aneuploidy (Ciciarello et al., 2007; Nigg, 2002; Sanderson and Clarke, 2006).
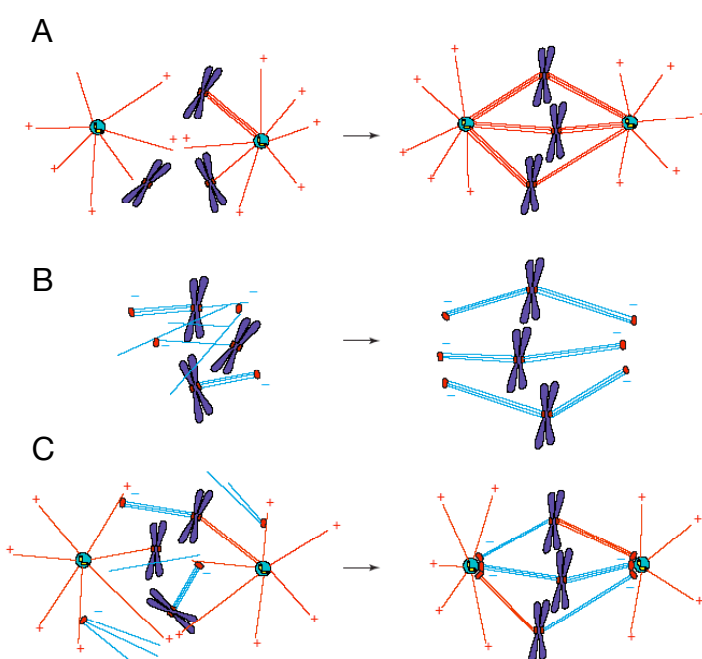
Figure 4. Two pathways cooperate in spindle formation
(A) In the classical "search-and-capture" mechanism sister chromatids are captured by centrosomal MTs at the kinetochore and congress to the middle of the cell after bipolar attachment has been established.
(B) The chromosome-mediated spindle assembly pathway in acentrosomal cells depends on the nucleation of MTs around the chromatin which then self-organize into a bipolar spindle.
(C) The extended "search-and-capture" pathway demonstrates how captured KMTs are transported along centrosomal MTs and incorporated into the spindle apparatus (adapted from Wadsworth and Khodjakov, 2004).

1.3.2 Chromosome-induced Ran-regulated spindle formation

The original "search-and-capture" mechanism is complemented by a centrosome-independent spindle assembly pathway that has been investigated primarily in *Xenopus* egg extracts (Carazo-Salas et al., 2001; Gruss et al., 2001; Gruss and Vernos, 2004; Heald et al., 1996; Heald et al., 1997). In this system, spindle formation relies on MT nucleation and organization in the vicinity of chromosomes, with the small GTPase, Ran, identified as the key regulator of centrosome-independent spindle assembly (Dasso, 2002; Gruss and Vernos, 2004; Heald and Weis, 2000; Wilde et al., 2001). Because the GTP-exchange factor (GEF) for Ran (RCC1) is associated with chromosomes, whereas the GTPase (RanGAP) is mostly cytoplasmic, a RanGTP gradient is generated (Figure 5), which favors MT assembly in the vicinity of chromosomes (Carazo-Salas et al., 2001; Carazo-Salas et al., 1999; Caudron et al., 2005; Dasso, 2002; Kalab et al., 2002; Karsenti and Vernos, 2001; Li and Zheng, 2004). How exactly RanGTP regulates spindle assembly remains to be fully understood, but the RanGTP-induced release of spindle assembly factors from inhibitory complexes with the nuclear import factors importin α and β is thought to be critical.

Extensive searches for RanGTP-regulated spindle assembly factors have identified TPX2 (Gruss et al., 2001), NuMA (Nachury et al., 2001; Wiese et al., 2001), XCTK2 (Ems-McClung et al., 2004), Xnf7 (Maresca et al., 2005), Rae1 (Blower et al., 2005), Kid (Tahara et al., 2008; Trieselmann et al., 2003), Rhamm (Groen et al., 2004), and NuSAP (Ribbeck et al., 2006; Ribbeck et al., 2007); and other factors almost certainly await discovery (Ciciarello et al., 2007). The first Ran target analyzed in more detail was TPX2, a non-motor spindle protein that stimulates MT bundling and nucleation. Moreover, TPX2 recruits the mitosis-specific kinase Aurora-A and is involved in spindle pole formation (Kufer et al., 2002; Tsai et al., 2003). Except for Rae1, which directly binds to importin β, all of the RanGTP targets described so far, are inhibited by interaction with importin β in complex with importin α.

Overall, the Ran gradient represents a RanGTP-driven reaction-diffusion system that generates concentration gradients of spindle proteins around the chromosomes (Figure 5). The concentration-dependent activity of these proteins in turn, induces local modifications in protein interactions which triggers their incorporation into the mitotic spindle network (Bastiaens et al., 2006).

INTRODUCTION
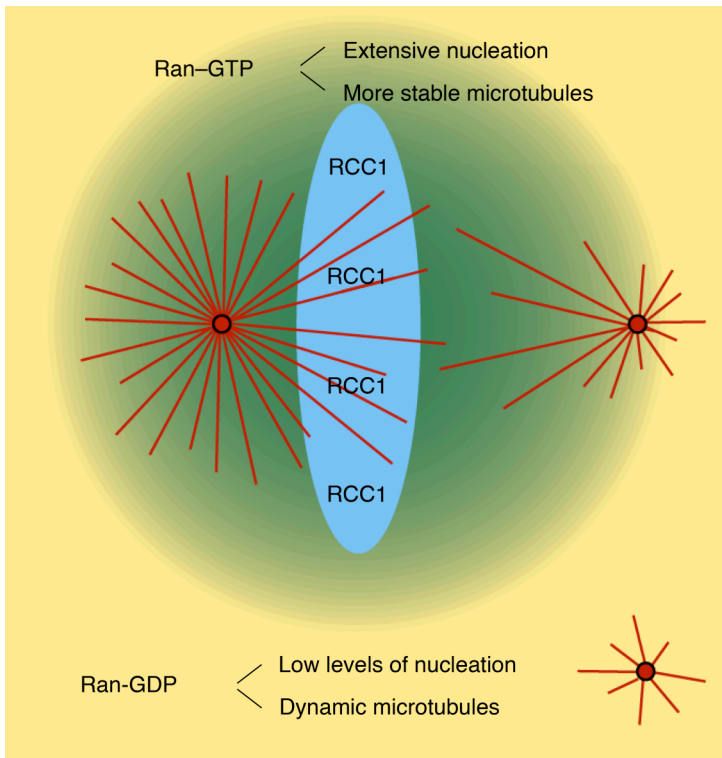
Figure 5. The RanGTP gradient in mitosis
Chromatin-bound RCC1 generates an increased concentration of RanGTP around the chromosomes. The high RanGTP levels promote the nucleation and stabilization of microtubules by release of spindle assembly factors from their inhibitory complexes with importin β (green = RanGTP; yellow = RanGDP) (adapted from Carazo-Salas et al., 2001).

The described Ran/importin-regulated pathway is expected to be particularly important in cells that lack centrosomes, including many animal oocytes. However, recent studies provide convincing results that it operates also in somatic cells, although, initially these cells were regarded as too small to establish a RanGTP gradient (Gorlich et al., 2003). Thus, spindles can still form in vertebrate cells from which centrosomes have been removed, using either microsurgery or laser ablation (Hinchcliffe et al., 2001; Khodjakov et al., 2000), and, similarly, spindle formation occurs in *Drosophila* mutants that fail to assemble functional centrosomes (Basto et al., 2006; Bonaccorsi et al., 1998; Megraw et al., 2001).

Although there is compelling evidence for the contribution of the chromosome-mediated spindle assembly pathway, it does not seem to be the driving force for spindle assembly in cells that contain centrosomes. Attenuation of the Ran gradient in somatic cells only disrupts the early steps of spindle formation, while later stages remain unaffected. This indicates that RanGTP is not involved in spindle maintenance (Kalab et al., 2006). However, the RanGTP gradient provides a kinetic advantage that accelerates the speed of spindle MT incorporation (O'Connell and Khodjakov, 2007). In conclusion, the centrosome and chromosome spindle assembly pathways are not mutually exclusive, but share a synergistic relationship in the promotion of mitotic spindle formation.

1.4 Stabilizing and destabilizing microtubule-associated proteins

Microtubule-associated proteins and kinesin-related motors assist in the generation of the bipolar array of MTs that forms the spindle. These spindle assembly factors can either directly act on MTs by changing the MT turnover or by modifying the spindle architecture through cross-linking and organizing the microtubule lattice (Figure 6).

One important group of MAPs, involved in changing MT dynamics is the kinesin-13 family (KinI family), also called catastrophe factors. These proteins decrease the length of MTs by increasing the frequency of catastrophe. The members of the kinesin-13 family are not motors, although they are structurally related to other kinesins. Rather, they associate with MT ends, where they disrupt lateral interactions between protofilaments and induce the dissociation of curved tubulin structures (Desai et al., 1999). MCAK, a prominent mammalian member of this family, has been reported to stabilize these tubulin rings in the presence of AMP-PNP and induce MT bracelets *in vitro,* which can be observed by electron microscopy (Tan et al., 2006). It has been speculated that these structures represent the higher eukaryotic counterpart of the Dam1-DASH complex (Davis and Wordeman, 2007; Santarella et al., 2007), which is required for kinetochore-microtubule attachment in budding yeast (Westermann et al., 2005). However, the presence of these MT structures was not confirmed in mammalian cells so far. Another popular MT destabilizer is OP18/stathmin that promotes catastrophe through its interaction with free tubulin, thereby decreasing the concentration of active tubulin dimers (Belmont and Mitchison, 1996).

The destabilizing impact of catastrophe factors is antagonized by MAPs that stabilize MTs. XMAP215, a prominent member of this group, belongs to the Dis1 family, which is essential for cell division in eukaryotes (Wittmann et al., 2001) and has also been proposed as a Ran target (Wilde and Zheng, 1999). XMAP215 was first described in *Xenopus,* as a MAP that promotes MT growth. It binds to MT plus ends and thereby inhibits the interaction with catastrophe factors, like XKCM1, another KinI kinesin family member (Gard and Kirschner, 1987; Tournebize et al., 2000). Other microtubule-associated proteins, like CLASP, EB1 and Clip170 specifically bind to growing microtubule plus ends and therefore, have been classified as plus end-tracking proteins (+TIPs) (Schuyler and Pellman, 2001).

INTRODUCTION

CLASP, for example, stabilizes MT plus ends by locally reducing the MT turnover and hence promotes rescue (Maiato et al., 2003; Maiato et al., 2002). Altogether, these proteins influence kinetochore-microtubule attachments during chromosome segregation by controlling MT dynamics (Carvalho et al., 2003; Galjart, 2005). NuMA, a non-motor spindle protein, that stabilizes MTs, is also regulated by the Ran pathway (Nachury et al., 2001; Wiese et al., 2001). NuMA has been proposed to play an important role, especially in acentrosomal spindle assembly because it cross-links MT minus ends and focuses them at the spindle pole (see below) (Merdes et al., 2000; Wiese et al., 2001). This function is assisted by motor proteins, specifically the minus end-directed motor dynein (Sun and Schatten, 2006). Finally, TPX2, another Ran target that promotes MT nucleation (Gruss et al., 2001), also becomes translocated to the spindle pole, in a dynein-dependent manner (Wittmann et al., 2000). TPX2 is important for centrosome integrity and spindle pole formation by recruitment of the mitotic kinase Aurora-A (Kufer et al., 2002; Tsai et al., 2003).
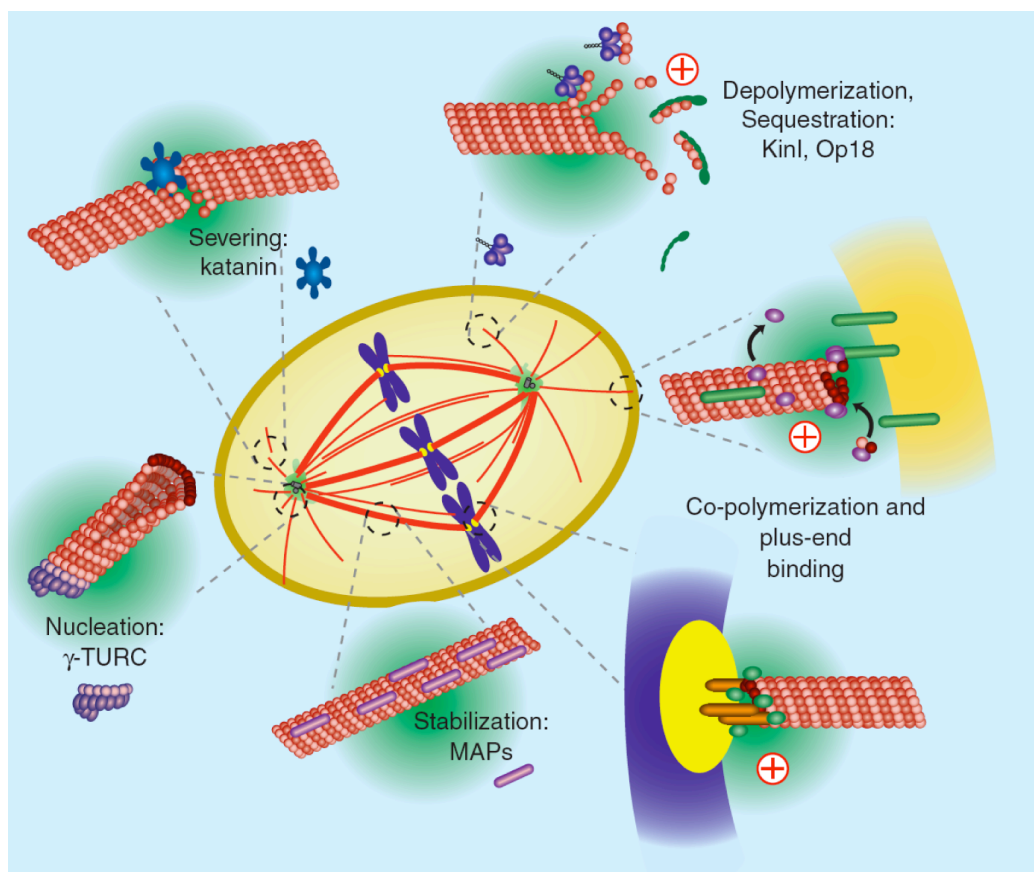
Figure 6. Regulation of spindle dynamics by MAPs
Several families of MT-associated proteins affect the spindle architecture by changing MT dynamics: MT nucleation is promoted by γTuRC; MT capture and stabilization is carried out by stabilizing MAPs, as for example XMAP215; MT depolymerization is performed by kinesin-13 family members or Op18/stathmin and severing is done by katanin. (Adapted from Gadde and Heald, 2004)

1.5 Motor proteins organize the spindle

MT-based motor proteins are mechanochemical ATPases that provide essential forces for the bipolar organization of spindle MTs and chromosome movement. They consist of a globular motor domain that is activated through protein dimerization. Subsequent ATP hydrolysis by the catalytical domain then serves as energy source for the motor to travel along the MTs. In addition, motor proteins generally have domains that bind MTs and interact with other proteins, in order to transport cargo or move the MTs themselves (Wittmann et al., 2001). There are several different groups of motor proteins in higher eukaryotes that migrate in different directions on the microtubules. The dynein/dynactin complex for example, only moves towards MT minus ends, whereas, the kinesin superfamily, contains mainly plus end-directed motors (Figure 7).

The plus end-directed kinesin-5 proteins of the BimC family, such as Eg5, play an important role during spindle assembly (Figure 7B). These tetrameric proteins have two complete motor domains and cross-link antiparallel MTs (IMTs) in the spindle midzone. Inactivation of Eg5 by the small molecule monastrol, results in the formation of monopolar spindles. This observation originally led to the conclusion that Eg5 is essential to separate the poles and maintain the bipolar array of spindle MTs during mitosis (Kapoor et al., 2000; Mayer et al., 1999). The action of the tetrameric kinesins is counteracted by minus end-directed kinesins of the kinesin-14 family (C-terminal motor-domain kinesins) (Figure 7C). These kinesins also cross-link IMTs, but in contrast to the kinesin-5 proteins, they pull the poles together, and thereby precisely regulate centrosome separation before nuclear envelope break down. XCTK2, the *Xenopus* homolog of this family, has been described as a Ran target (Ems-McClung et al., 2004) and together with NuMA functions in a dynein-dependent manner to focus microtubules on the spindle poles (see below). Another important class of kinesins are the plus end-directed chromokinesins of the kinesin-4 and kinesin-10 family. Chromokinesins simultaneously interact with MTs and chromatin, and thus push the chromosome arms away from the poles. In contrast to the kinesin-14 family, these chromokinesins separate the spindle poles in early mitosis and contribute to the chromosome positioning at the metaphase plate (Figure 7E). Although Xkid, a member of the kinesin-10 family (Antonio et al., 2000; Funabiki and Murray, 2000;

INTRODUCTION

Levesque and Compton, 2001; Tokai et al., 1996; Yajima et al., 2003), and Xklp1, a member of the kinesin-4 family (Vernos et al., 1995) share characteristics, like plus end-directed motility, and association with mitotic chromatin, these motors perform nonredundant functions. Depletion experiments in *Xenopus* egg extracts have shown that Xkid is essential for chromosome alignment and contributes to the polar ejection force (see below) but is not required for bipolar spindle assembly (Antonio et al., 2000; Funabiki and Murray, 2000; Levesque and Compton, 2001; Tokai et al., 1996; Yajima et al., 2003). In contrast, Xklp1 contributes to the assembly of a functional bipolar spindle, presumably by affecting MT polymerization (Castoldi and Vernos, 2006). Finally, dynein itself, is a minus end-directed motor that cross-links microtubules and is involved in many processes during spindle formation. Importantly, dynein forms a complex with dynactin, and transports spindle assembly factors like NuMA and TPX2 towards the pole (Figure 7D) (Wittmann et al., 2000). It is therefore crucial for spindle pole organization and has an essential function especially in acentrosomal spindle assembly. Moreover, dynein also associates with plus ends of AMTs and connects them to the cell cortex (Figure 7A). This promotes the positioning of the spindle poles and the orientation of the cell (Brouhard and Hunt, 2005; Heald, 2000; Rieder and Salmon, 1994; Vernos and Karsenti, 1995).
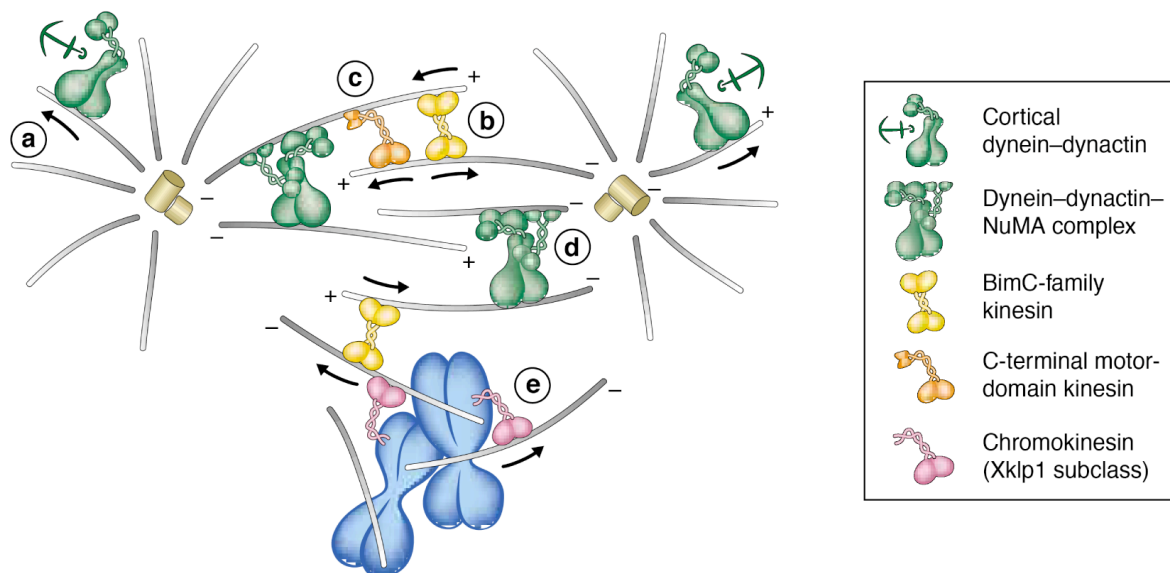
Figure 7. Microtubule-associated motor proteins establish and maintain the spindle bipolarity
(A) Cortical dynein connects AMTs to the cell cortex to position the spindle and maintain centrosome separation.
(B) Plus end-directed tetrameric kinesins of the BimC-family (kinesin-5 family, Eg5) slide MTs poleward and organize the antiparallel MTs in the spindle midzone.
(C) Minus end-directed C-terminal motor domain kinesins of the KinC family (kinesin-14 family, XCTK2) control spindle pole separation.

16

(D) The dynein/dynactin complex, bound to NuMA, focuses the spindle pole by cross-linking MT minus ends.
(E) Plus end-directed chromokinesins of the kinesin-4 (Xklp1) and kinesin-10 family (Xkid) simultaneously associate with MTs and chromatin and push the chromosome arms away from the spindle poles. (Adapted from Wittmann et al., 2001)

1.5.1   Poleward forces

In mitosis, multiple forces affect chromosome movement. After capture of a kinetochore by spindle MTs, chromosomes are pulled poleward to enable proper spindle-kinetochore attachment. The main force driving this movement is generated at the kinetochores themselves. Catastrophe factors of the kinesin-13 family are recruited to the MT plus end and induce MT depolymerization. Indeed, photobleaching experiments have shown that KMTs depolymerize primarily at the kinetochore (Gorbsky et al., 1988). This originally led to the conclusion that the kinetochore, by inducing MT disassembly, "chews" its way to the pole in a "pacman"-like manner (Desai et al., 1998; Maddox et al., 2003). In addition, kinetochore-associated dynein moves the monooriented chromosomes towards the pole (Sharp et al., 2000), while CENP-E, in turn directs them in the opposite direction. As a result the chromosomes oscillate between the poles, driven by MT depolymerization at the leading (poleward, P) kinetochore and polymerization at the lagging (away from the pole, AP) kinetochore (Figure 8A) (Compton, 2000), which finally leads to chromosome congression (Kapoor et al., 2006). Together with their involvement in MT attachment, kinetochore proteins are hence also required to trigger alignment of monooriented chromatid pairs (Kapoor and Compton, 2002).

Another poleward force, superimposed on the kinetochore forces, is MT flux (see above). This poleward movement of tubulin results from the dynamic instability of MTs and is supported by motor proteins (Figure 8A). The kinesin-5 protein Eg5 is a major contributor to MT flux (Kwok and Kapoor, 2007), and inhibition of Eg5 significantly decreases the flux rate (Miyamoto et al., 2004).

1.5.2   Polar ejection force

Polar ejection forces balance the poleward forces, generated by the kinetochores and MT flux, in order to enable chromosome congression in metaphase (Figure 8B). These forces, which are occasionally also referred to as 'polar wind', reflect the action of kinesin-related motors that push chromosome arms away from the spindle poles and thus facilitate chromosome movement towards the spindle equator

INTRODUCTION

(Brouhard and Hunt, 2005; Heald, 2000; Rieder and Salmon, 1994; Vernos and Karsenti, 1995). Consequently, it has been proposed that the balance between the two force gradients, generated along the spindle, drives chromosome congression: poleward force from MT flux, peaking at the kinetochores in the middle of the spindle, and the polar ejection force, increasing towards the poles. In this model, when a chromosome, driven by poleward force, moves to one pole, increasing polar ejection force opposes this movement, changing the polymerization state of the leading kinetochore microtubule. This in turn, promotes the congression of chromosomes to the centre of the spindle, where polar ejection forces are balanced (Kapoor and Compton, 2002).

In vertebrates, the polar ejection force is primarily due to the chromokinesin Kid, a plus end-directed motor protein of the kinesin-10 family (see above) (Antonio et al., 2000; Funabiki and Murray, 2000; Levesque and Compton, 2001; Tokai et al., 1996; Yajima et al., 2003), which links non-kinetochore microtubules to chromosome arms (Levesque and Compton, 2001; Yajima et al., 2003). The interaction of Kid with microtubules has been reported to be inhibited by importin α/β, whereas, the recruitment to the chromatin seems to be promoted by the high RanGTP levels in the vicinity of the chromosomes (Tahara et al., 2008; Trieselmann et al., 2003). At the metaphase to anaphase transition, Kid is targeted for degradation via the APC.
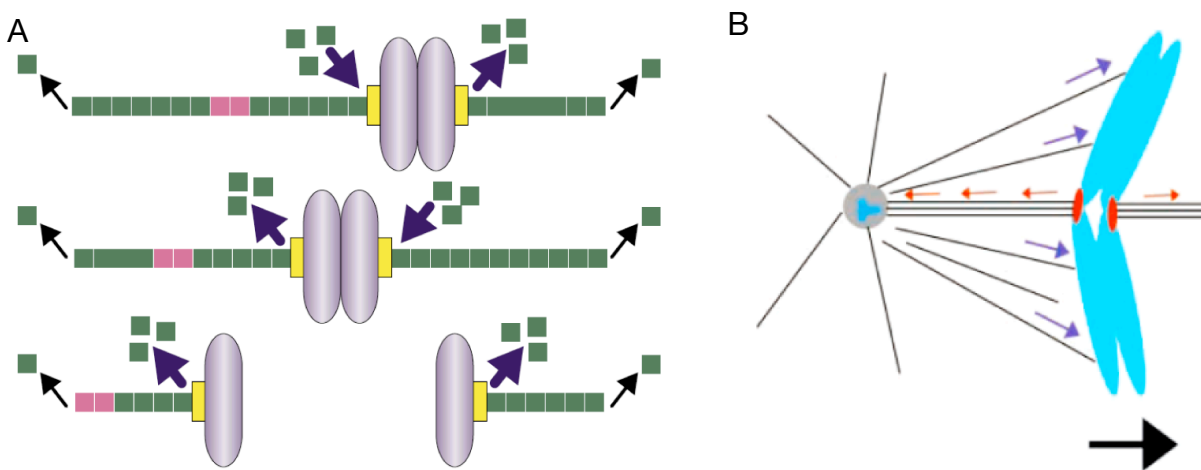
Figure 8. Forces acting on chromosome movement
(A) Poleward force is generated by MT flux. MTs depolymerize at the poles and either polymerize or depolymerize at the kinetochores (yellow rectangle). The different polymerization dynamics at the kinetochore microtubules then drive chromosome movement. The red mark represents a fiduciary mark, as used in photobleaching and photoactivation experiments to track the tubulin migration. (Adapted from Mitchison and Salmon, 2001)
(B) The poleward force (red arrows) is counteracted by polar ejection forces (blue arrows) mediated by chromosome-associated chromokinesins of the Kid subclass (kinesin-10 family) that push chromosome arms away from the poles. (Adapted from Kapoor and Compton, 2002)

18

1.6 Regulation by phosphorylation

Mitotic progression is regulated by reversible protein phosphorylation and irreversible protein degradation. Protein phosphorylation and proteolysis are closely linked, since the proteolytic machinery is regulated by phosphorylation. Conversely, a number of mitotic kinases are down regulated by degradation. The master regulator in the orchestration of M-phase events is the Cyclin-dependent kinase, Cdk1 (Nigg, 2001). While Cdk1 protein levels are constant throughout the cell cycle, its activity is tightly regulated by phosphorylation and protein-protein interactions. The regulatory interaction partners of Cdk1 are Cyclin A and B. Whereas Cyclin A begins accumulating in S-phase, Cyclin B is highly expressed shortly before M-phase. Subsequent association of Cyclin B with Cdk1 initiates a series of events that lead to entry into mitosis. In mammalian cells, activation of Cdk1 at the G2/M transition depends on the net dephosphorylation at two neighboring residues (Thr14 and Tyr 15) by the dual-specificity phosphatase Cdc25C that overcomes the inhibitory phosphorylation by the two kinases Wee1 and Myt1 (Nigg, 2001). The Cdk1/Cyclin B complex afterwards promotes its own activation in a positive feedback loop. Fully activated Cdk1/Cyclin B has many phosphorylation targets, involved in all fundamental mitotic stages. In early mitosis, nuclear envelope breakdown, chromatin condensation, centrosome separation and spindle assembly are initiated by Cdk1-mediated phosphorylation of nuclear lamins (Peter et al., 1991), condensins (Kimura et al., 1998), kinesin related motors and microtubule binding proteins (Blangy et al., 1995). At anaphase onset, Cdk1/Cyclin B complexes are involved in the regulation of the ubiquitin-dependent proteolytic machinery via the APC that triggers the timely degradation of several mitotic regulators, including securin and Cyclin B itself (Morgan, 1997). The continuous proteolysis orders late mitotic events, like spindle disassembly, nuclear envelope reformation and cytokinesis. Finally, Cyclin degradation results in Cdk1 inactivation which in turn allows the dephosphorylation of Cdk1 substrates by phosphatases, and leads to mitotic exit (Sullivan and Morgan, 2007).

1.6.1 Mitotic kinases

In addition to Cdk1, there are several other kinases, which play an important role in mitotic progression. Among them, the well characterized Polo-like kinases (Plk).

INTRODUCTION

Plk1, a member of this family has been studied to great extent and reported to be involved in almost all phases of mitosis. This particular kinase is highly dynamic. It localizes to centrosomes and kinetochores during early mitosis and the central spindle in telophase (Barr et al., 2004), and hence promotes centrosome maturation and separation in early mitosis (Barr et al., 2004; Glover, 2005), APC/C-mediated chromosome separation at anaphase onset (Barr et al., 2004; Uhlmann, 2004; Watanabe, 2005) as well as cytokinesis (Neef et al., 2003). Members of the Plk-family are classified by a C-terminal polo-box domain (PBD) that is required for the substrate targeting and subcellular localization of Plk1 (Elia et al., 2003). The PBD functions as a phosphopeptide-binding motif that recognizes previously phosphorylated docking proteins (Elia et al., 2003). It has been proposed that the binding of the PBD results in a conformational change that liberates the kinase domain of Plk1, which is then capable to phosphorylate either the docking protein itself or other downstream targets. Cdk1/Cyclin B has been reported to activate Plk1 by pre-phosphorylating Plk1 docking proteins (Elia et al., 2003), but Plk1 can also function as its own "priming" kinase (Neef et al., 2003).

Another family of mitosis-specific kinases comprises the Aurora kinases. As in the case of Plk1 (Golsteyn et al., 1995), the expression of Aurora-A is increased in mitosis and the enzyme is activated by phosphorylation at multiple sites (Littlepage et al., 2002). Binding to TPX2 keeps Aurora-A in a conformationally-active state and protects its phosphorylated activation segment from inactivation by protein phosphatase 1 (PP1) (Bayliss et al., 2003; Kufer et al., 2002; Tsai et al., 2003). In addition, TPX2 targets Aurora-A to the spindle pole in early mitosis, in a RanGTP-dependent manner (Bayliss et al., 2003; Kufer et al., 2002; Tsai et al., 2003) and thus promotes its function in centrosome maturation (Glover et al., 1995) and spindle assembly (Roghi et al., 1998). Most of the identified Aurora-A targets localize to the centrosome, such as TPX2 and Eg5 (Cochran et al., 2004; Kufer et al., 2002; Tsai et al., 2003). Nevertheless, HURP (hepatoma upregulated protein), a protein that localizes to spindle MTs (Sauer et al., 2005; Tsou et al., 2003) has also been reported to be controlled by Aurora-A phosphorylation, at least *in vitro* (Li and Li, 2006; Yu et al., 2005). However, it is still unclear which of the predicted Aurora-A substrates are actually phosphorylated *in vivo,* and new targets almost certainly await discovery*.*

20

2 Aim of the work

The mitotic spindle is a highly dynamic entity, providing the infrastructure for directional chromosome movement. Despite major progress in understanding the spatial and temporal regulation of the spindle apparatus, its function and composition are not fully understood. In order to achieve a more complete inventory of the spindle components, a proteomic survey has been carried out in our laboratory (Sauer et al., 2005). In this study, 147 known spindle-associated spindle components and 144 new potential spindle proteins were identified by mass spectrometry (Sauer et al., 2005). Among the 17 candidates analyzed in detail, 6 localized to the spindle. Three of these new spindle proteins have been successfully studied in our laboratory and their subcellular localization is shown below by transient expression of myc-tagged constructs in HeLa S3 (Figure 9): HURP (hepatoma upregulated protein), Ska1 (Spindle and kinetochore-associated 1) (Hanisch et al., 2006) and a previously non-described protein, C20Orf129 (later called CHICA by Dr. Anna Santamaria).

The specific goal of my PhD-thesis was to identify the physiological function of these proteins, with particular interest on their possible contributions to the stabilization of K-fibers. Originally, work was initiated on two proteins a) C20Orf129 and b) HURP. In this thesis, results on C20Orf129 will be described only very briefly, because after initial results were positive for both proteins, the study of C20Orf129 was continued primarily by Dr. Anna Santamaria in the laboratory.
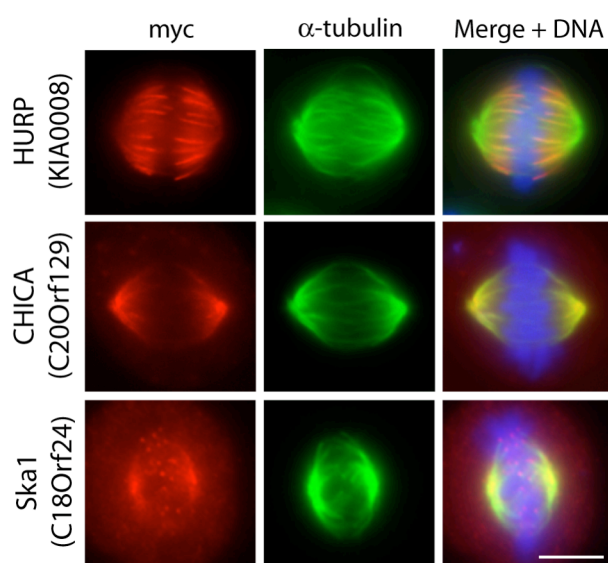
Instead, my own work focused on a detailed analysis of HURP, especially its regulation by the recently discovered Ran-dependent spindle assembly pathway in human somatic cells.

Figure 9. Spindle localization of novel proteins N-terminally myc-tagged proteins were overexpressed in HeLa S3 and stained for myc in red, α-tubulin in green, and DNA was stained with DAPI (blue). Scale bar = 10 µm. (Adapted from Sauer et al., 2005)

3 Results

3.1 Initial characterization of the new spindle protein C20Orf129 (CHICA)

C20Orf129 was identified as a novel spindle protein in the course of our proteomic survey of the human mitotic spindle. It was an interesting candidate for further study by virtue of its apparent localization to the spindle MTs (Sauer et al., 2005; Tsou et al., 2003). Having confirmed that C20Orf129 is a bonafide spindle component, it was shown subsequently by Dr. Anna Santamaria that C20Orf129 functionally interacts with the chromokinesin Kid. Consequently, the protein has been renamed CHICA (CHICA = Spanish for 'girl', partner of Kid).

For the initial characterization of CHICA, we first analyzed the primary structure using Pfam (Finn et al., 2006), which revealed similarities with several other human proteins, most of which have not previously been described (Fam83A-G). This is reflected by the presence of a domain, termed DUF1669 (Figure 10, residues 8-297). Within this domain, CHICA harbors a conserved motif $(H(X)K(X)_4D)$, characteristic of phospholipase D or nuclease function (Ponting and Kerr, 1996; Xie et al., 1998) (Figure 10). However, the significance of this motif is presently unknown.
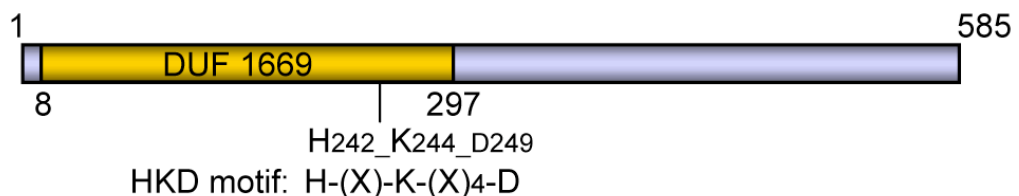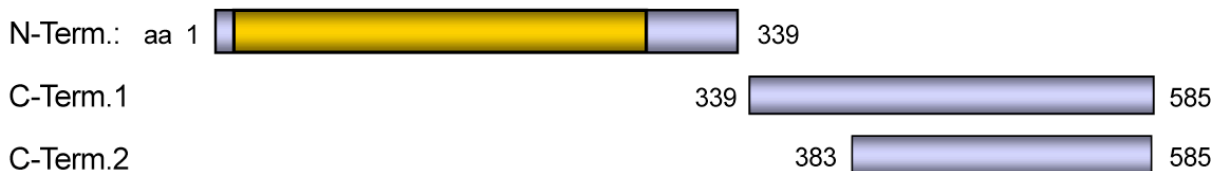
Figure 10. Primary structure of the protein CHICA
The conserved domain DUF1669 is shown in orange and key residues of the HKD domain are depicted. N-and C-terminal CHICA fragments are shown below: N-Term.: aa 1-339, C-Term.1: aa 339-585, and C-Term.2: aa 383-585.

3.1.1 CHICA localizes to the proximity of the spindle poles

To determine the localization of endogenous CHICA, rabbit polyclonal antibodies were generated. To this end, different N-and C-terminal His-tagged CHICA fragments were produced in *E. coil* and tested for their expression and solubility. Expression of the N-terminus (N-Term.: aa 1-339), as well as the C-terminus (C-Term.1: aa 339-585) of CHICA could not be induced by IPTG, however, a shorter C-terminal fragment (C-Term.2: aa 383-585) was highly expressed. Therefore, this C-terminal fragment (C-Term.2) of CHICA was purified under denaturing conditions and used as an immunogen for injection into rabbits. The serum obtained at day 73 after immunization was tested for reactivity on mitotic HeLa S3 cells by immunofluorescence microscopy and antibodies were then affinity purified with membrane bound antigen to obtain CHICA-specific antibody (Figure 11A). In Western blots, the anti-CHICA antibody recognized a band at around 66 kDa (the expected molecular mass of CHICA) in asynchronous cells, but a doublet in M phase samples (Figure 11B), suggesting that CHICA is modified during mitosis.
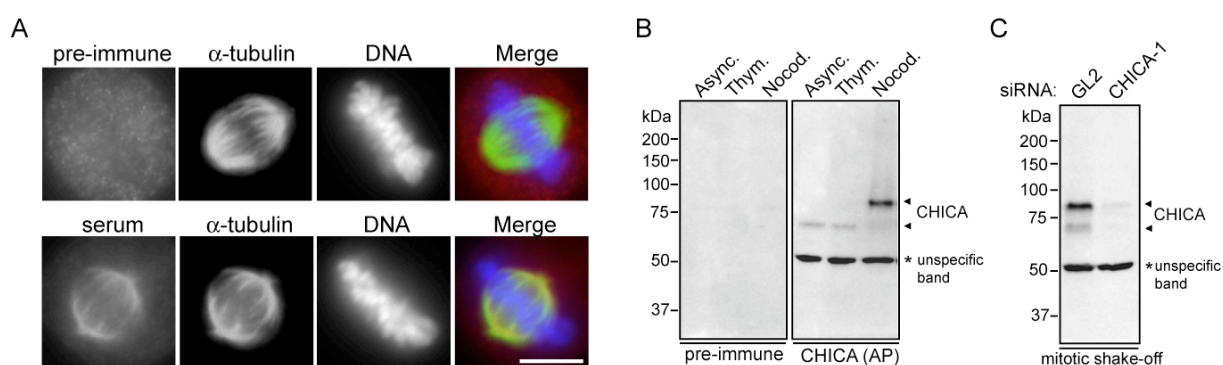
Figure 11. Anti-CHICA serum specifically detects CHICA on spindle MTs and in cell lysates
(A) Pre-immune serum and serum from day 73 were tested for reactivity on mitotic HeLa S3 cells by immunofluorescence microscopy. Cells were stained with pre-immune serum and serum against CHICA (red), anti-α-tubulin antibody (green), and DNA with DAPI (blue). Scale bar = 10 μm
(B) Lysates (60 μg) from asynchronously growing, thymidine and nocodazole arrested cells were resolved by SDS-PAGE and probed with pre-immune serum or affinity purified antibody (AP). Two bands corresponding to CHICA are marked (arrows).
(C) Mitotic lysates of nocodazole-treated cells (isolated by mitotic shake-off) representing either GL2- or CHICA-depleted cells were resolved by gel electrophoresis and analyzed by Western blotting with the CHICA affinity purified antibody. The asterisk indicates a cross-reacting band, observed with the CHICA antibody (The blots, shown in B and C were kindly provided by Dr. Anna Santamaria).

As shown by indirect immunofluorescence microscopy, endogenous CHICA was observed only as a faint, primarily cytoplasmic staining in interphase cells. During mitosis, CHICA associated with the spindle pole of the forming bipolar

spindle in prophase and then persisted on the spindle caps until anaphase (Figure 12). No spindle staining was observed with pre-immune IgGs (Figure 11A) or after depletion of CHICA by siRNA (Figure 11C and Figure 12, right). These data validate the specificity of the anti-CHICA polyclonal antibody and confirm that CHICA is a genuine component of the mitotic spindle.
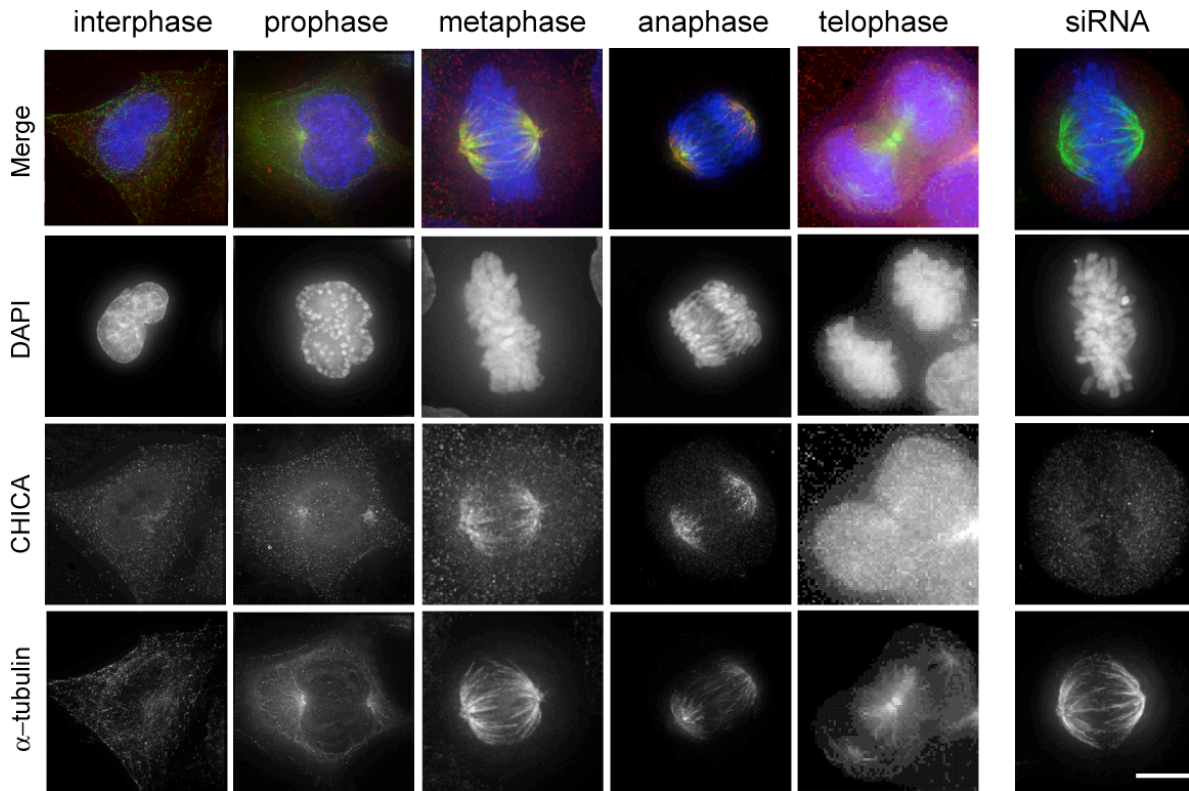
Figure 12. CHICA localizes to the mitotic spindle
Immunofluorescence images of HeLa S3 cells at different cell-cycle stages and HeLa S3 cells treated with CHICA siRNA-1 for 36 hr. Cells were stained with antibodies against CHICA (red), and α-tubulin (green). DNA was stained with DAPI (blue). Scale bar = 10 μm

3.2 CHICA does not play a role in K-fiber stabilization

CHICA localizes preferentially to non-kinetochore MTs at the spindle pole caps, as demonstrated by the near-exclusive localization of myc-CHICA and HURP, the later specifically localizing to K-fibers in the vicinity of the chromosomes (Koffa et al., 2006; Sillje et al., 2006) (Figure 13A). However, this does not rigorously exclude a contribution of CHICA to K-fiber stabilization. We thus tested the stability of K-fibers by exposing both CHICA- and HURP-depleted cells to a 20 min cold treatment (Rieder, 1981). Whereas cold treatment did not impair K-fibers in GL2-treated control cells, it resulted in the rapid disappearance of most K-fibers from HURP-depleted cells (Figure 13B), as reported previously (Sillje et al., 2006). In contrast, depletion of CHICA did not have an effect on K-fiber stability, compared to

GL2-treated cells analyzed for control (Figure 13B). Moreover, depletion of CHICA did not show a significant reduction of inter-kinetochore distances (CHICA-1: 1.48±0.03, and CHICA-2: 1.50±0.03 μm, respectively), as compared to control cells (GL2: 1.51±0.01), in contrast to nocodazole (1.05±0.09 μm) or taxol-treated (1.08±0.02 μm) cells (Figure 13C). Taken together, these observations suggest that the absence of CHICA does not significantly affect K-fiber stability. Moreover, CHICA was absent from K-fibers resisting cold treatment (Figure 13B, GL2), which also argues against a critical role for this protein in the formation or function of K-fibers.
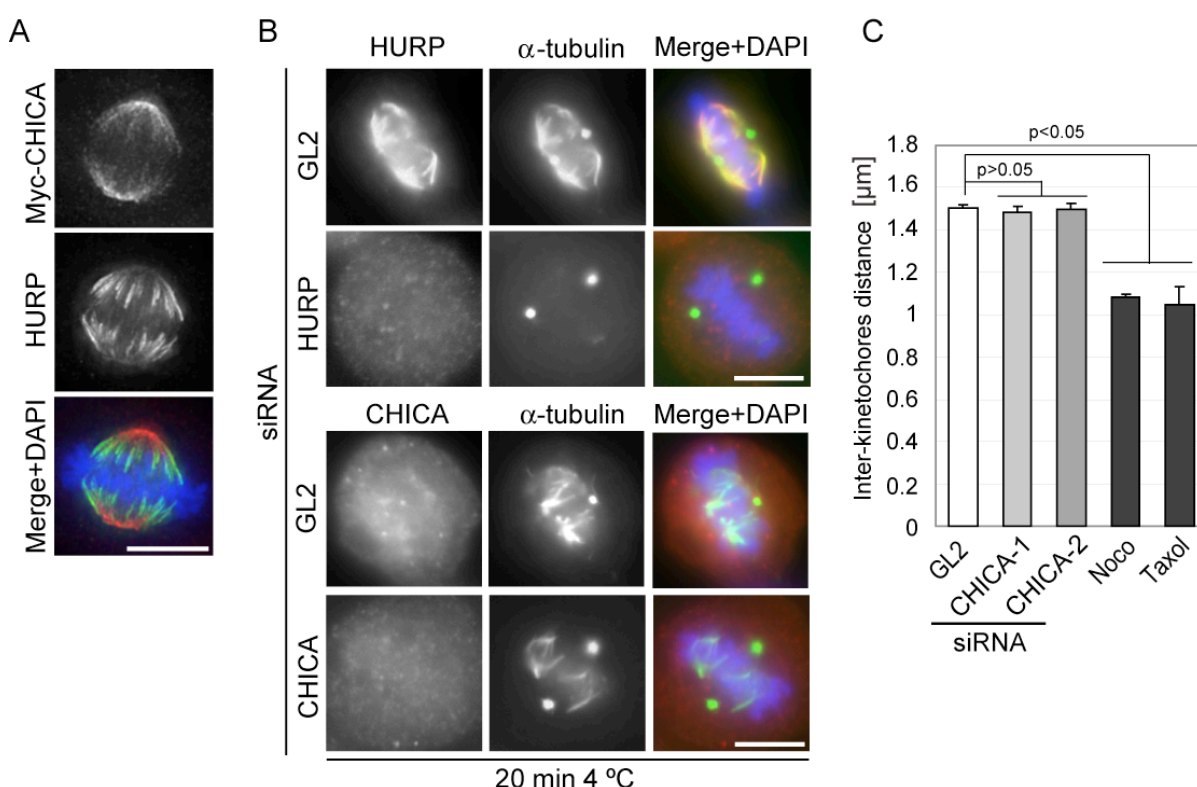
Figure 13. CHICA depletion does not affect K-fiber stability
(A) HeLa cells were transfected with a myc-tagged CHICA construct and then permeabilized and fixed with PTEMF. Cells were stained with anti-myc 9E10 (red), and anti-HURP (green) antibodies and DNA was stained with DAPI (blue). Scale bars always equal 10 μm.
(B) Control (GL2), HURP, or CHICA- depleted HeLa S3 cells were placed on ice for 20 min and then fixed and permeabilized with PTEMF. Cells were stained with anti-α-tubulin antibody (green), anti-HURP or anti-CHICA antibody (red), respectively and DNA was stained with DAPI (blue).
(C) Analysis of the inter-kinetochore distance on sister chromatids. HeLa cells were transfected with GL2 (control), and CHICA siRNA for 48 hr. Cells were collected after a thymidine block for 12 hr, followed by a 12 hr release into 20 μm MG132 for the last 2 hr, or treated with 200 nM nocodazole or 1 μM taxol for 12 hr. Kinetochore pairs on sister chromatids were observed by inner kinetochore CREST staining and flanking Hec1 staining. ~20 kinetochore pairs were counted in each cell and 20 cells were counted per condition, in 3 independent experiments.

Having confirmed, that the previously identified candidate spindle component CHICA (C20Orf129) indeed interacts with the mitotic spindle apparatus, the project

was continued by Dr. Anna Santamaria, a postdoc in our laboratory, while my own work was focused on HURP. In her study, Dr. Anna Santamaria further characterized the function and phenotype of CHICA and uncovered a functional interaction with the chromokinesin Kid, which indicates a role for a CHICA-Kid complex in the generation of polar ejection forces.

3.3 HURP a new target of the Ran-importin β-regulated spindle assembly pathway

HURP was originally identified as a protein upregulated in human hepatocellular carcinoma and shown to be a component of the spindle apparatus (Sauer et al., 2005; Tsou et al., 2003). A bioinformatic analysis of HURP using ClustalW, SMART and ProtParam software revealed that the protein has a basic N-terminus (pI: 9.9), including two predicted coiled coil domains (CC1: aa 22-42; CC2: aa 94-120) followed by a guanylate kinase-associated protein domain (GKAP: aa 310-607) of unknown function (Tsou et al., 2003) (Figure 14) (Appendix: Alignments). The C-terminus (aa 402-846 pI: 5.5), in contrast, is acidic and contains Aurora-A and Cdk1 phosphorylation sites that have been previously described to be involved in HURP stability and degradation (Hsu et al., 2004; Yu et al., 2005). Furthermore, HURP contains a N-terminal [32]KEN[34]-Box within the first coiled coil domain and a D-Box (aa 573-581) at the end of the GKAP domain, implying that HURP might be an APC substrate (Pfleger and Kirschner, 2000).
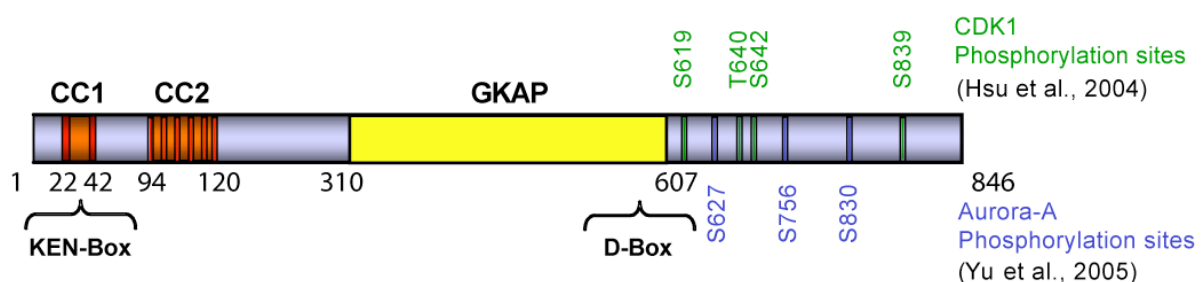
Figure 14. Primary structure of HURP
The conserved coiled coil (CC1: aa 22-42, CC2: aa 94-120) domains are depicted in orange, the guanylate kinase-associated protein domain (GKAP: aa 310-607) is shown in yellow and conserved, predicted Cdk1- and Aurora-A phosphorylation sites in green and blue, respectively. The [32]KEN[34]-Box within the first coiled coil domain and the D-Box (aa 573-581) within the GKAP domain are marked with brackets.

3.3.1 HURP localizes to microtubules in the vicinity of chromosomes

To allow its functional characterization, a specific rabbit polyclonal antibody was generated against the amino-terminal half of HURP (aa 1–401) (Figure 14). Analysis of cells released from a nocodazole block showed that HURP protein levels changed during the cell cycle, being high during early mitosis and then gradually decreasing during mitotic exit (Figure 16A). These results are in line with a recent study, showing that the F-box protein Fbx7 targets HURP for degradation (Hsu et al., 2004). Compared to its migration in SDS-PAGE in asynchronously growing (interphase) cells, HURP showed reduced electrophoretic mobility during early mitosis (Figure 16A), presumably reflecting phosphorylation (Hsu et al., 2004). By means of high-resolution SDS-PAGE, two closely associated bands could also be identified in lysates from asynchronously growing cells (Figure 16A). Both bands were similarly reduced in response to siRNA-mediated depletion of HURP (Figure 18A, below), suggesting that multiple forms of HURP are present throughout the cell cycle.

To investigate the subcellular localization of endogenous HURP, indirect immunofluorescence microscopy was performed. In interphase cells, only a faint, predominantly cytoplasmic staining was observed (Figure 16B). However, in cells with partially condensed chromosomes, HURP localization was mostly nuclear, suggesting that HURP accumulates in the nucleus shortly before the onset of mitosis (Figure 16B). In mitotic cells, HURP staining became much more prominent (Figure 16C), in agreement with its higher abundance during M-phase (Figure 16A). In prometaphase cells, HURP colocalized with spindle MTs and, most strikingly, the protein was concentrated in the vicinity of mitotic chromosomes. This unequal labeling of spindle MTs was even more pronounced in metaphase and early anaphase cells, when HURP was present on MTs close to chromosomes but absent from the polar regions. During late anaphase, HURP localized to MTs directly adjacent to both sides of the segregating chromatids but was excluded from the central spindle. Finally, HURP staining gradually diminished during telophase and only weak signals could be seen around chromosomes (Figure 16C).
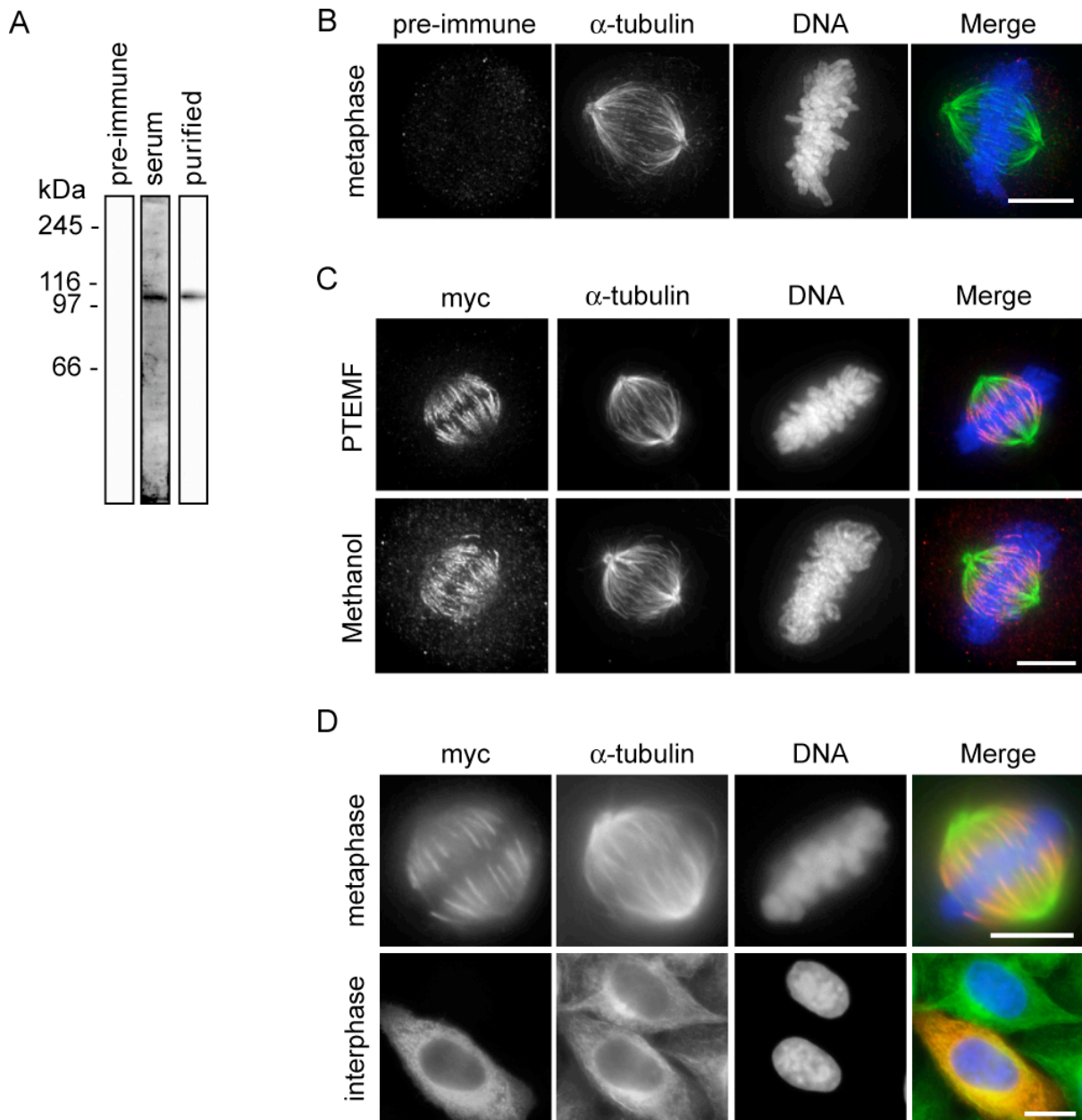
Figure 15. Specificity of anti-HURP polyclonal antibody and HURP localization
(A) Cell extracts from exponentially growing HeLa S3 cells were separated by SDS-PAGE and probed by Western blotting with pre-immune serum, anti-HURP serum, and affinity purified anti-HURP antibodies, respectively. A specific band, at around 100 kDa was observed with the anti-HURP serum and the affinity-purified anti-HURP antibody.
(B) HeLa S3 cells were fixed and permeabilized with PTEMF and probed with pre-immune IgG (red) and anti-α-tubulin antibody (green), and DNA was stained with DAPI (blue). Scale bars equal 10 μm.
(C) HeLa S3 cells were fixed and permeabilized with PTEMF or methanol, respectively and probed with anti-myc 9E10 antibody (red) and anti- α-tubulin antibody (green). DNA was stained with DAPI (blue). Scale bars equal 10 μm.
(D) Myc-tagged HURP was transiently expressed in HeLa S3 cells for 24 hr. After paraformaldehyde fixation and Triton-X100 permeabilization, cells were stained with anti-myc 9E10 antibody (red) and anti-α-tubulin antibody (green), and DNA was stained with DAPI (blue). Scale bars equal 10 μm.

The spindle localization of HURP was independent of the fixation method (Figure 15C), and no spindle staining was observed with pre-immune IgGs (Figure 15A, 15B). Finally, staining of a transiently expressed myc-tagged HURP protein with anti-myc (9E10) antibodies (Figure 15D) confirmed the localizations established for endogenous HURP. These results indicate that HURP associates with a select subset of spindle MTs and, throughout mitosis, displays a striking enrichment in the vicinity of chromosomes.

3.3.2   HURP localizes predominantly to kinetochore microtubules

To better understand the observed HURP localization, we costained cells with antibodies against HURP and the kinetochore marker Hec1 (Figure 17A). In early prometaphase cells, HURP staining of MTs showed a comet-like pattern and, as revealed by higher magnification, the HURP-positive comet tails were directly adjacent to Hec1-positive kinetochores (Figure 17A, top panel).

Similarly, in metaphase and anaphase cells, HURP-positive MTs almost invariably ended at Hec1-stained kinetochores (Figure 17A, middle and bottom). These results strongly suggest that HURP localizes predominantly to kinetochore MTs. To investigate, whether normal MT dynamics were required for HURP localization, we treated cells with nocodazole or taxol (paclitaxel). At the low concentration of nocodazole used, monopolar spindles were formed and HURP still localized to MTs close to chromosomes (Figure 17B). Interestingly, occasional long MTs extending toward the cell cortex were always devoid of HURP (Figure 17B, arrowheads). In cells treated with taxol, spindle MTs formed multiple clusters, often at the cell periphery (Figure 17B). Yet, HURP remained localized predominantly in the vicinity of chromosomes, often showing comet-like staining suggestive of kinetochore-associated MTs. These observations indicate that HURP remained confined to the vicinity of chromosomes, even when normal MT dynamics were disturbed, further supporting the conclusion that HURP localizes only to a subset of MTs.
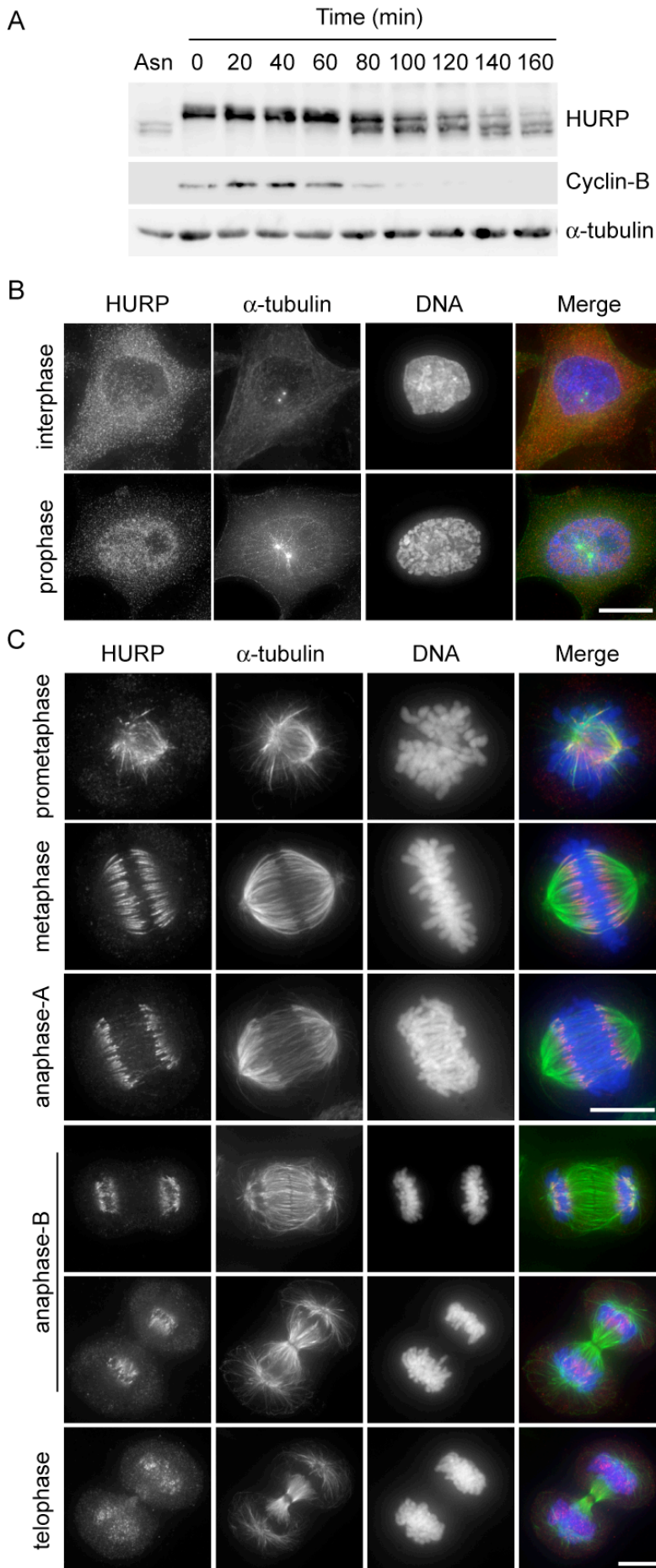
Figure 16. Cell cycle-regulated HURP localizes to mitotic spindle microtubules in the vicinity of chromosomes

(A) HeLa S3 cells were synchronized by a sequential aphidicolin/nocodazole block and release protocol. After nocodazole release, cell samples were taken every 20 min. For comparison, asynchronously (Asn) growing cells were analyzed in parallel. Equal amounts of cell extracts were separated by SDS-PAGE and probed by Western blotting with the indicated antibodies.

(B) HeLa S3 cells were fixed with paraformaldehyde followed by permeabilization with Triton-X100. Cells were probed with anti-HURP antibody (red) and anti-α-tubulin antibody (green), and DNA was stained with DAPI (blue).

(C) HeLa S3 cells were fixed and permeabilized with PTEMF and probed with anti-HURP antibody (red) and anti-α-tubulin antibody (green), and DNA was stained with DAPI (blue). Scale bars equal 10 μm.
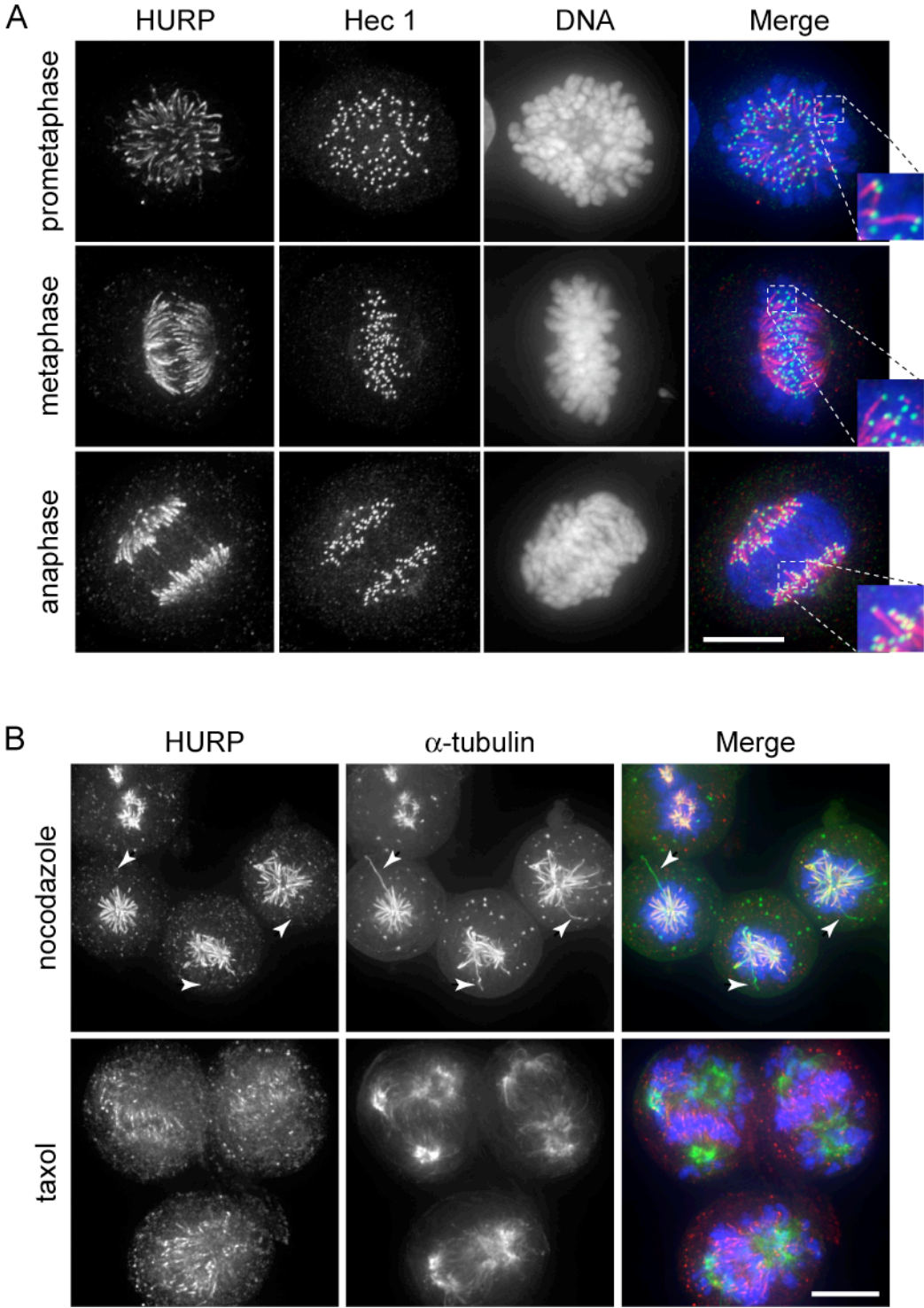
Figure 17. HURP localizes predominantly to kinetochore microtubules

(A) HeLa S3 cells were grown on coverslips and subsequently fixed and permeabilized with PTEMF. Cells were then stained with anti-HURP antibody (red) and anti-Hec1 antibody (green), a kinetochore marker, and DNA was stained with DAPI (blue). Insets show a 2.5 times magnification of the indicated areas.

(B) HeLa S3 cells were grown on coverslips and either treated with a low dose of nocodazole (40 ng/ml) or with taxol (1 μg/ml) (bottom) for 12 hr, before fixation and permeabilization with PTEMF. Cells were stained with anti-HURP antibody (red) and anti-α-tubulin antibody (green). DNA was stained with DAPI (blue). Arrowheads indicate long astral MTs that are devoid of HURP. Scale bars equal 10 μm.

3.3.3 HURP is required for stabilization of K-fibers

To determine the consequences of HURP depletion, two siRNA oligonucleotide duplexes targeting HURP were tested in comparison to a control (GL2) duplex (Elbashir et al., 2001). As shown by Western blot analysis and immunofluorescence microscopy (Figures 18A and 18B and Figure 19A), both siRNAs caused extensive depletion of HURP. This caused an increase in the number of cells with partly congressed chromosomes, while metaphase cells with properly aligned chromosomes became correspondingly less abundant (Figures 18B and 18C and Figure 19A). Nevertheless, HURP depletion did not result in a mitotic arrest, as indicated by the presence of cells at later mitotic stages. To analyze these apparent mitotic defects in more detail, live-cell imaging was performed (Figures 18D–18F and Figure 19B). A HeLa S3 cell line expressing a histone H2B-GFP fusion protein was subjected to a synchronization/siRNA protocol, as depicted in Figure 18D, and time-lapse immunofluorescence microscopy was initiated 8 hr after release from an aphidicolin block (Figures 18E and 18F, Figure 19B). In control (GL2-treated) cells, the time interval between prophase and anaphase onset was about 33 min, and only 4% of cells required more than 60 min to enter anaphase (Figure 18G). In contrast, in HURP-depleted cells treated with siRNA-1 or -2, the mean duration of prophase to anaphase onset was 90 min (siRNA-1) or 120 min (siRNA-2), and 55% or 82% of the cells, respectively, required more than 60 min to enter anaphase (Figure 18G). This delay clearly indicates that HURP-depleted cells experienced problems with chromosome congression, but, eventually, virtually all cells succeeded to align their chromosomes. After anaphase onset, no obvious differences between control and HURP-depleted cells could be observed, although it is difficult to exclude occasional chromosome segregation defects. Altogether, these results show that depletion of HURP substantially delayed chromosome alignment but did not ultimately prevent completion of mitosis.
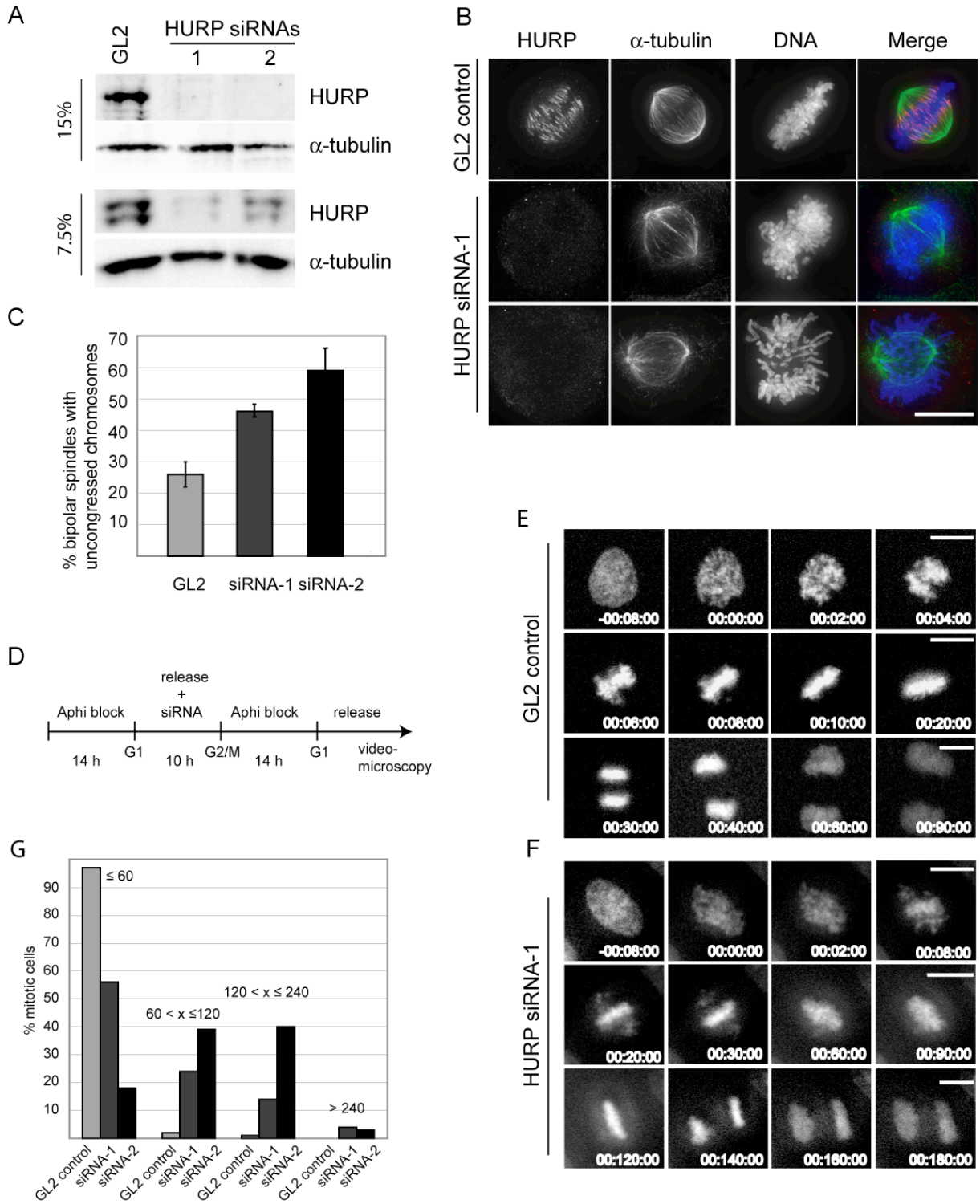
Figure 18. Depletion of HURP results in a chromosome congression delay
(A) HeLa S3 cells were treated for 48 hr with control (GL2) and two different HURP-specific siRNAs (siRNA-1 and siRNA-2), respectively. Equal amounts of cell extracts were separated by 15% (top) and 7.5% (below) SDS-PAGE and probed by Western blotting with anti-HURP antibody. Detection of α-tubulin was used as a loading control.
(B) HeLa S3 cells were treated for 48 hr with control (GL2) and HURP siRNA-1 and then fixed and permeabilized with PTEMF. Cells were probed with anti-HURP antibody (red) and anti-α-tubulin antibody (green), and DNA was stained with DAPI (blue).

(C) Quantitative analysis of the number of bipolar spindles with uncongressed chromosomes in control (GL2) and HURP siRNA-depleted cells. Histogram shows the results of three independent experiments (>200 cells each) and bars indicate standard deviations.

(D) Schematic depiction of the synchronization/siRNA protocol used for live-cell imaging. After release from a G1/S phase aphidicolin block, HeLa S3 cells stably expressing histone H2B-GFP were treated with control (GL2) or HURP siRNAs. 10 hr after the release, a second aphidicolin block was imposed for 14 hr, and 8 hr after a second release, time-lapse immunofluorescence microscopy was started. Pictures were taken at 2 min intervals.

(E) Selected images show H2B-GFP stained chromosomes of a control (GL2) treated cell progressing through mitosis (188 cells analyzed). T = 0 was defined as the time point at which chromosome condensation became evident.

(F) As in (E), except that cells were treated with HURP siRNA-1 (201 cells analyzed).

(G) The duration of prophase to anaphase onset was calculated from time-lapse movies of control (GL2) and HURP siRNA-treated cells, as described in (E) and (F). T = 0 was defined as in (E) (onset of chromosome condensation) and anaphase onset was defined as the last frame at which chromosome segregation had not yet occurred. Histogram shows the percentages of mitotic cells that had progressed from prophase to anaphase onset within 60 min, within 60-120 min, within 120-240 min, and those that had required more than 240 min. Scale bars equal 10 μm.
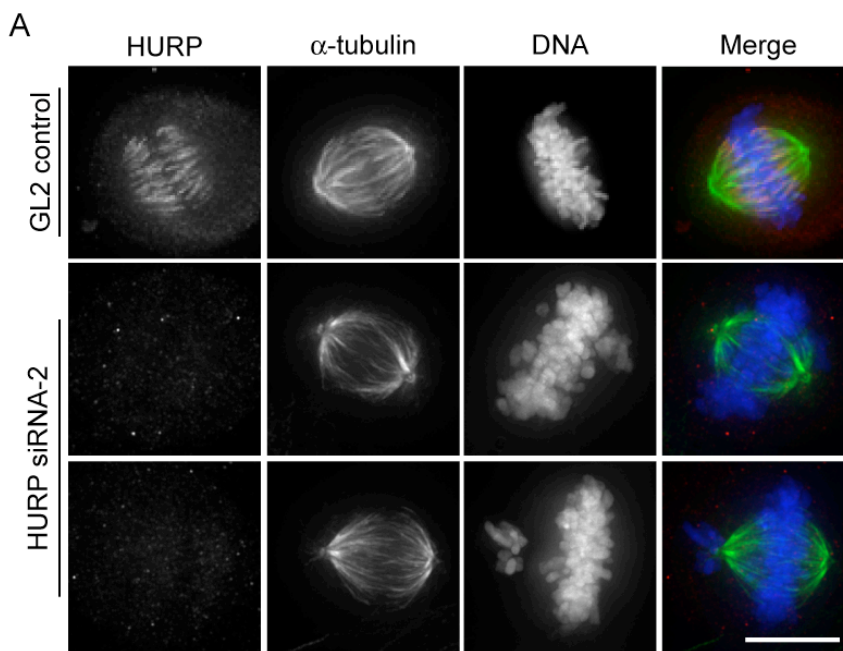
Figure 19. Mitotic progression in cells depleted of HURP by means of siRNA-2

(A) HeLa S3 cells were treated for 48 hr with either control siRNA (GL2) or the HURP siRNA-2 and then fixed and permeabilized with PTEMF. Cells were probed with anti-HURP antibody (red), anti-α-tubulin antibody (green), and DAPI (blue).

(B) HeLa S3 cells stably expressing histone H2B-GFP were subjected to a synchronization/siRNA protocol, as described in Figure 18D and analyzed exactly as described in Figure 18E.

Scale bars equal 10 μm.
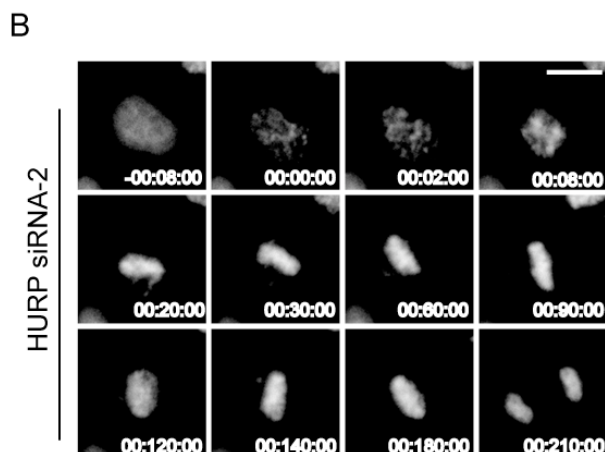
To determine whether the observed chromosome congression defect was related to the integrity of K-fibers, cells were subjected to cold treatment. Under such conditions, K-fibers remain relatively stable, whereas most other MTs depolymerize (Rieder, 1981). In HeLa S3 cells exposed to the control duplex (GL2), cold treatment for 20 min resulted in a disappearance of most MTs, except for K-fibers and central spindle/midbody MT bundles, as expected (Figure 20A, top). In contrast, no cold-resistant K-fibers could be observed in HURP-depleted metaphase cells, and only centrosomal tubulin remained (Figure 20A, bottom). Central spindle/midbody MTs in anaphase cells were nearly as stable in HURP-depleted cells as in control cells (Figure 20A). Similar results were obtained with HURP siRNA-2, attesting to their specificity (Figure 21). These data indicate that HURP is involved in the formation and/or stabilization of K-fibers, but not of other MT bundles, in agreement with its specific localization.
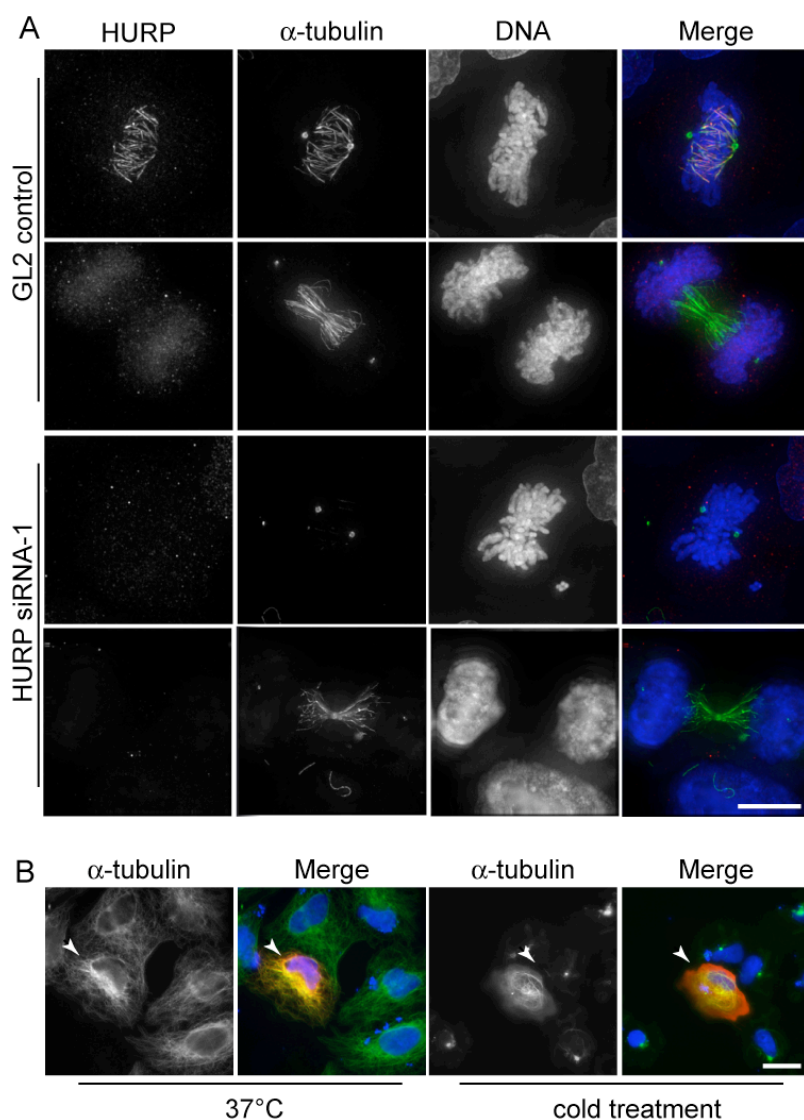
Figure 20. HURP stabilizes kinetochore microtubules
(A) HeLa S3 cells were treated for 48 hr with control (GL2) and HURP siRNA-1. Before fixation and permeabilization with PTEMF, cells were incubated for 20 min in ice-cold growth medium. Cells were stained with anti-HURP antibody (red) and anti-α-tubulin antibody (green), and DNA was stained with DAPI (blue).
(B) HeLa S3 cells transiently expressing myc-tagged HURP were either directly fixed and permeabilized with PTEMF or after a 30 min cold treatment. Cells were stained with anti-myc 9E10 antibody (red) and anti-α-tubulin antibody (green), and DNA was stained with DAPI (blue). Arrowheads indicate transfected cells. Scale bars equal 10 μm.

| | HURP | α-tubulin | DNA | Merge |

Figure 21. HURP stabilizes kinetochore MTs
HeLa S3 cells were treated for 48 hr with control (GL2) and HURP siRNAs, respectively. Before fixation and permeabilization with PTEMF, cells were incubated for 20 min in ice-cold growth medium. Cells were stained with anti-HURP antibody (red), anti-α-tubulin antibody (green), and DAPI (blue). Note that depletion of HURP with either siRNA 1 or 2 causes a very similar cold sensitization of K-fibers. Scale bar equals 10 μm.

We next asked whether the overexpression of HURP would lead to MT stabilization at ectopic sites. Indeed, when myc-tagged HURP was expressed to sufficiently high levels, this resulted in the formation of cold-resistant MT bundles even in interphase HeLa S3 cells (Figure 20B). The fact that overexpressed HURP is able to stabilize MTs also in interphase cells suggests that levels of functional HURP protein must be tightly controlled during the cell cycle.

3.3.4   HURP binds, bundles, and stabilizes microtubules *in vitro*

Having uncovered a function of HURP in MT stabilization *in vivo*, we next asked whether HURP could directly bind to MTs *in vitro*. To this end, human HURP was expressed from a baculovirus in Sf9 insect cells. Purified recombinant HURP was then incubated with or without taxol-stabilized MTs and centrifuged through a glycerol cushion (Figure 22A, top). In the presence of MTs, most of the recombinant HURP was recovered in the pellet fraction, whereas the protein was soluble in the absence of MTs. Bovine serum albumin (BSA), analyzed under identical conditions, remained in the soluble fraction both in the presence and absence of MTs (Figure 22A, bottom). Next we asked, whether purified HURP would be able to bundle and stabilize MTs *in vitro*. Specifically, we analyzed rhodamine-labeled MTs, which in the absence of any added protein appeared as faintly stained fibers under the immunofluorescence microscope (Figure 22B). Addition of BSA to these MTs had no effect on their appearance, but addition of HURP rapidly resulted in a strong bundling (Figure 22B, top). These HURP-induced MT bundles were highly stable and

resisted even prolonged (16 hr) cold treatment, whereas only amorphous material could be observed in cold-treated control samples (Figure 22B, bottom). These results indicate that HURP is able to bind, bundle, and stabilize MTs *in vitro*.
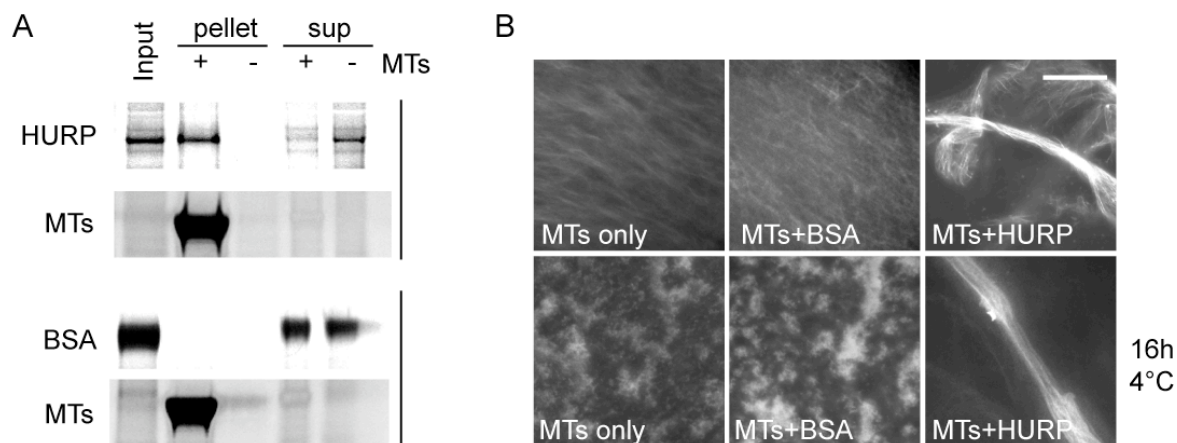
Figure 22. HURP directly binds, bundles, and stabilizes MTs *in vitro*
(A) Purified recombinant HURP was mixed with *in vitro* produced microtubules (+MTs), or as a control with buffer (-MTs). Subsequently, these samples were spun through a glycerol cushion and the supernatant (sup), and pellet fractions were then analyzed for the presence of HURP by Coomassie blue staining of SDS-PAGE gels. In parallel, the same experiment was performed with BSA, instead of HURP (bottom).
(B) MTs were produced *in vitro* with rhodamine-labeled tubulin. These MTs were then incubated with buffer (only), BSA, and recombinant HURP, respectively. Immunofluorescence microscopy was carried out, either after 5 min incubation at RT, or after 5 min incubation at RT followed by 16 hr incubation at 4°C (bottom). Scale bar equals 10 μm.

3.3.5 HURP interacts with importin β and shuttles between the cytoplasm and nucleus

To explore the mechanisms underlying HURP localization and/or function, we searched for interacting proteins. As a first approach, co-immunoprecipitation experiments were performed on mitotic HeLa S3 cells by means of the HURP antibody and pre-immune IgG as a negative control. Immunoprecipitated proteins were separated by SDS-PAGE and visualized by Coomassie blue staining. Two prominent proteins migrating at about 100 and 90 kDa were observed only in the anti-HURP immunoprecipitates (Figure 23A). Mass spectrometry identified these proteins as HURP and the nuclear import factor importin β, respectively (Figure 24). Importin β was also readily detected in anti-myc immunoprecipitates from cells expressing myc-tagged HURP, ruling out antibody crossreactivity (Figure 23B). In a second approach, we also searched for HURP-interacting proteins with a N-terminal HURP fragment (aa 1-550) in a yeast two-hybrid screen. As illustrated by a

representative two-hybrid interaction (Figure 23C), this screen yielded different cDNA clones encoding C-terminal fragments of human importin β. Together, these data demonstrate that HURP interacts with the nuclear import factor importin β.
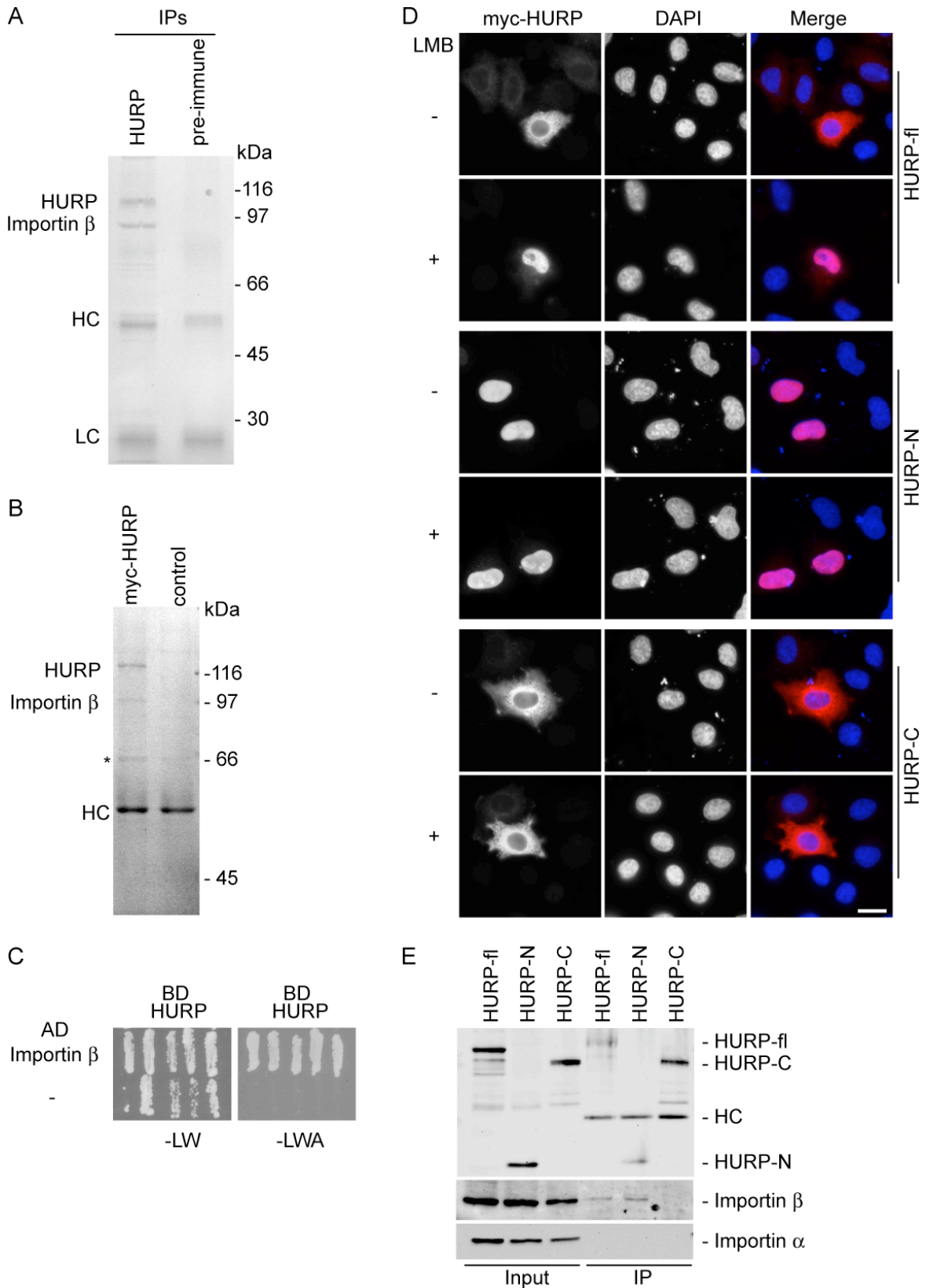
Figure 23. HURP interacts with importin β and shuttles between the cytoplasm and the nucleus
(A) Mitotic HeLa S3 cell lysates were used for immunoprecipitions (IPs) with anti-HURP antibody and pre-immune IgGs, respectively. The isolated protein complexes were separated by SDS-PAGE and proteins visualized by Coomassie blue staining. Two specific bands were identified in the anti-HURP IP. Mass spectrometry analysis (see Figure 24) revealed that these were human HURP and importin β, respectively, as indicated. HC and LC indicate antibody heavy and light chains, respectively.
(B) Similar as in (A), except that anti-myc 9E10 antibody immunoprecipitations were performed on cell lysates from control and myc- HURP-expressing HEK293T cells, respectively. Proteins were again identified by MS analysis. Asterisk indicates a non-specific interacting protein.
(C) Yeast two-hybrid interaction between N-terminal HURP (residues 1-550) expressed from a binding domain vector and a C-terminal importin β fragment expressed from an activation domain (AD) vector. As a negative control, the empty AD (-) vector was used. Interactions were reflected by growth on selective medium (-LWA, at right). For control, growth on nonselective (-LW) plates is shown.
(D) HeLa S3 cells were transiently transfected for 48 hr with myc-HURP full-length, myc-HURP N-terminal (1-201) (HURP-N), and myc-HURP C-terminal (201-846) (HURP-C) encoding constructs, respectively. Cells were then treated with (+) or without (-) leptomycin B (LMB, 0.4 ng/ml) for 40 min before fixation with paraformaldehyde, followed by Triton-X100 permeabilization. Cells were stained with anti-myc 9E10 antibody (red), and DNA was stained with DAPI (blue). Scale bar equals 10 μm.
(E) Immunoprecipitations with the anti-myc 9E10 antibody were performed on cell lysates from HEK293T cells transiently expressing myc-tagged HURP full-length, HURP-N (1-201), and HURP-C (201-846), respectively. Equal amounts of cell lysates and IPs were separated by SDS-PAGE and probed by Western blotting with anti-myc 9E10, anti-importin β, and anti-importin α antibodies, as indicated. HC indicates antibody heavy chains.
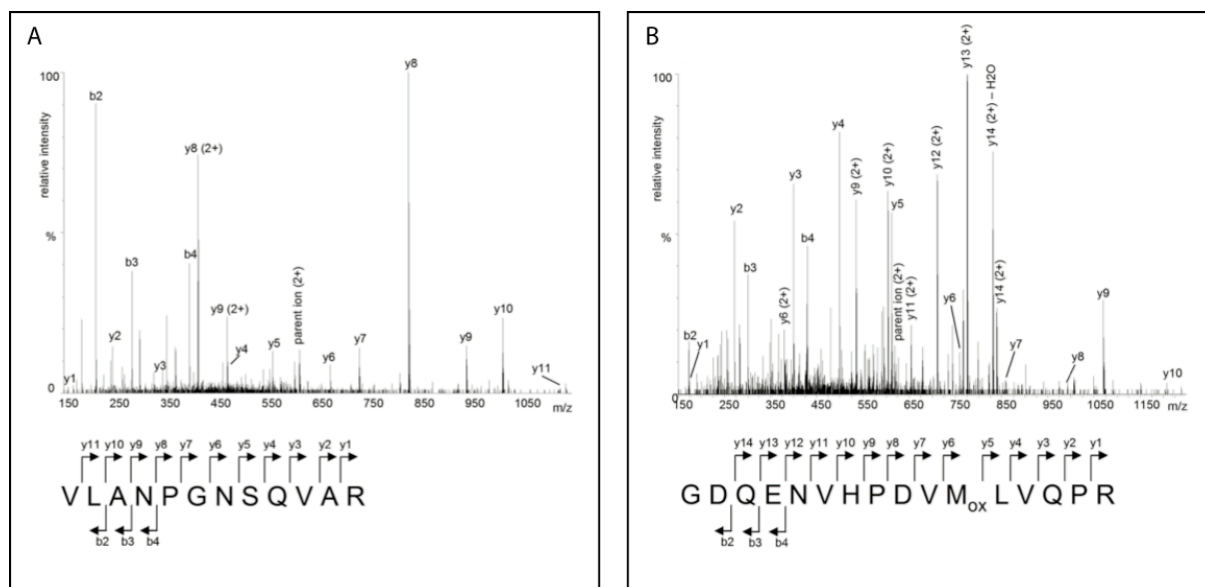
Figure 24. Identification of importin β by mass spectrometry
Collision-induced dissociation (CID) mass spectra of importin β (SWISS-PROT: Q14974)-derived peptides VLANPGNSQVAR (A) and GDQENVHPDVMoxLVQPR (B). C-terminal and N-terminal fragments of the peptides are marked as y-ions and b-ions, respectively, and (2+) denotes doubly charged ions. The observed peptide fragments are also marked within the peptide sequences below the spectra. Mox in (B) denotes oxidized methionine. Both spectra were acquired on a quadrupole time-of-flight mass spectrometer (Q-TOF Ultima, Waters, Manchester, UK).

Since the low amounts of HURP present in interphase cells were located primarily in the cytoplasm of both HeLa S3 and Cos 7 cells, we suspected that HURP might shuttle between the cytoplasm and the nucleus. To test this idea, cells were transfected with myc-tagged full-length HURP, as well as N- and C-terminal fragments, and then treated with leptomycin B (LMB), a drug that inhibits nuclear export via irreversible binding to the nuclear export factor Crm1 (Nishi et al., 1994). Whereas full-length myc-tagged HURP was predominantly cytoplasmic in untreated cells, it clearly accumulated in the nucleus after LMB treatment (Figure 23D). The N-terminal fragment of HURP (1-201) localized to the nucleus already in the absence of LMB, whereas the C-terminal fragment (201-846) localized to the cytoplasm, even in the presence of LMB (Figure 23D). This strongly suggests that HURP contains a nuclear localization signal (NLS) in the N-terminal domain and a nuclear exclusion signal (NES) in the C-terminal domain.

In support of this conclusion, co-immunoprecipitation experiments showed that importin β bound only to full-length HURP and the N-terminal fragment, but not to the C-terminal domain (Figure 23E). Interestingly, importin α could not be detected in any of these immunoprecipitates (Figure 23E), indicating that HURP binds directly to importin β. Together, these results indicate that Ran-regulated importin β transports HURP to the interphase nucleus through binding of an N-terminal NLS, but that HURP is also rapidly exported from the nucleus through a C-terminal NES, so that its steady-state distribution reflects the balance of import and export activities.

3.3.6   Importin β regulates the mitotic spindle localization and function of HURP

The interaction between HURP and importin β raised the intriguing possibility that the RanGTP pathway could regulate the function of HURP. To explore this hypothesis, myc-tagged HURP-importin β complexes were immunoprecipitated from cells and incubated with either recombinant RanQ69L, a Ran mutant locked in the GTP bound state that is known to displace cargo from importin β (Bischoff et al., 1994; Klebe et al., 1995; Ren et al., 1993), or with RanT24N, a nucleotide-free Ran mutant (Dasso et al., 1994; Klebe et al., 1995). As shown in Figure 25A, incubation with RanQ69L prompted the release of importin β from myc-HURP, whereas the

complex remained stable in the presence of RanT24N. Thus, the nucleotide state of Ran regulates the HURP-importin β interaction.

We also asked, whether importin β could regulate the MT bundling activity of HURP. Rhodamine-labeled MTs were incubated either with HURP only or with HURP together with an excess of importin β. Strikingly, the addition of importin β completely prevented the bundling of MTs by HURP (Figure 25B). Such an inhibition was not observed upon addition of a similar amount of importin α, indicating that it was specific for importin β (Figure 25B). The inhibitory action of importin β could be abolished by the addition of RanQ69L but not RanT24N (Figure 25B). Taken together, these data demonstrate that the Ran-importin β pathway can regulate the MT bundling function of HURP.
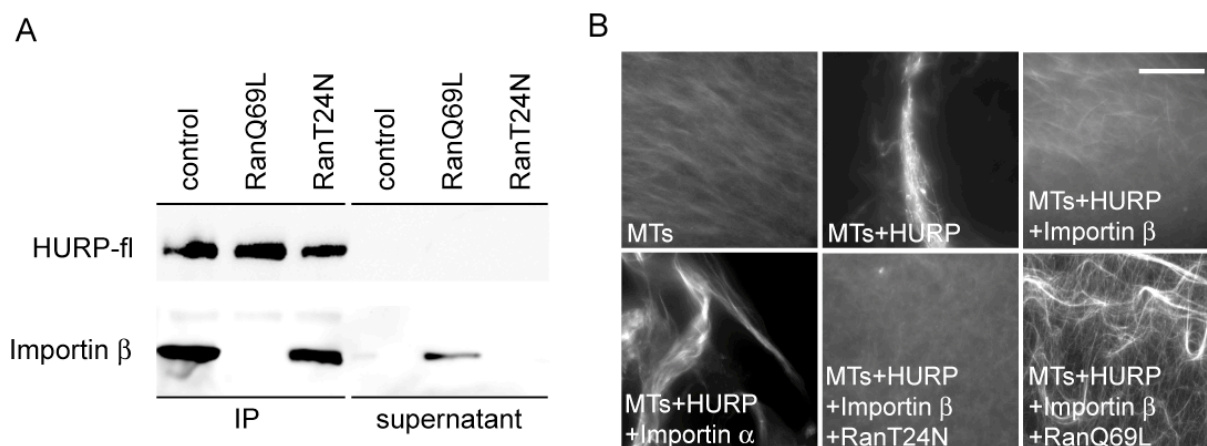
Figure 25. Regulation of HURP activity by the nucleotide state of Ran
(A) Myc-HURP-fl was transiently overexpressed in HEK293T cells, and the *in vivo* formed myc-HURP/importin β complex was purified with anti-myc 9E10 antibody beads. This bead bound complex was then incubated with recombinant RanQ69L, RanT24N, and buffer (control), respectively. After centrifugation, the amount of importin β bound to the myc-HURP beads and released into the supernatant was analyzed by Western blot analysis.
(B) MTs were produced *in vitro* with rhodamine-labeled tubulin. These MTs were then incubated with the indicated recombinant proteins for 5 min at RT before immunofluorescence microscopy was carried out. Scale bar equals 10 μm.

Finally, two types of experiments were carried out to demonstrate a critical role for the Ran-importin β pathway in the regulation of HURP *in vivo*. First, we analyzed the localization of HURP in Cos 7 cells after transient transfection of myc-tagged importin β or mutant Ran proteins. Transfected cells entered mitosis with bipolar spindles, indicating that interference with interphase nuclear transport was not a concern over the time course of these experiments. HURP association with the

mitotic spindle was strongly diminished in the presence of excess myc-importin β (Figure 26A), indicating that importin β negatively regulates HURP interaction with the spindle. Furthermore, the spindle association of HURP was strongly diminished, upon overexpression of myc-RanT24N, which acts as an inhibitor of RCC1 (Klebe et al., 1995), but enhanced when RanQ69L was overexpressed (Figure 26A). Under these latter conditions, HURP also localized to the spindle poles, confirming that the precise localization of HURP is sensitive to RanGTP levels.

In a second, complementary experiment, we examined HURP localization in tsBN2 cells. These cells harbor a temperature-sensitive RCC1 protein (the sole GEF for Ran), so that their incubation at the restrictive temperature (39°C-40°C) results in rapid proteolysis of RCC1 (Nishitani et al., 1991). Upon incubation of these cells at the restrictive temperature, HURP association with the spindle diminished progressively and was clearly decreased by 4 hr (Figure 26B). Taken together, these results demonstrate that the Ran-importin β pathway controls HURP localization to the mitotic spindle *in vivo*.
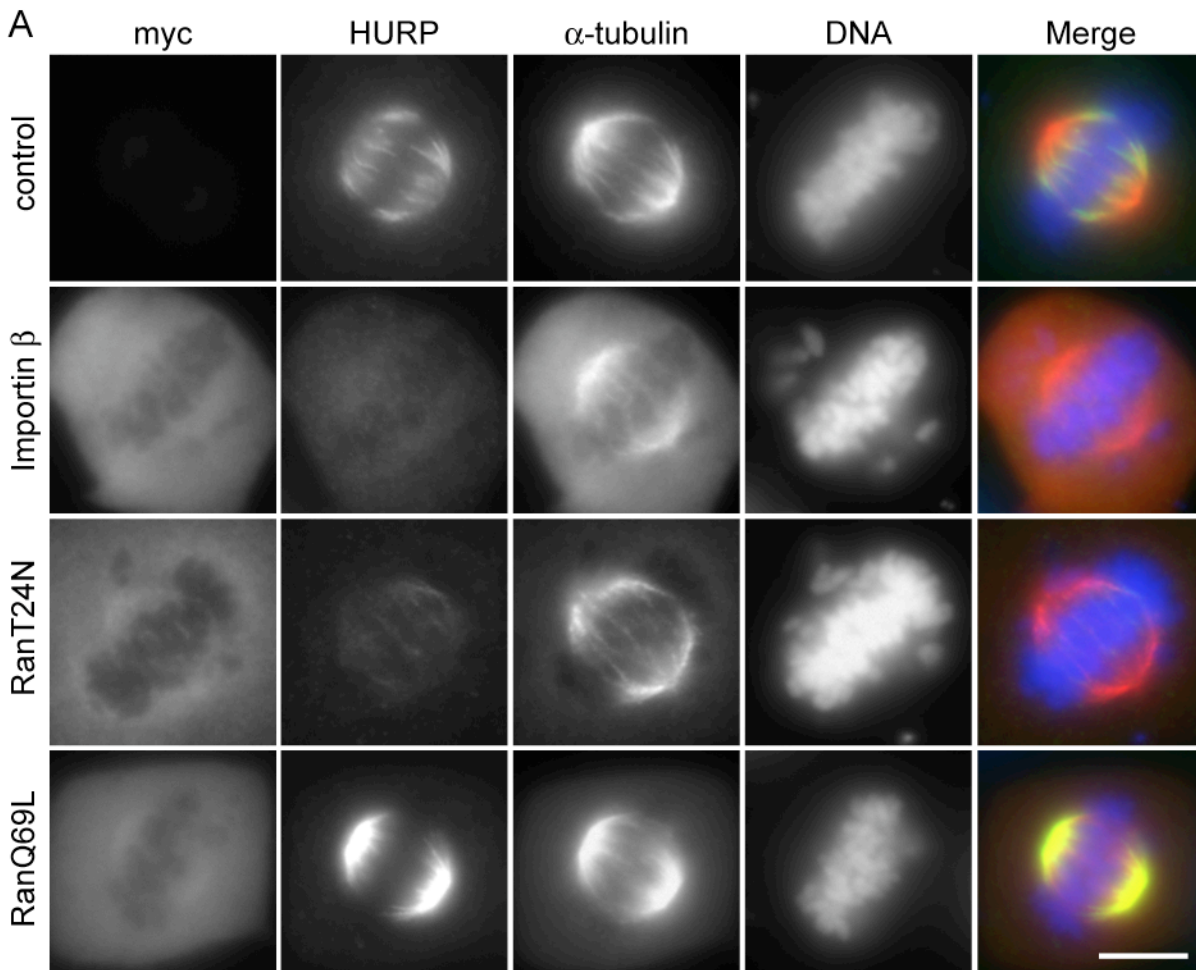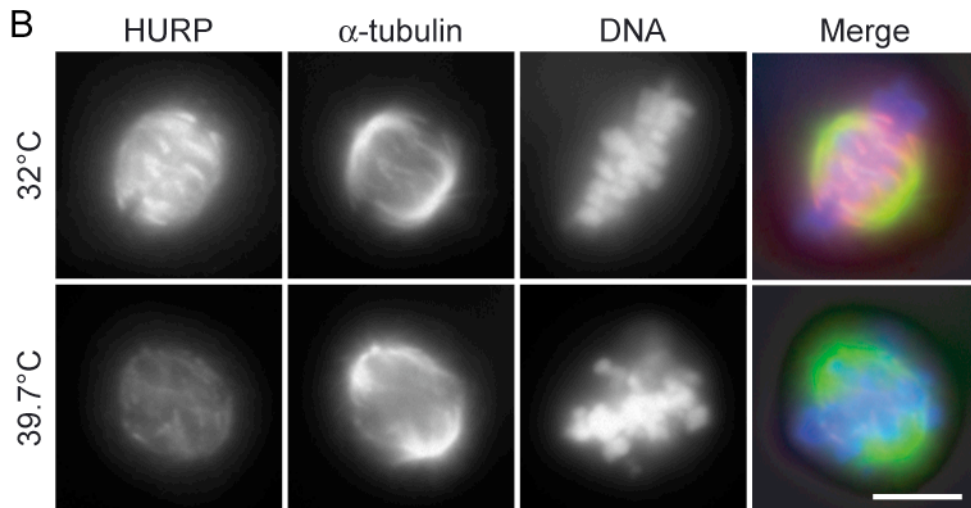
Figure 26. Regulation of HURP localization by the Ran-importin β pathway
(A) Myc-tagged importin β, RanT24N, and RanQ69L, respectively, were transiently overexpressed for 24 hr in Cos 7 cells. After fixation and permeabilization with PTEMF, cells were stained with anti-myc 9E10 (far red), anti-HURP (green), and anti-α-tubulin antibodies (red), and DNA was stained with DAPI (blue). At the right, merged images are shown with HURP in green, α-tubulin in red, and DNA in blue. The top row shows a control spindle in a nontransfected cell.
(B) Temperature-sensitive tsBN2 cells (normally grown at 32°C) were incubated for 4 hr at either the permissive temperature (32°C) or the restrictive temperature (39.7°C). Cells were then fixed and permeabilized with PTEMF and stained with anti-HURP (red) and anti-α-tubulin (green) antibodies and DNA was stained with DAPI (blue). Scale bars equal 10 μm.

3.4 How is HURP specifically localized to K-fibers?

3.4.1 Structure-function analysis of different HURP-domains

To better understand how the localization of HURP to kinetochore microtubules is controlled, we carried out a structure-function analysis, focusing on different HURP-domains. Based on the primary structure (Figure 14), we designed myc-tagged HURP fragments for mammalian expression and His-tagged HURP fragments for recombinant expression, to study their effects on microtubule stability (Table 1). In order to determine their subcellular localization, the different myc-tagged HURP fragments (fl: 1-846, N2: 1-201, N3: 1-404, N6: 1-505, C2: 202-846) were expressed for 48 hr in HeLa S3 cells, fixed with paraformaldehyde (PFA) and analyzed by microscopy, using the Deltavision instrument (Figure 27). Whereas the full-length protein (fl: 1-846) localized to kinetochore microtubules in the vicinity of the chromosomes and was typically excluded from the poles (Figure 27, top), the HURP fragments lacking the C-terminus (N6: 1-505, and to greater extent N3: 1-404) displayed an increased staining over the entire spindle (Figure 27, middle). The N-terminus of HURP (N2: 1-201) even, accumulated in proximity to the spindle poles, while the C-terminus (C2: 202-846) did not localize to the mitotic spindle at all (Figure 27, bottom). These observations show that the C-terminus, including the GKAP domain is important for localizing HURP to the plus ends of K-fibers, although the N-terminus appears to be necessary for the initial spindle targeting of the protein. During interphase, the N-terminal fragments (N2: 1-201 and N3: 1-404) accumulated in the nucleus, although the longer N-terminus (N3: 1-404) was also found on cytoplasmic MTs (Figure 27, middle-bottom). In contrast, the C-terminus (C2: 201-846) and the full-length (fl: 1-846) protein localized to the cytoplasm (Figure 27, top and bottom). This indicates that HURP may have an NES at around aa 400-550. Although we identified many conserved leucine residues in this region, we have not been successful to map the exact NES site (Appendix: Alignment C, NetNES) (la Cour et al., 2004).
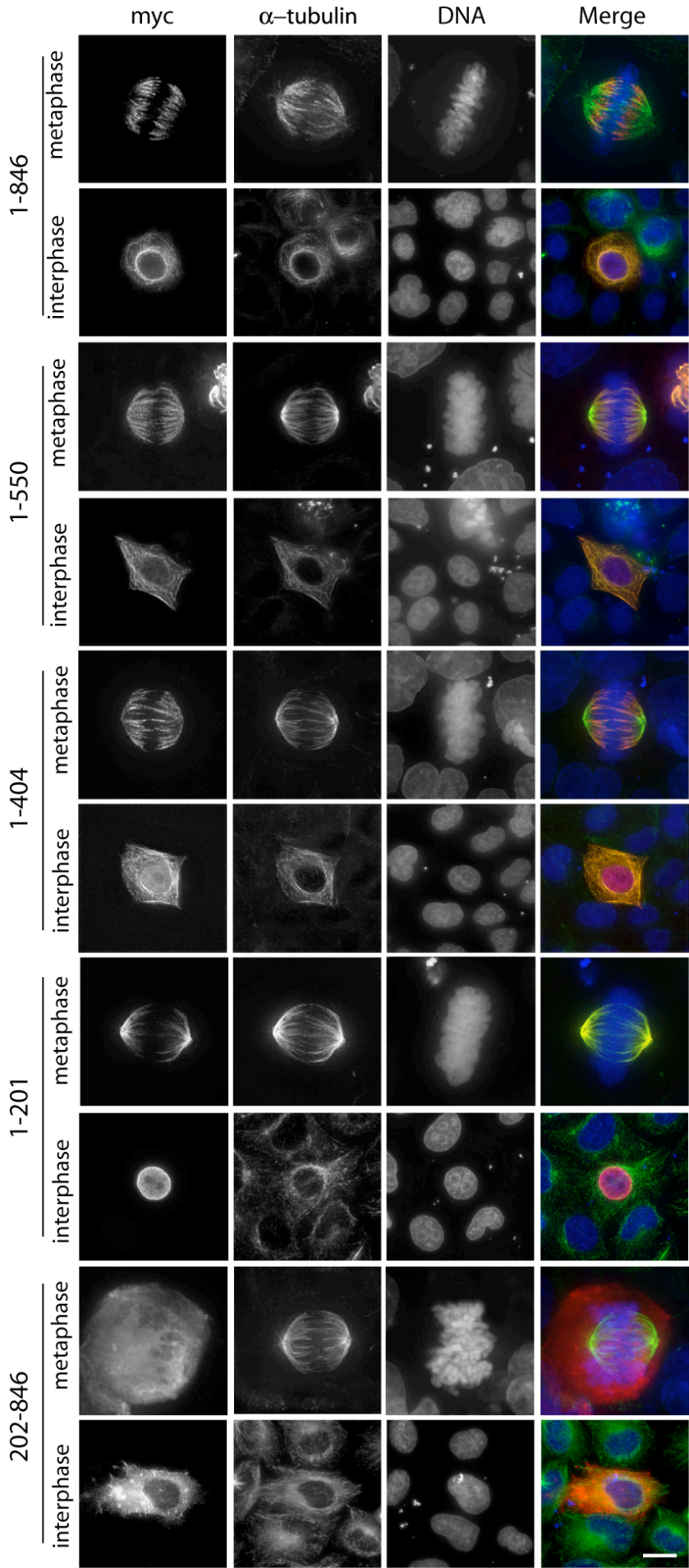
Figure 27. A C-terminal region of HURP (aa 300-600) is necessary for KMT plus end targeting
HeLa S3 cells were transiently transfected for 48 hr with myc-tagged HURP fragments (fl: aa 1-846, N6: aa 1-550, N3: aa 1-404, N2: aa 1-201 and C2: aa 202-846). Afterwards, cells were fixed with PFA followed by permeabilization with Triton-X100. Cells were probed with anti-myc 9E10 antibody (red), anti-α-tubulin antibody (green), and DNA was stained with DAPI (blue). Scale bar is 10 μm.

45

3.4.1.1 The coiled coil regions are necessary to load HURP onto the spindle MTs

As we have shown, HURP directly binds and bundles MTs *in vitro* (Sillje et al., 2006). Other MT stabilizing proteins perform this function either by oligomerization, as for example NuMA (Haren and Merdes, 2002), or have several MT binding sites like TOGp, the human homolog of XMAP215 (Spittle et al., 2000).

To test whether HURP dimerizes, FLAG- and myc-tagged full-length-, N-terminal- (1-404) and C-terminal- (405-846) HURP fragments were produced by *in vitro* coupled transcription translation (IVT) and tested for their ability to interact by co-immunoprecipitation (Figure 28). As a positive control, we used FLAG- and myc-tagged CHICA, and as a negative control, we used myc-tagged Salvador, that has previously been shown to be monomeric (Chan et al., 2005). The constructs were co-immunoprecipitated in different combinations, using anti-myc and anti-FLAG antibody-coated beads, respectively. As observed in our laboratory previously, myc- and FLAG-tagged CHICA co-immunoprecipitated, demonstrating dimerization, whereas Salvador did not (Figure 28). In contrast, neither full-length HURP, nor the N- or C-terminus co-immunoprecipitated under these conditions, suggesting that HURP does not dimerize despite the presence of 2 coiled coil domains.
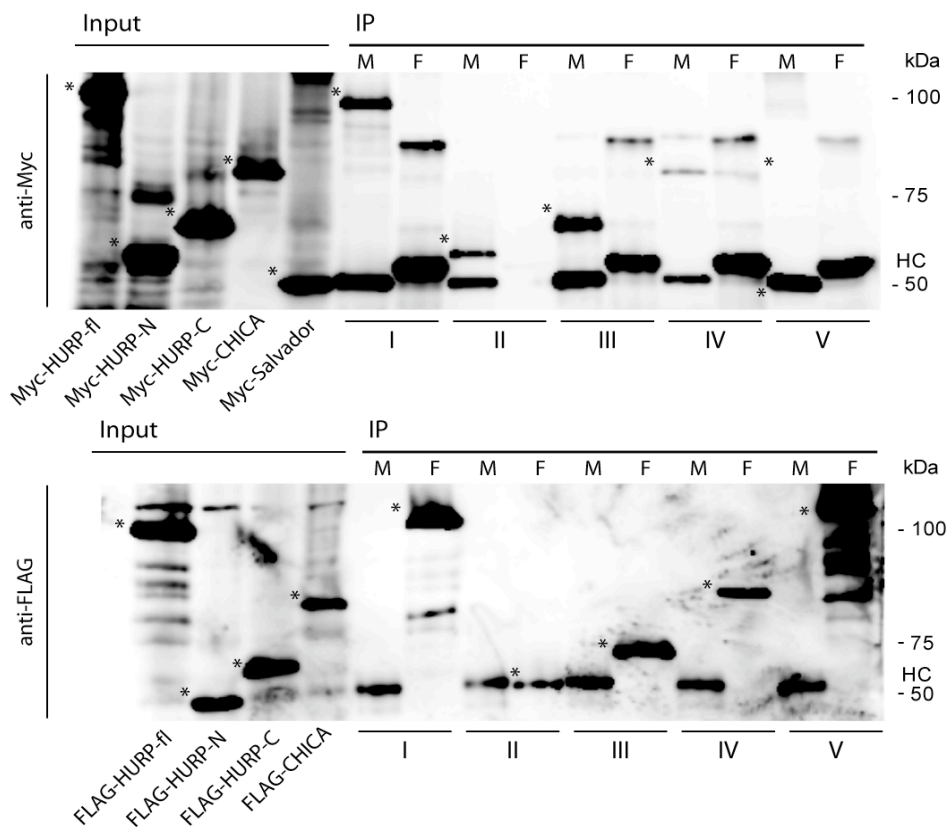
Figure 28. HURP does not dimerize in the IVT lysate
Myc- and FLAG-tagged full-length (1-846), N-terminal (1-404) and C-terminal (405-846) HURP and myc- and FLAG-tagged CHICA (positive control), as well as myc-tagged Salvador (negative control) were generated by *in vitro* coupled transcription translation (IVT) and co-immunoprecipitated with anti-myc- (M) and FLAG- (F) beads, respectively in the following combinations I: myc-HURP-fl + FLAG-HURP-fl II: myc-HURP-N + FLAG-HURP-N III: myc-HURP-C + FLAG-HURP-C IV: myc-CHICA-fl + FLAG-CHICA-fl V: myc-Salvador-fl + FLAG-HURP-fl. The complexes were separated by 7.5% SDS-PAGE and probed by Western blotting with anti-myc 9E10 and anti-FLAG antibodies. Stars (*) indicate relevant bands and HC indicates antibody heavy chain.

Next, we analyzed potential MT binding sites, focusing on the N-terminus of HURP because the C-terminus did not localize to MTs *in vivo*, as shown by immunofluorescence microscopy (Figure 27). To this end, different N-terminal HURP fragments (N1: 1-116, N2: 1-201, N3: 1-404, N5: 1-150, and N7: 60-150) were purified from *E.coli* and cleared by ultracentrifugation. To analyze which parts of HURP directly bind to microtubules, these fragments were subsequently used in a MT co-sedimentation assay. Specifically, the recombinant HURP fragments, or BSA as a negative control, were incubated with or without taxol-stabilized MTs and centrifuged through a glycerol cushion (Figure 29A).

In the presence of MTs, all of the recombinant protein representing the different fragments was recovered in the pellet fraction, whereas at least half (N3: 1-404, N2: 1-201, N5: 1-150, and N1: 1-116), if not most, of the protein (N7: 60-150) was found in the supernatant in the absence of MTs. As a control, similar amounts of BSA remained in the supernatant, independent of the presence of MTs (Figure 29A). This suggests that all N-terminal HURP fragments analyzed were able to directly bind MTs *in vitro*. One interpretation of this result is that HURP has several MT binding sites within the N-terminus, which may include the N-terminal coiled coil domains.

Since coiled coil domains are often involved in protein-protein interactions (Burkhard et al., 2001), we focused on these HURP domains (CC1: aa 22-42 and CC2: aa 94-120), in order to investigate which protein regions are involved in the initial loading of HURP onto the spindle MTs. Different myc-tagged fragments of the HURP N-terminus were expressed in HeLa S3 cells for 48 hr and analyzed by immunofluorescence microscopy (Figure 29B). The HURP fragments analyzed comprised either both coiled coil domains (N2: 1-201) or the first and part of the second (N1: 1-116), or only the second coiled coil domain (N7: 60-150).
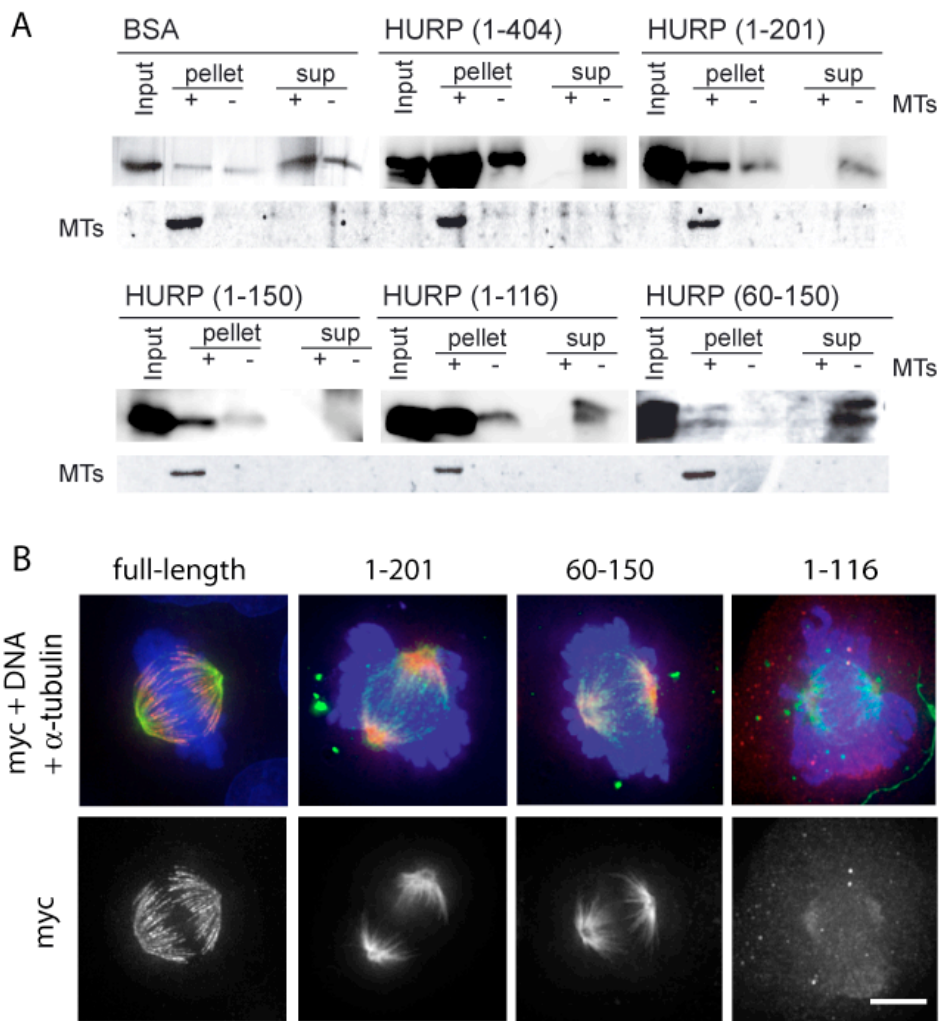
Figure 29. The N-terminus of HURP binds to MTs *in vitro* and *in vivo*
(A) The following recombinant HURP fragments: N1: 1-116, N2: 1-201, N3: 1-404, N5: 1-150, and N7: 60-150, were purified from *E. coli* and mixed with *in vitro* produced microtubules (+MTs), or as a control with buffer (-MTs). BSA was used as negative control. Subsequently, these samples were spun through a glycerol cushion and the supernatant (sup), and pellet fractions were separated by SDS-PAGE and probed by Western blotting with anti-HURP antibody. BSA and the presence of MTs were analyzed by Coomassie blue staining of the SDS-PAGE gels.
(B) HeLa S3 cells were transiently transfected for 48 hr with the following myc-tagged HURP fragments: full-length: 1-846, N1: 1-116, N2: 1-201, and N7: 60-150. Afterwards, cells were directly permeabilized and fixed with PTEMF and stained with anti-myc 9E10 antibody (red), anti-α-tubulin antibody (green), and DNA was stained with DAPI (blue). Scale bar equals 10 μm.

As shown before, the full-length protein, concentrated on the KMT plus ends, although it sometimes spreads more along the spindle MTs than endogenous HURP, depending on the overexpression levels (Figure 29B, left). In contrast, the N-terminal HURP fragment including both coiled coil regions (N2: 1-201), accumulated on the spindle pole caps, and similar results were obtained with a construct lacking the far N-terminus, but including the second coiled coil region (N7:

60-150). However, the fragment with the first and only part of the second coiled coil domain (N1: 1-116) did not localize to the spindle at all, but rather showed a diffuse pattern throughout the cytosol (Figure 29B, right). Having shown above that all N-terminal fragments were able to directly bind MTs *in vitro* (Figure 29A)*,* this latter observation was surprising. Together the above results suggest that the region spanning residues 60-150, including the second coiled coil domain, is essential to target HURP to the mitotic spindle *in vivo*. In contrast to the full-length protein, overexpression of the N-terminal fragments caused chromosome congression defects in some cells (Figure 29B), which may be an indirect effect of the mislocalized HURP fragments.

3.4.1.2 Both coiled coil regions of HURP are essential to stabilize MTs

As the N-terminus of HURP appears to be required for MT binding and spindle targeting, we next asked which one of the coiled coil domains are involved in the MT stabilizing function of HURP. The recombinant N-terminal HURP fragments described above were incubated with rhodamine-labeled MTs and MT bundling was analyzed by immunofluorescence microscopy (Figure 30A). As described before, the addition of full-length HURP (fl: 1-846) resulted in strong bundling of the fibers, which otherwise appeared faintly stained in the presence of buffer or BSA (Sauer et al., 2005). A similar stabilization effect was observed with the HURP N-terminal fragments (N5: 1-150, N2: 1-201, and N3: 1-404), which include both coiled coil domains. The thickest fibers were induced by the addition of the N-terminal fragment 1-404, which also contains part of the GKAP domain of HURP (GKAP: aa 310-607). These MT bundles were resistant to prolonged cold treatment (16 hr), similar to the MT fibers formed in the presence of full-length HURP (Figure 30A, top/right). In contrast, a shorter N-terminal fragment (N1: 1-116), with a deficient second coiled coil domain, as well as the N-terminal fragment lacking the first coiled coil region (N7: 60-150), did not have an effect on MT stability (Figure 30A, left), similar to BSA which served as negative control (Figure 30A, bottom/right).

From these observations we conclude that the N-terminus of HURP (1-150) is able to bundle MTs *in vitro*. Whereas both coiled coil regions of HURP (CC1: aa 22-42; CC2: aa 94-120) are essential for this function, the amino acids downstream of these domains (120-404) may contribute to further MT stabilization.

RESULTS
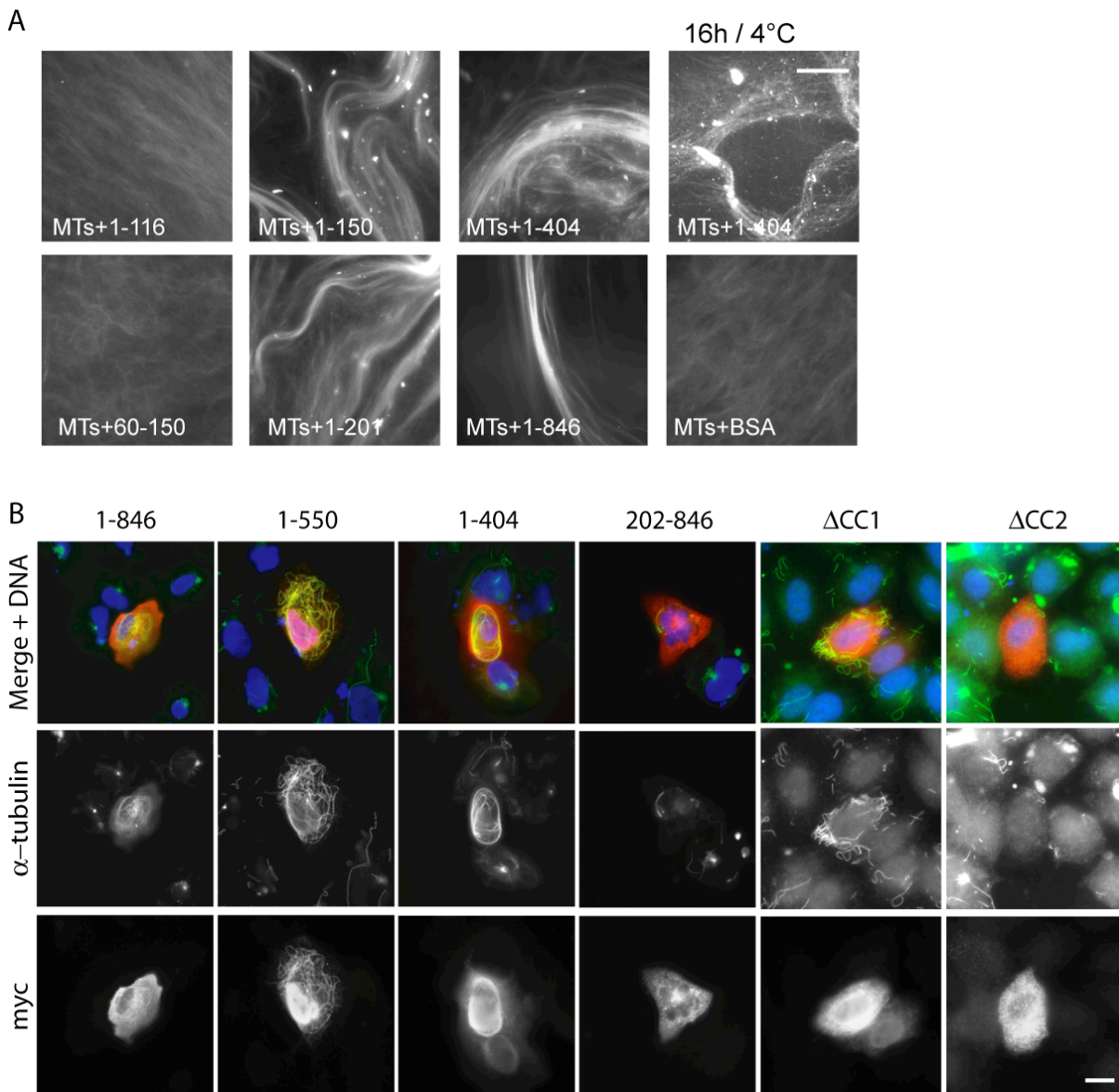
Figure 30. The N-terminus of HURP bundles MTs *in vitro* and *in vivo*

(A) MTs were polymerized *in vitro* from rhodamine-labeled tubulin. These MTs were then incubated with full-length recombinant HURP (fl: 1-846), N-terminal HURP fragments (N1: 1-116, N7: 60-150, N5: 1-150, N2: 1-201, N3: 1-404) and BSA, as a negative control, respectively. Immunofluorescence microscopy was carried out either after 5 min incubation at RT or after 5 min incubation at RT, followed by a 16 hr incubation at 4°C (top right). Scale bar equals 10 μm.

(B) HeLa S3 cells were transiently transfected for 48 hr with the following myc-tagged HURP constructs: fl: 1-846, N6: 1-550, N3: 1-404, C2: 202-846, ΔCC1: 60-846, and ΔCC2: 1-88+120-846. Afterwards, cells were incubated at 4°C for 30 min and fixed with PFA followed by permeabilization with Triton-X100. Then, cells were stained with anti-myc 9E10 antibody (red), anti-α-tubulin antibody (green), and DNA was stained with DAPI (blue). Scale bar equals 10 μm.

In order to investigate the contribution of the HURP domains to the MT stability in cells, we performed a MT-depolymerizing assay by cold treatment of HeLa S3 that have previously been transfected with different constructs encoding myc-tagged HURP fragments. We analyzed N- and C-terminal fragments of HURP (N6: 1-550, N3: 1-404, and C2: 202-846) that localize to the cytoplasm in interphase

50

cells, as shown by IF (Figure 27), and compared these with constructs lacking the first (ΔCC1: 60-846) or the second coiled coil region (ΔCC2: 1-88+120-846) (Figure 30B). Consistent with our *in vitro* results, cold-stable MT bundles were induced only when the full-length protein (fl: 1-846) or the N-terminal fragments (N5: 1-550, and N3: 1-404), including both coiled coil domains, were expressed at high levels (Figure 30B, left). In contrast, the overexpression of the C-terminus (C2: 202-846), as well as the HURP constructs lacking one of the coiled coil domains (ΔCC1 and ΔCC2), did not influence MT stability (Figure 30B, middle and right). Altogether, these results indicate that the HURP N-terminus is able to stabilize MTs *in vitro* and *in vivo,* and that the coiled coil domains play an important role in this process.

The results of our structure-function study of the different HURP domains are summarized below (Table 1). The Table shows that the two N-terminal coiled coil domains of HURP are involved in the binding and bundling of MTs and are also essential for the initial spindle loading of HURP. However, the C-terminus that contains the GKAP domain is required for the specific targeting of HURP to the MT plus ends.

HURP plasmids	Mitosis		Interphase		MT binding	MT stabilization		Importin ß binding
	Spindle plus ends	Spindle poles	Cytoplasm	Nucleus	*in vitro*	*in vitro*	*in vivo*	
fl HS268	+	-	+	-	+	+	+	+
N6 HS308	+	-	+	-	n.d.	+	+	n.d.
N3 HS291	+/-	+/-	-	+	+	+	+	n.d.
N2 HS295	-	+	-	+	+	+	n.d.	+
N5 HS307	-	+	-	+	+	+	n.d.	+
N1 HS304	-	-	-	+	+	-	n.d.	+
N4 HS310	-	+	-	+	n.d.	n.d.	n.d.	+
N7 HS309	-	+	+	+	+	-	n.d.	+
C2 HS296	-	-	+	-	n.d.	n.d.	-	-
C1 HS290	-	-	+	-	n.d.	-	-	n.d.
CC1 SN25	-	-	NE	+	n.d.	n.d.	n.d.	+
ΔCC1 SN20	-	+	+	-	n.d.	n.d.	-	-
ΔCC2 SN26	-	-	+	-	n.d.	n.d.	-	+/-
NLSIA SN21	-	+	+	-	n.d.	n.d.	+/-	+
NLSIB SN22	-	+	+	-	n.d.	n.d.	+/-	+

Table 1. Summary of results from the structure-function analysis of different HURP-domains
The Table shows the primary structures of the different N-and C-terminal HURP fragments that have been generated and analyzed with regard to their mitotic and interphase localization, their MT binding and stabilization capability, as well as their binding to importin β. Positive results are indicated with +, negative results with -, n.d. means not determined, NE = nuclear envelope.

3.4.2   Identification of the importin β binding site within the HURP N-terminus

As described above, the N-terminus (1-201) of HURP binds to importin β and this interaction is required for its nuclear localization. Proteins that interact with importin β classically do so via an NLS sequence (R/H/KX$_{(2-5)}$PY) (Chook and Blobel, 2001; Lee et al., 2006). We therefore performed a sequence analysis of HURP to predict the residues required for its interaction with importin β. Although this analysis revealed several clusters of conserved basic residues within the N-terminus of HURP (Appendix: Alignment A), none matched the typical NLS-consensus sequence. Furthermore, this protein area contains the two predicted coiled coil domains (as described above), which play an important role in spindle targeting and the MT bundling function of HURP.

In order to determine the exact importin β binding site on HURP, mutations in conserved basic clusters were analyzed. To this end, selected lysine and arginine residues were changed to alanine (NLSIA: R9A/R11A/K12A, NLSIB: R26A/K27A, NLSIIA: R90A/K91A, NLSIIB: K112A/K114A/R115A). Co-immunoprecipitation analysis of these mutants and the previously described constructs, lacking one of the two coiled coil domains (ΔCC1 and ΔCC2), showed that the capability of HURP to bind importin β is slightly decreased in the construct without the second coiled coil domain (ΔCC2), and completely lost when the first coiled coil region (ΔCC1) is removed (Figure 31A). The fragment containing only residues 1-60 (CC1) was present in the nucleus, upon overexpression in HeLa S3 cells, and did not localize to the mitotic spindle (Figure 31B), unlike the larger N-terminal fragment (N2: 1-201), described above. However, in interphase cells this HURP fragment (CC1) colocalized with importin β on the nuclear envelope, which indicates that the far N-terminus of HURP indeed interacts with importin β. The importin β binding abilities of the mutated N-terminal fragments were also analyzed by treatment with LMB, a nuclear export inhibitor (Figure 32). Cells were transfected with the potential NLS-mutants (HURP-NLSIA, HURP-NLSIB, HURP-NLSIIA, HURP-NLSIIB, HURPΔCC1, and HURPΔCC2), as well as wild-type (WT) HURP as control, and then treated with LMB for 40 min. Wild-type myc-tagged HURP, as well as the NLS point mutants (HURP-NLSIA, HURP-NLSIB, HURP-NLSIIA & HURP-NLSIIB) accumulated in the nucleus after LMB treatment. However, the construct without the second

coiled coil (HURPΔCC2) was found in the cytoplasm, in 50% of the cells and the fragment lacking the first coiled coil (HURPΔCC1) remained in the cytoplasm even in the presence of LMB. This demonstrated that the nuclear import of these HURP constructs was impaired, which indicates that the NLS was at least partially disrupted in the first case and completely lost upon removal of the first 60 residues. However, selected mutations in the basic clusters of the HURP sequence were not sufficient to affect the nuclear import.
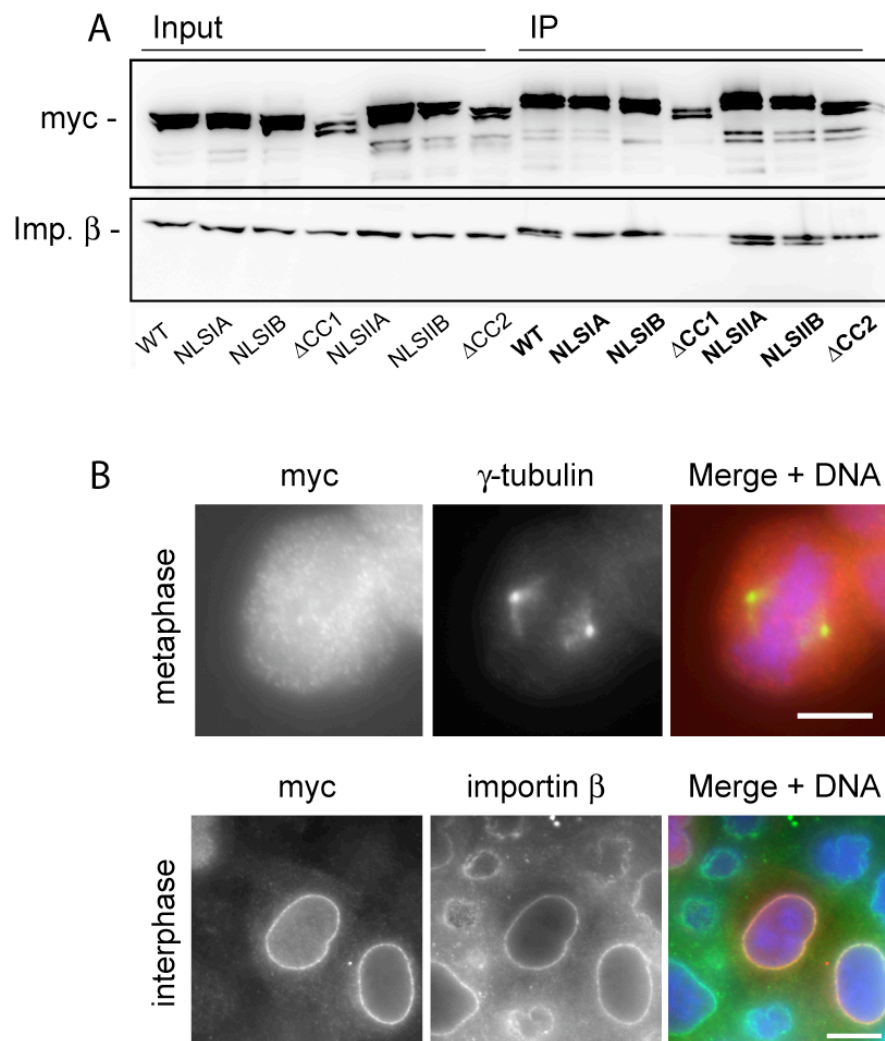
Figure 31. The far N-terminus of HURP interacts with importin β
(A) Immunoprecipitations with the anti-myc 9E10 antibody were performed on cell lysates from HEK293T cells transiently expressing myc-tagged HURP constructs: HURP-WT, HURP-NLSIA, HURP-NLSIB, HURP-ΔCC1, HURP-NLSIIA, HURP-NLSIIB and HURP-ΔCC2, respectively. Equal amounts of cell lysates and IPs were separated by SDS-PAGE and probed by Western blotting with anti-myc 9E10 and anti-importin β antibodies, as indicated.
(B) HeLa S3 cells were transiently transfected for 48 hr with myc-HURP-CC1 (1-60) and directly permeabilized and fixed with PTEMF. Cells were stained with anti-myc 9E10 (red), and anti-γ-tubulin or anti-importin β antibodies (green), respectively. DNA was stained with DAPI (blue). Scale bar equals 10 μm.
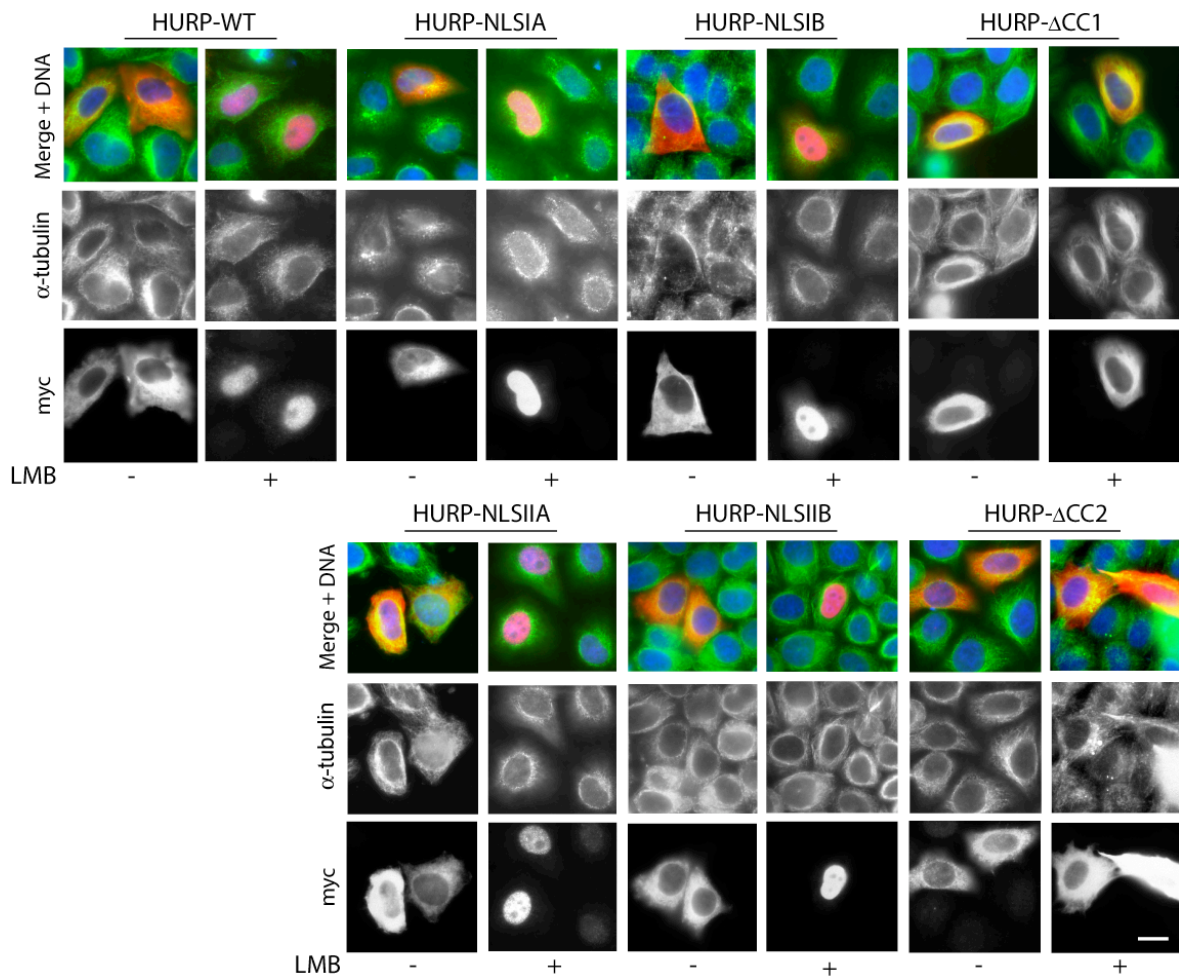
Figure 32. The NLS mutants of HURP are insensitive to LMB
HeLa S3 cells were transiently transfected for 48 hr with myc-tagged HURP constructs as follows: HURP-WT, HURP-NLSIA, HURP-NLSIB, HURP-ΔCC1, HURP-NLSIIA, HURP-NLSIIB and HURP-ΔCC2. Cells were then treated with (+) or without (-) LMB (0.4 ng/ml) for 40 min, before fixation with PFA followed by Triton-X100 permeabilization. Cells were stained with anti-myc 9E10 (red) and anti-α-tubulin antibodies (green). DNA was stained with DAPI (blue). Scale bar = 10 μm.

The results from the study of the interaction between different N-terminal HURP mutants and importin β demonstrate a requirement for HURP's coiled coil domains, in particular CC1 (aa: 1-60). Hence, the NLS of HURP is most likely found within the first 60 amino acids. However, selected point mutations within this area (HURP-NLSIA and HURP-NLSIB) did not disrupt the interaction of HURP with importin β, which suggests that binding can occur via different basic patches. Interestingly, not only the importin β binding ability, but also the spindle localization was affected in these mutants (Figure 33A). In contrast to full-length myc-tagged HURP that localized to the KMT plus ends, as reported earlier (Sillje et al., 2006) (Figure 33A, left), myc-tagged HURPΔCC1 was only present at the spindle pole (Figure 33A, middle) and myc-tagged HURPΔCC2 was mostly displaced from the spindle altogether (Figure 33A, right). Moreover, HURP-NLSIA and HURP-NLSIB were

54

displaced to the spindle pole caps, although importin β binding was not affected in these cases, suggesting that these domains might also play an important role in the initial spindle targeting of the protein. This is in line with the finding that although the MT bundling activity of HURP is inhibited by importin β, HURP is still able to bind MTs in the presence of importin β in MT co-sedimentation assays (Figure 33B).

Taken together, the results from the NLS mutagenesis and the previous structure-function analysis of the different HURP domains demonstrate a requirement for the coiled coil domains in the spindle localization of HURP, importin β binding and MT stabilization capability. Furthermore, our observations suggest that importin β binding to one of the two coiled coil domains still allows the spindle association of HURP, although the MT bundling capability is inhibited.
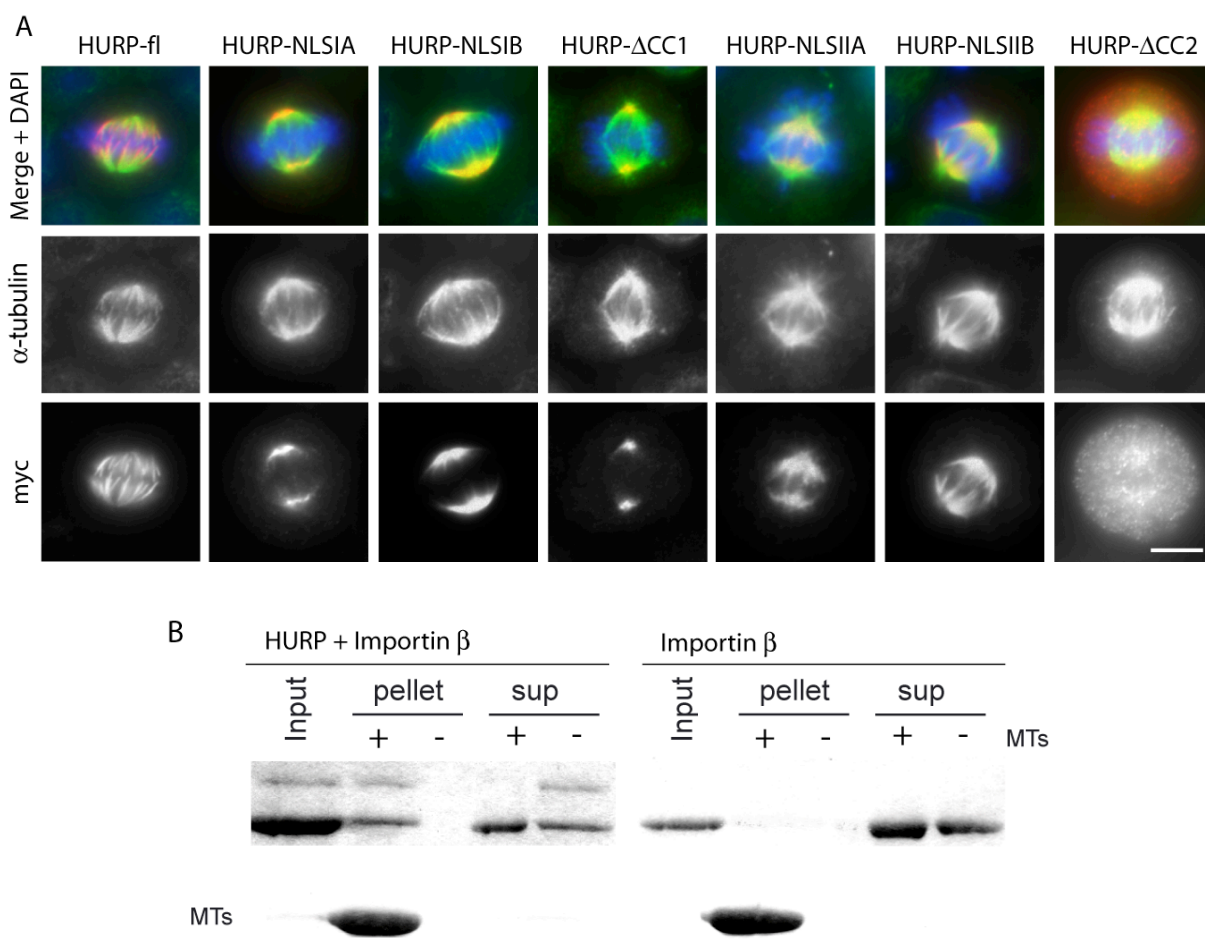
Figure 33. The spindle localization of the NLS mutants of HURP is aberrant
(A) HeLa S3 cells were transiently transfected for 48 hr with myc-tagged HURP constructs: HURP-WT, HURP-NLSIA, HURP-NLSIB, HURP-ΔCC1, HURP-NLSIIA, HURP-NLSIIB and HURP-ΔCC2. Cells were directly permeabilized and fixed with PTEMF and then stained with anti-myc 9E10 (red) and anti-α-tubulin antibodies (green). DNA was stained with DAPI (blue). Scale bar = 10 μm.
(B) Purified recombinant HURP and importin β were mixed with microtubules (+MTs), or buffer (-MTs) as a control. The samples were spun through a glycerol cushion and the supernatant and pellet fractions were analyzed for HURP and importin β by Coomassie blue staining of SDS-PAGE gels.

3.4.3 Regulation of HURP by phosphorylation

The function of most mitotic proteins is regulated by phosphorylation. HURP itself has been reported to be phosphorylated by Aurora-A and Cdk1 (Hsu et al., 2004; Yu et al., 2005). In order to search for new mitosis-specific phosphorylation sites of HURP, a spindle preparation was carried out. Endogenous HURP was immunoprecipitated from the purified spindles and analyzed by MS, after phosphopeptide enrichment via immobilized metal ($Fe3+$) affinity chromatography (IMAC) (Andersson and Porath, 1986). Thus, phosphorylation of a conserved TP-site was identified at T330, within the GKAP domain of HURP. This site has been proposed before to be phosphorylated by Cdk1, as a prerequisite for HURP degradation by the SCF complex (Hsu et al., 2004). As demonstrated by overexpression of the different HURP fragments described above, we identified the GKAP domain as important for targeting HURP to the K-fibers. To better understand whether phosphorylation plays a role in this process, myc-tagged alanine (A) and asparagine (D) mutants were generated of the predicted Cdk1 phosphorylation site (HURP-WT, HURP-T330A and HURP-T330D) and studied in HeLa S3 cells. The detailed immunofluorescence analysis of these cells showed that the phosphorylation site mutant HURP-T330A localized along the entire spindle, whereas the myc-tagged HURP-WT was concentrated at the MT plus end region (Figure 34A). Interestingly, the phosphomimic mutant HURP-T330D behaved like the wild-type protein. To quantify these results, the myc-fluorescence signals of 5 representative cells were measured from pole-to-pole and plotted in a histogram (Figure 34B). As inferred from these fluorescence intensities, the signal of cells overexpressing HURP-WT and HURP-T330D had two peaks (arbitrary units = 100) (Figure 34B, top and bottom), approximately 4-5 μm away from each pole. Furthermore, the myc-signal decreased to half of its maximum intensity (arbitrary units = 50) already 2-3 μm away from the poles, which confirmed the concentration of myc-tagged HURP-WT and HURP-T330D at the MT plus ends. In contrast, the myc-signal of cells overexpressing HURP-T330A decreased to its half maximum fluorescence intensity less than 1 μm away from the poles and most of these cells had their fluorescence maxima at a distance of approximately 3-5 μm from each pole (Figure 34B,middle), indicating that the myc-signal of this HURP

phosphorylation site mutant (T330A) spreads further towards the spindle poles. In conclusion, these data suggest that Cdk1 phosphorylation may contribute to regulate the localization of HURP along the spindle.
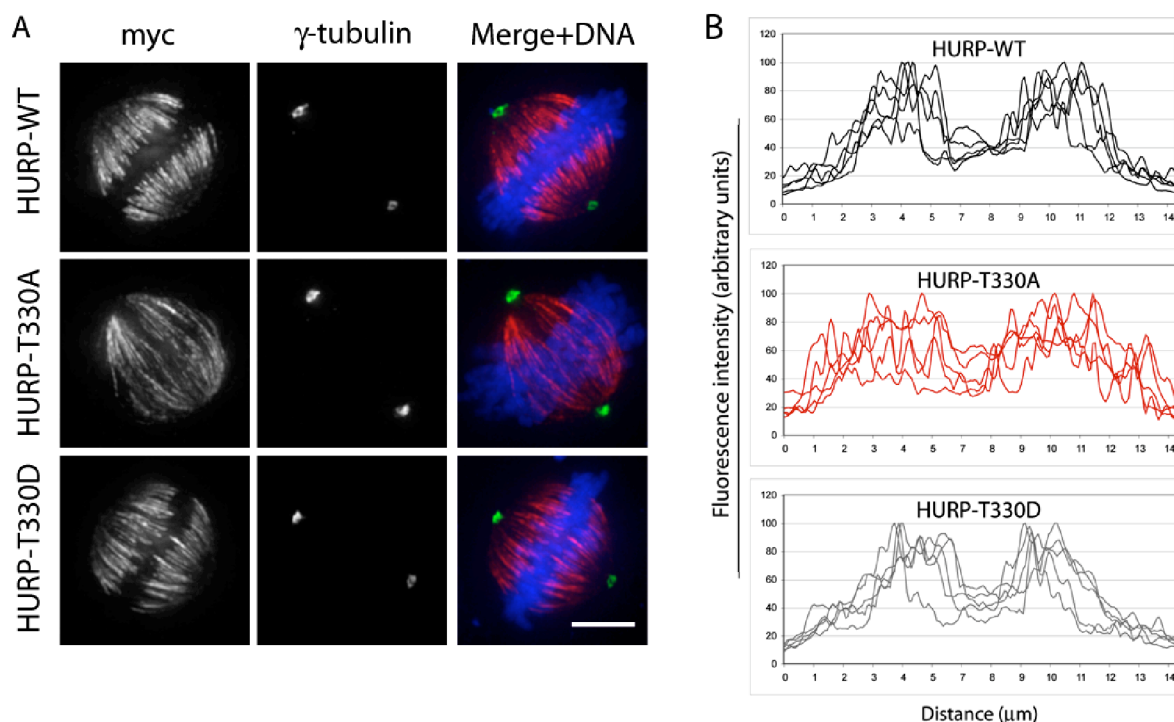
Figure 34. HURP-T330A spreads over the spindle MTs
(A) HeLa S3 cells were transiently transfected for 48 hr with constructs encoding myc-HURP-WT, myc-HURP-T330A and myc-HURP-T330D, respectively. Cells were permeabilized and fixed with PTEMF and stained with anti-myc 9E10 antibody (red) and anti-γ-tubulin antibody (green). DNA was stained with DAPI (blue). Scale bar equals 10 μm.
(B) Quantitative analysis of the distribution of myc-signal in HeLa S3 cells transiently transfected for 48 hr with myc-HURP-WT, myc-HURP-T330A and myc-HURP-T330D, respectively. Histograms show the fluorescence intensity from pole-to-pole of 5 representative cells, as measured by ImageJ.

Since HURP strongly stabilizes MTs and has also been described to be involved in MT-nucleation (Sillje et al., 2006; Wong and Fang, 2006), the protein levels and localization need to be tightly regulated. In consequence, small modifications could already have significant effects on spindle architecture. To investigate whether the displaced HURP phosphorylation site mutant (HURP-T330A) has an influence on MT stability, we carried out a cold-treatment of Cos 7 cells that highly overexpressed phosphorylation site mutant HURP constructs (Figure 35). In line with our previous results (Sillje et al., 2006), the overexpression of HURP-WT lead to stabilization of KMTs, as seen by prominent MT staining, in comparison to control cells, where only a few K-fibers were left after 30 min at 4°C (Figure 35, middle and left). The overexpression of the potential HURP Cdk1-phosphorylation

site mutant (HURP-T330A) caused even stronger α-tubulin signal, representing highly stabilized spindle MTs (Figure 35, right). Moreover, the cells that overexpressed HURP-T330A had a broad metaphase plate and many uncongressed chromosomes (Figure 34A and 35), which indicates that chromosome alignment was also affected in these cells. In conclusion, the phosphorylation of HURP, presumably by Cdk1, seems to influence the localization of the protein, which in turn affects spindle MT stability and chromosome congression.
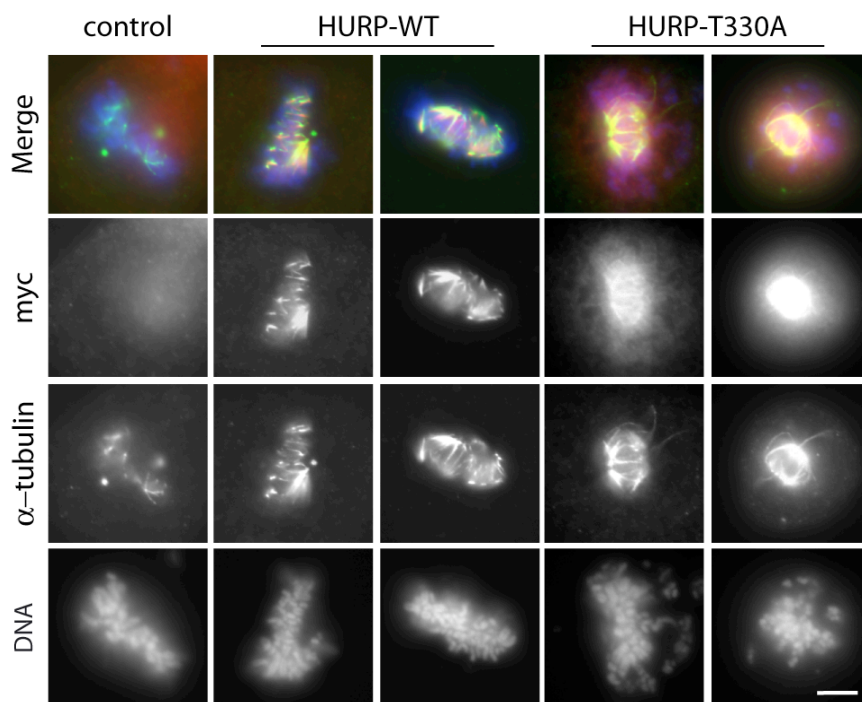
Figure 35. Stabilization of spindle KMTs by overexpression of HURP constructs
Cos 7 cells were transiently transfected with myc-HURP-WT and myc-HURP-T330A for 48 hr and incubated at 4°C for 30 min, before being directly permeabilized and fixed with PTEMF. Cells were stained with anti-myc 9E10 antibody (red) and anti-α-tubulin antibody (green). DNA was stained with DAPI (blue). Scale bar indicates 10 μm.

To analyze the effect of the HURP phosphorylation site mutant s under physiological conditions, live-cell imaging was performed (Figure 36). Cherry-tagged constructs of HURP-WT, HURP-T330A and HURP-T330D were generated and transiently overexpressed for 36 hr in HeLa S3 cells that stably expressed histone H2B-GFP. To increase the proportion of transfected mitotic cells, cells were pre-synchronized by thymidine block for 12 hr and then filmed by time-lapse microscopy 8 hr after release into drug-free medium (Figure 36A). Cells transfected with Cherry-tagged HURP-WT required 40 min, on average, to progress from prophase to anaphase (Figure 36B, top). The vast majority of these cells succeeded to congress and segregate their chromosomes, as well as to complete cytokinesis properly, although 2 out of 20 transfected cells died after cytokinesis. Cells transfected with Cherry-tagged HURP-T330A took approximately 46 min to reach

anaphase and went through mitosis without any apparent problems. However, 11 out of 20 cells died after cytokinesis (Figure 36B, middle), possibly from chromosome segregation defects or problems in later cell cycle stages. Cells transfected with the phosphomimic mutant HURP-T330D took approximately 44 min to get to anaphase and 6 of 20 cells also died after cytokinesis (Figure 36B, bottom). These results suggest that an aberrant phosphorylation state of HURP can be lethal during cell cycle progression, underlining our previous observations that HURP levels need to be tightly regulated. From the phosphorylation site mutant study we can conclude that the localization of HURP on the KMT plus ends is influenced by phosphorylation and that mislocalization of HURP causes problems in cell cycle progression. In addition to the Ran gradient, phosphorylation by Cdk1 therefore seems to be involved in restricting HURP to K-fibers.
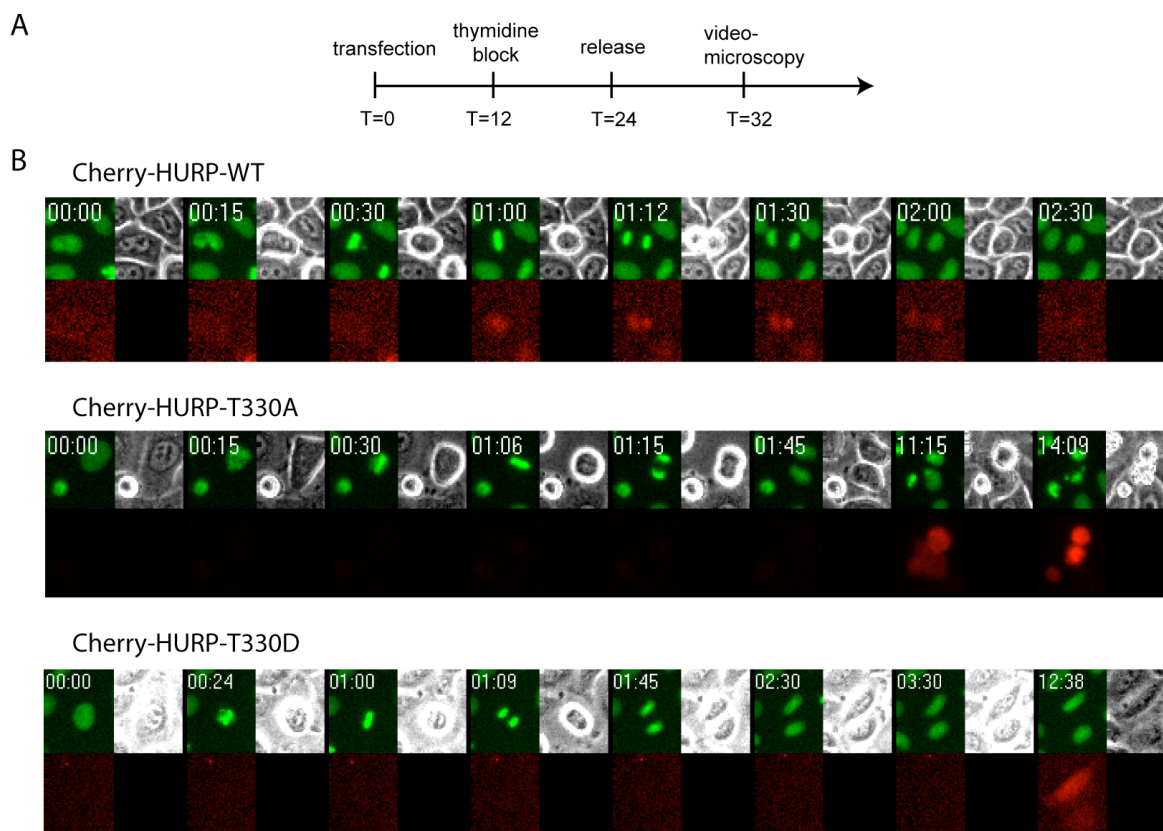
Figure 36. Time-lapse videomicroscopy of cells expressing Cherry-HURP constructs
(A) Schematic representation of Cherry-HURP transfection, and videomicroscopy protocol. Cells were simultaneously transfected with the indicated Cherry-HURP constructs and arrested by addition of thymidine 12 hr later. After further 12 hr, they were released from the block and imaging was started 8 hr later for a total duration of 12 hr (adapted from Elowe et al., 2007).
(B). Selected images show control (Cherry-HURP-WT) and phosphorylation site mutant (Cherry-HURP-T330A, Cherry-HURP-T330D) overexpressing cells, which were identified through the Cy3 signal (red, lower panel). The same cell is followed through mitosis with phase contrast (grey, upper panel) and the GFP-signal (green, upper panel), which visualizes the chromosomes. Images were acquired at the indicated time points after the start of chromosome condensation (T=0).

3.4.4 Search for a recruitment factor targeting HURP to the KMT plus ends

3.4.4.1 Analysis of potential HURP interacting proteins

As described above, the spindle localization of HURP is regulated by the Ran-importin pathway. High levels of RanGTP around the chromosomes localize HURP on KMT plus ends. Yet, it still remains unclear how HURP specifically localizes to K-fibers and is excluded from the spindle poles. One possibility would be that HURP is loaded close to the spindle poles and then transported along the microtubules towards the kinetochores by a plus end-directed motor. The most prominent candidate in this regard is Eg5, a plus end-directed kinesin that pushes antiparallel MTs poleward and is involved in maintaining spindle bipolarity (Kapitein et al., 2005). In *Xenopus* egg extract, HURP has been identified to be part of a Ran-dependent complex together with Eg5, TPX2, Aurora-A and XMAP215 (Koffa et al., 2006). To explore the existence of a similar complex in higher eukaryotes, we tested the HURP-Eg5 interaction in human somatic cells. To this end, we immunoprecipitated endogenous HURP from mitotic and asynchronously growing HeLa S3 cells (Figure 37A). Equal amounts of lysates and IPs were separated by SDS-PAGE and subsequently probed by Western blotting with anti-HURP, anti-Eg5, anti-TPX2 and anti-NuSAP antibodies. We tested for NuSAP (nucleolar and spindle-associated protein) in these samples as, to the best of our knowledge, it is the only other protein that has a similar localization to HURP and stabilizes MTs around the chromatin (Raemaekers et al., 2003; Ribbeck et al., 2006; Ribbeck et al., 2007). In our analysis, HURP strongly accumulated in the HURP immunoprecipitation from the mitotic extract, while no clear HURP signal was detected in the lysate from asynchronous cells. Furthermore, Eg5 also appeared as a weak band in the HURP IP, which showed hat HURP and Eg5 co-immunoprecipitated in the mitotic extract. (Figure 37A). To investigate this potential interaction, we performed an immunofluorescence analysis on HeLa S3 cells that had been depleted of Eg5 or Plk1, as negative control. If Eg5 would be the kinesin that brings HURP to the microtubule plus ends, one may have expected that in the Eg5-depleted cells HURP would not be excluded from the poles anymore,. However, on the resulting monopolar spindles (Mountain et al., 1999; Sumara et al., 2004), HURP was still

mostly absent from the centrosomes, similar to the situation in the Plk1 control (Figure 37B). Hence, Eg5 depletion did not detectably affect the localization of HURP on these monopolar spindles. Neither NuSAP nor TPX2 were detected in the immunoprecipitation of HURP, arguing against an interaction between these proteins (Figure 37A). Moreover, in HURP depleted mitotic cells, the spindle localization of NuSAP was not affected (Figure 37C). In some of the abnormal spindles seen in NuSAP-depleted cells, HURP spread along the MTs. However, this could be an indirect effect resulting from the NuSAP depletion, because NuSAP is important for chromatin MT-interactions *in vitro* (Raemaekers et al., 2003), and may thereby influence the localization of HURP on the K-fibers (Sillje et al., 2006). Altogether, we did not observe any direct interaction between HURP and NuSAP or TPX2. However, as seen by the co-immunoprecipitation, there could be a transient interaction between HURP and Eg5 during mitosis.
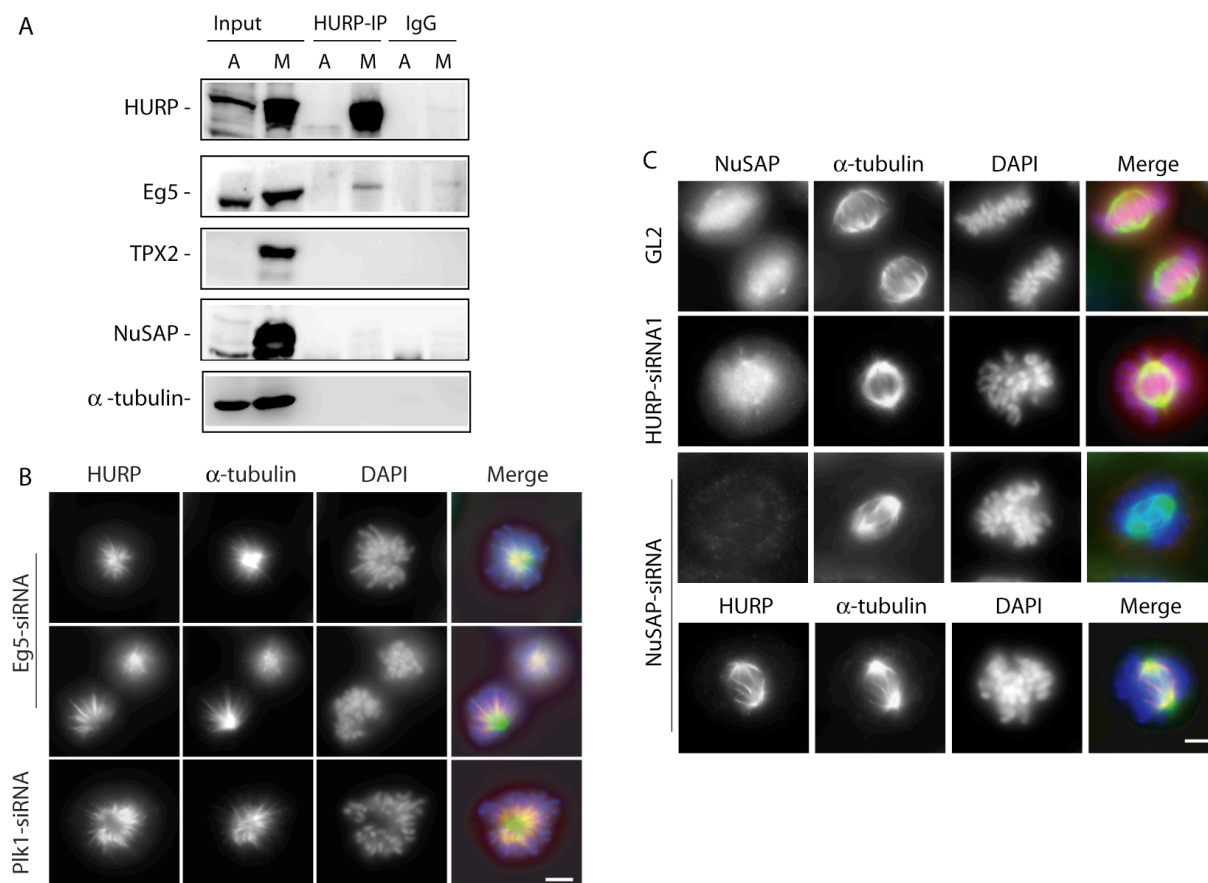
Figure 37. HURP may interact with Eg5 in mitotic cells
(A) Asynchronous and mitotic (nocodazole block and release) HeLa S3 cell lysates were immunoprecipitated with anti-HURP antibody and pre-immune IgGs, respectively. The isolated protein complexes were separated by 12% SDS-PAGE and probed by Western blotting with anti-HURP, anti-Eg5, anti-TPX2 and anti-NuSAP antibodies, as well as anti-α-tubulin antibody, as a loading control.

(B) HeLa S3 cells were treated with Eg5- and Plk1-siRNA for 48 hr and permeabilized and fixed at the same time with PTEMF. Afterwards, cells were stained with anti-HURP (red) and anti-α-tubulin (green) antibodies and DNA was stained with DAPI (blue). Scale bar equals 10 μm.
 (C) HeLa S3 cells were treated with GL2, HURP- and NuSAP-siRNA for 48 hr and permeabilized and fixed at the same time with PTEMF. Next, cells were stained with anti-NuSAP-or anti-HURP antibodies (red), respectively, as well as with anti-α-tubulin antibody (green), and DNA was stained with DAPI (blue). Scale bar equals 10 μm.

3.4.4.2 Isolation of a HURP complex reduced in importin β

We have shown previously that HURP forms a complex with importin β (Sillje et al., 2006; Wilde, 2006). Since this complex possibly interferes with other transient interactions, we attempted to identify potential HURP interaction partners in an importin β-free environment. To this end, interphase and mitotic lysates were produced from HeLa S3 cells synchronized by a double thymidine block (interphase lysate), or a thymidine block followed by a nocodazole block and release (mitotic lysate), respectively. Then, samples were compared by gel filtration (Appendix, Figure 43: Chromatogram of Superose 12). Afterwards, HURP and importin β were detected by Western blot analysis (Figure 38A). In contrast to the interphase extract, where the peak fraction of HURP co-eluted with the peak fraction of importin β (Figure 38A, left, E11), the elution profile of HURP from the mitotic extract appeared to have two peaks (Figure 38A, right, A10 & A12). One fraction of HURP co-eluted with importin β (A12), while the majority of HURP eluted at a higher molecular weight fraction that was almost devoid of importin β, but contained Eg5 (A10). This result indicates that HURP forms different complexes, depending on the cell cycle phase. During mitosis, HURP possibly exists in two populations, one bound to importin β and another one devoid of importin β. The latter fraction might instead allow more transient interactions with other spindle proteins. Thus the resulting larger HURP complex possibly assembles upon release from importin β. However, whether this complex is only created in the absence of importin β was not examined.
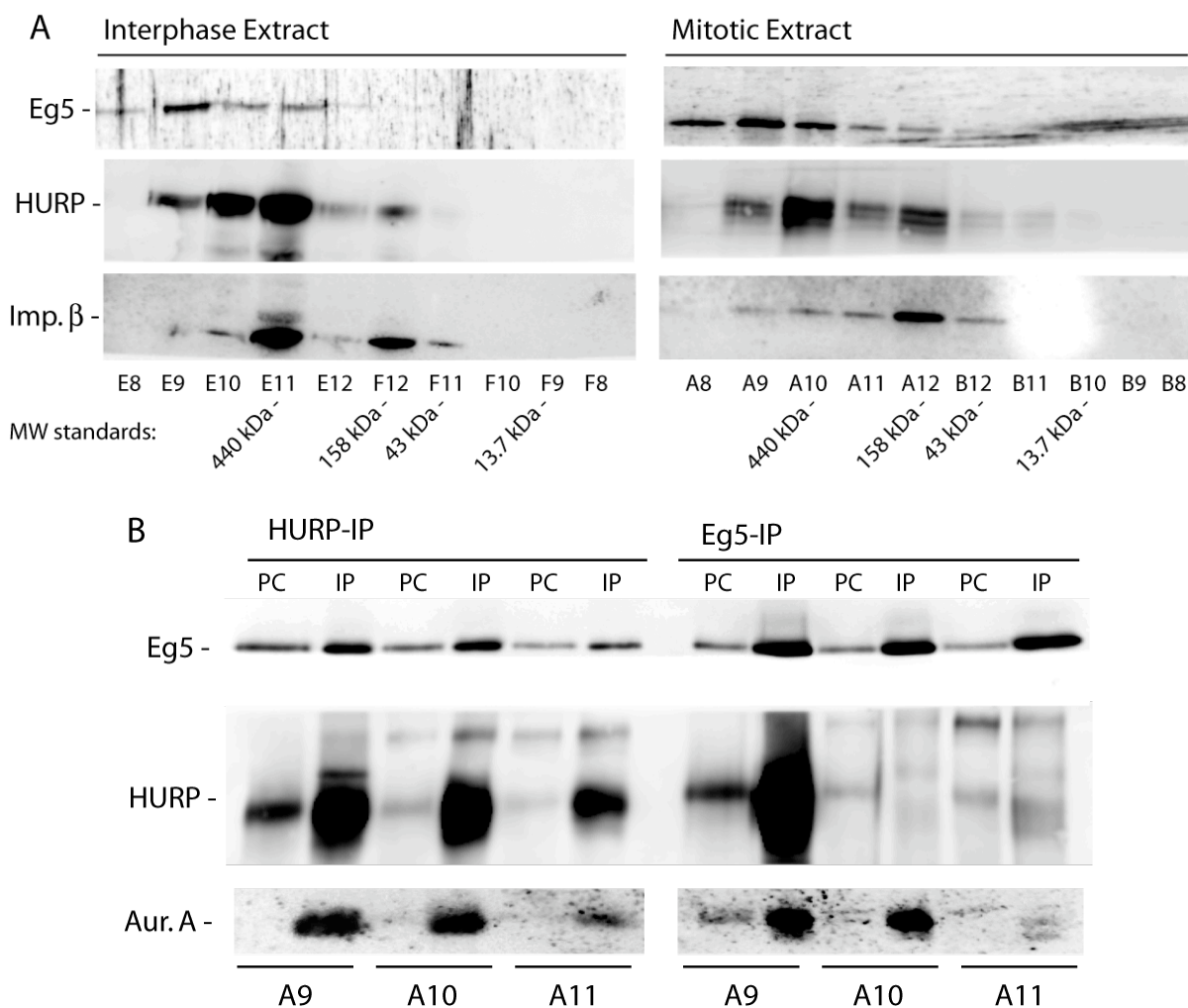
Figure 38. Analysis of the potential HURP/Eg5/Aurora-A complex in human somatic cells
(A) Interphase and mitotic extracts from HeLa S3 were separated by gel filtration on a superose 12 column. Equal amounts of the peak fractions were then analyzed by SDS-PAGE and probed by Western blotting with anti-Eg5, anti-HURP, and anti-importin β antibodies (Imp. β). Corresponding molecular weights were determined with a standard curve before (MW standards).
(B) A mitotic extract from HeLa S3 was separated by gel filtration on a superose 12 column and peak fractions (A9-A11) were pre-cleared (PC) with IgGs, followed by IP with anti-HURP- and anti-Eg5-antibody, respectively. The isolated protein complexes were separated by SDS-PAGE and probed by Western blotting with anti-Eg5, anti-HURP, and anti-Aurora-A (Aur.A) antibodies.

In order to analyze in more detail whether HURP and Eg5 interact directly in the HURP peak from the fractionated mitotic lysate (Figure 38A, A10), HURP and Eg5 were immunoprecipitated from these fractions (Figure 38B, A9/A10/A11). Equal amounts of the different fractions were separated by SDS-PAGE and probed by Western blotting with anti-HURP, anti-Eg5, and anti-Aurora-A antibodies, respectively. Eg5 and Aurora-A both co-immunoprecipitated with HURP in the peak fractions (Figure 38, left, A9, A10). This result could be confirmed by performing the experiment in reverse order, that is an immunoprecipitation of Eg5, followed by Western blotting HURP and Aurora-A (Figure 38, right).

RESULTS

These data suggest that HURP may, at least transiently, interact with Eg5 and Aurora-A, when released from importin β during mitosis. Phosphorylation of HURP by Aurora-A has been reported to contribute to protein stability *in vitro* (Yu et al., 2005), but further investigations will be necessary to clarify the physiological relevance of these potential mitotic HURP interaction partners.

3.4.4.3 Search for new mitotic HURP interactors

Our fractionation studies demonstrated that it is possible to isolate HURP under importin β-reduced conditions. This approach gave us the intriguing opportunity to seek for new mitosis-specific HURP interactors that may target and maintain the protein on the K-fibers, after RanGTP-driven release of HURP from importin β, in the vicinity of the chromosomes.

In order to identify the components of this putative mitotic HURP complex, the peak fractions (A10, A12) from the gel filtration of the mitotic lysate were pre-cleared with rabbit IgGs and immunoprecipitated with the anti-HURP antibody (Figure 39). The samples were separated by a gradient NuPAGE gel and distinct Coomassie stained bands from the HURP/importin β peak (A12), the importin β-reduced HURP peak (A10), and rabbit IgGs (as negative control) were cut, in-gel digested with trypsin and analyzed by MS (performed by René Lenobel and Roman Körner). Both peak fractions contained HURP and importin β, although importin β was strongly reduced in the HURP peak, which corresponded to the higher molecular weight fraction (Figure 39, A10). Moreover, several possible binding partners co-immunoprecipitated with HURP. Among them were spindle-associated proteins (NuMA and Nucleophosmin), proteins involved in the spindle checkpoint (Cdc20 and Bub3), proteins playing a role in RanGTP turnover (for example: RacGAP1, Nucleolar GTP-binding protein 1 and Nucleostemin) and Nup153, a nucleoporin that was identified previously in a large-scale immunoprecipitation of HURP from a spindle preparation. Interestingly, many of the proteins found in the immunoprecipitation were either present only in the importin β-reduced fraction (NuMA, Cdc20 and Bub3), or highly enriched (Nup153, Nucleostemin and Nucleophosmin), as determined by the amount of peptides identified. We are therefore confident that we have identified a HURP complex from human somatic cells, which may contain new HURP interaction partners, other than importin β.
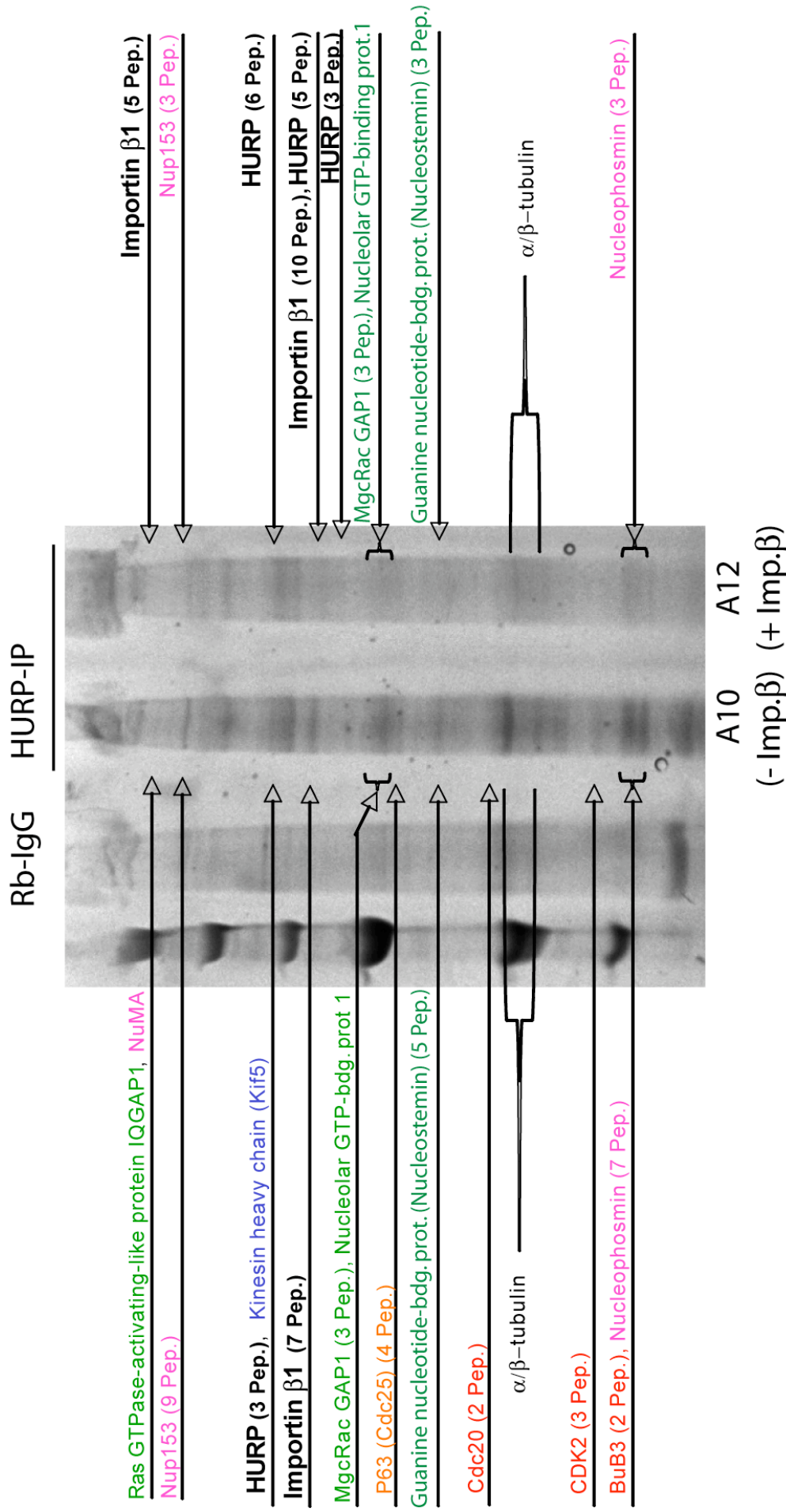
Figure 39. Identification of an importin β-reduced HURP complex
Two superose 12 peak fractions (A10 = importin β-reduced, A12 = HURP/importin β peak) of mitotic HeLa S3 cell lysate were used for immunoprecipitations with anti-HURP antibody and pre-immune IgGs, respectively. The isolated protein complexes were separated by a NuPAGE gradient gel and proteins were visualized by Coomassie blue staining. Distinct bands were cut and in-gel digested by trypsin. Mass spectrometry analysis identified HURP and importin β and revealed potential new HURP interactors. Selected candidates are listed next to the gel. The number of identified peptides is depicted in brackets (Pep.).

4 Discussion

4.1 Characterization of new spindle components

Chromosome alignment at the spindle equator defines the metaphase stage of the cell cycle. Microtubule-associated motor and non-motor proteins assist in the bipolar organization of spindle microtubules and kinetochore capture by K-fibers, prerequisites of chromosome congression. Here, the characterization of two novel non-motor spindle proteins, termed HURP and CHICA, is described. These proteins were originally identified in a proteomic survey of the human spindle apparatus (Sauer et al., 2005). We show that HURP and CHICA localize to the mitotic spindle and are both up-regulated and phosphorylated during mitosis. While HURP decorates the KMTs in the vicinity of the chromosomes, CHICA localizes to the proximity of the spindle poles. Moreover, both proteins directly bind to MTs *in vitro,* indicating that they could have an influence on spindle architecture. In contrast to HURP, CHICA was absent from cold-resistant K-fibers, demonstrating that these proteins bind to distinct subsets of spindle MTs. Altogether, their mutually exclusive spindle localization implied different functions for HURP and CHICA, especially concerning their contributions to the stabilization of K-fibers, which was the focus of the work described here.

4.1.1 CHICA is required for loading the chromokinesin Kid onto the mitotic spindle

Following up on my early studies, which demonstrated that CHICA is a genuine component of the spindle apparatus but does not significantly affect K-fiber stability, Dr. Anna Santamaria found that this protein plays a role primarily in the generation of polar ejection forces.

Dr. Anna Santamaria showed that CHICA-depleted cells fail to organize a proper metaphase plate, highly reminiscent of the phenotype observed upon depletion of the chromokinesin Kid, a key regulator of polar ejection forces (Antonio et al., 2000; Funabiki and Murray, 2000; Levesque and Compton, 2001; Tokai et al., 1996; Yajima et al., 2003). Moreover, upon depletion of either CHICA or Kid, chromosomes collapsed onto the poles of monastrol-induced monopolar spindles, indicating that the two proteins cooperate in the generation of polar ejection forces. Finally, it was proposed that CHICA is required for the spindle localization of Kid

(Figure 40). These data identify CHICA as an important interaction partner of the chromokinesin Kid and contribute to a better understanding of Kid function in chromosome congression.

Figure 40. The spindle localization of Kid depends on CHICA
The model illustrates the proposed mechanism of Kid loading onto the spindle by CHICA, which generates a gradient of polar ejection forces from the poles to the middle zone of the bipolar spindle.
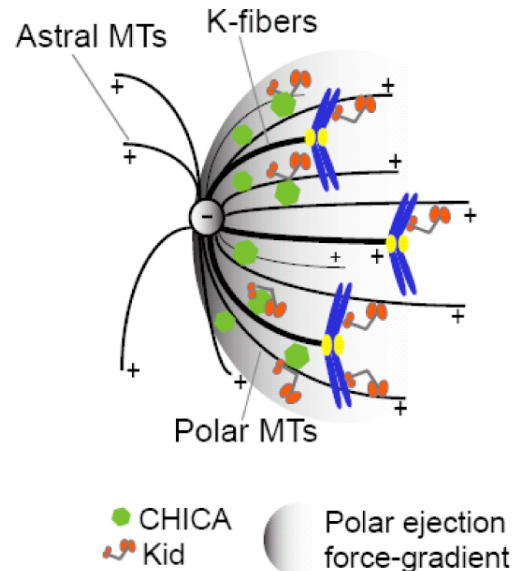
4.1.2 HURP, is a novel target of the Ran-regulated spindle assembly pathway

In contrast to CHICA, HURP specifically stabilizes K-fibers by virtue of its ability to bind and bundle microtubules. Upon HURP depletion, K-fiber stability is impaired, resulting in a chromosome congression delay. Furthermore, we found that HURP interacts with importin β, which inhibits its MT stabilization capability *in vitro*. *In vivo*, HURP localizes predominantly to the KMT plus ends and this localization is controlled by high RanGTP levels in the vicinity of the chromosomes. In addition to the RanGTP gradient the spindle localization of HURP is influenced by Cdk1-phosphorylation, which seems to restrict HURP to the K-fibers. In summary, our study identifies HURP as a novel component of the Ran-importin β-regulated spindle assembly pathway. Thus, the mechanism of Ran-dependent K-fiber stabilization by HURP will be discussed in more detail in the next paragraph.

4.2   Ran-regulated K-fiber stabilization by HURP

Bipolar spindle formation critically depends on the formation of K-fibers. In somatic cells, this process is thought to involve at least two partially redundant pathways, one based on centrosomes, the other based on RanGTP production in the vicinity of chromosomes (Rieder, 2005).

With the help of co-immunoprecipitation/mass spectrometry and yeast two-hybrid screens we revealed that HURP binds directly to importin β, a property shared with Rae1 (Blower et al., 2005). In contrast, TPX2, NuMA, XCTK2, Xnf7, and Kid interact with importin α (Ems-McClung et al., 2004; Gruss et al., 2001; Maresca et al., 2005; Nachury et al., 2001; Tahara et al., 2008; Wiese et al., 2001). Also, HURP localizes to kinetochore MTs and shows a striking enrichment in the close vicinity of chromosomes, whereas other RanGTP-responsive spindle assembly factors localize mostly toward the proximity of spindle poles (Blower et al., 2005; Gruss et al., 2002; Maresca et al., 2005; Wittmann et al., 2000). HURP still concentrated in the proximity of chromosomes when normal MT dynamics were altered by taxol or low doses of nocodazole, suggesting that MT flux is not a prime determinant for its localization. Most importantly, generation of low RanGTP levels, either by overexpression of RanT24N or by inactivation of RCC1 in the tsBN2 cell line, diminished HURP localization to spindles, as did overexpression of importin β. Conversely, high RanGTP levels, mimicked by overexpression of RanQ69L, resulted in enhanced spindle localization of HURP. Moreover, in the presence of RanQ69L, HURP could also be seen at spindle poles, indicating that the exact localization of HURP is exquisitely sensitive to RanGTP levels. Recent studies have argued for the existence of RanGTP gradients not only in eggs but also in somatic cells (Caudron et al., 2005; Li and Zheng, 2004). Therefore, depending on the steepness of this gradient and the concentration of RanGTP required to dissociate a HURP-importin β complex, this gradient might restrict the localization of HURP to the proximity of chromosomes. If so, HURP could be an excellent marker to monitor RanGTP levels and gradients in mitotic cells. Other, not mutually exclusive, mechanisms may also contribute to determine the localization of HURP. In particular, it is possible that MT-dependent motor activities could dynamically restrict the distribution of HURP. Alternatively, HURP localization could be determined by the asymmetric distribution of a specific MT-associated protein and/or the activities of kinases and

phosphatases. HURP has been reported to be phosphorylated by Aurora-A, at least *in vitro* (Yu et al., 2005), and given the concentration of Aurora-A on poleward spindle MTs (Bischoff et al., 1998; Kufer et al., 2003), it is possible that phosphorylation by this kinase displaces HURP from the spindle poles.

Upon siRNA-mediated reduction of HURP levels, a delay in chromosome congression was observed, but cells still progressed through mitosis, indicating that kinetochore-MT interactions were not abolished. Although it would be premature to exclude that a complete (genetic) knockout of HURP might reveal a more severe phenotype, the most obvious consequence of siRNA-mediated depletion of HURP concerned the stability of K-fibers. In particular, K-fibers in HURP-depleted cells showed a striking sensitivity to cold-induced depolymerization. This might contribute to explain the previous observation that K-fibers are less stable in tsBN2 cells at the restrictive temperature (Arnaoutov et al., 2005), but it is clear that other factors, including the RanBP2/Nup358-RanGAP complex, also contribute to K-fiber stabilization (Arnaoutov et al., 2005; Salina et al., 2003). Together with the ability of HURP to bind and bundle MTs *in vitro*, our data suggest that the primary function of HURP is to promote spindle formation through stabilization of K-fibers. Interestingly, antiparallel MT bundles, notably those in the central spindle, were not affected by the absence of HURP. This indicates that HURP functions primarily to stabilize parallel MTs. As shown here and by others (Hsu et al., 2004), HURP abundance is tightly regulated during the cell cycle. Thus, it is plausible that the amounts of HURP protein present in the cytoplasm in interphase cells are sufficiently low to prevent its action on MTs. In support of this view, endogenous HURP did not detectably bundle MTs during interphase of the cell cycle, although bundling could be induced by overexpression of HURP. Our data also show that the steady-state distribution of HURP is determined by continuous shuttling between cytoplasm and nucleus. Thus, it would be premature to exclude an interphase function for HURP.

In summary, we have characterized HURP, a novel spindle assembly factor, regulated by the Ran-importin β pathway (Figure 41). Most strikingly, the spindle localization of HURP is sensitive to the levels of importin β and RanGTP, and HURP function appears to be confined to the vicinity of chromosomes, the primary site of RanGTP production. Specifically, we show that HURP directly binds to MTs and selectively bundles K-fibers. These data strengthen the emerging view that K-fiber

formation depends not only on the classical "search-and-capture" mechanism, but also involves a RanGTP-regulated pathway, operating in the vicinity of chromatin.
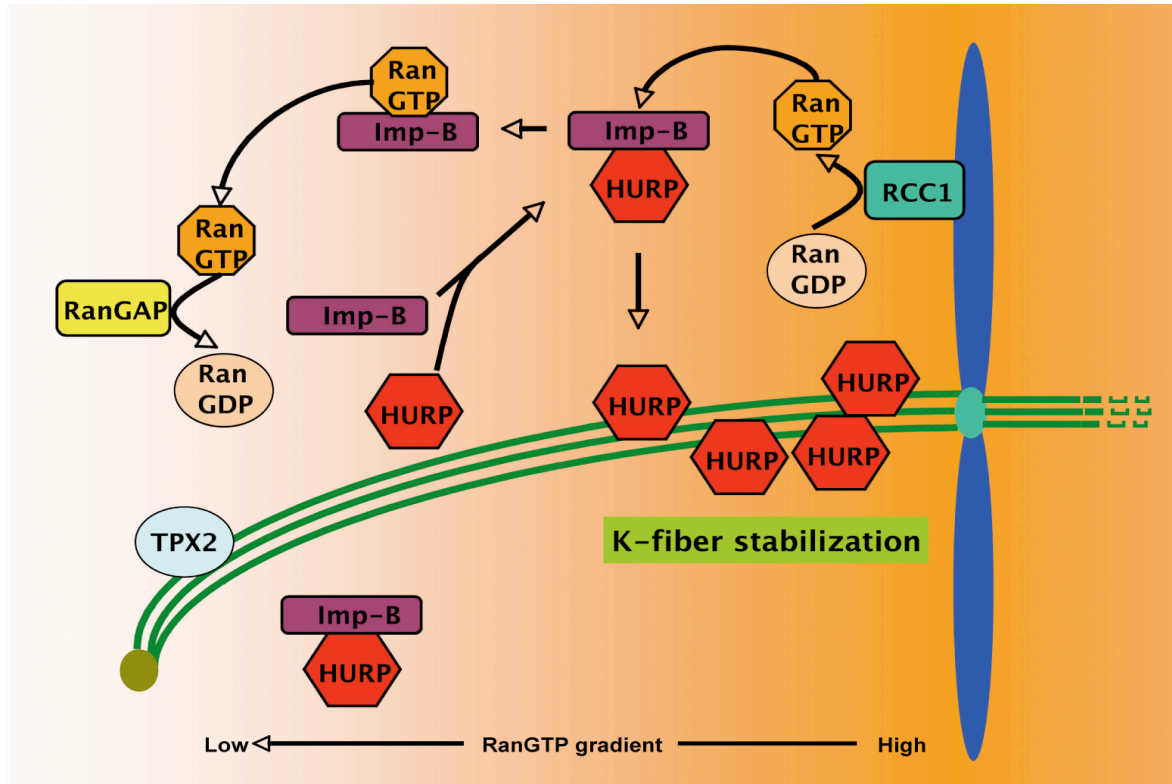
Figure 41. Ran-regulated K-fiber stabilization by HURP
Model of HURP regulation by Ran-importin during the chromatin-induced spindle assembly pathway. High RanGTP concentrations generated by the chromatin-bound RanGEF, RCC1 trigger the release of spindle assembly factors, like TPX2 and HURP from their inhibitory complex with importin β. HURP in turn, bundles KMTs creating stable K-fibers in the vicinity of the chromosomes.

4.3   How is HURP specifically recruited to K-fibers?

Having established that HURP stabilizes K-fibers in a Ran/importin-dependent manner (Sillje et al., 2006; Wilde, 2006), several aspects of this HURP function remained to be further characterized. Although we were able to show that HURP specifically localizes to the KMTs in the vicinity of the chromosomes (Sillje et al., 2006), how this specificity is achieved, and which domains of HURP are involved in this process remained unclear. We considered two possibilities for targeting HURP to the K-fibers, either a transport by plus end-directed motor proteins, or an asymmetrically distributed spindle recruitment factor. Moreover, it has been reported before that HURP protein levels are regulated by phosphorylation through Cdk1 and Aurora-A (Hsu et al., 2004; Yu et al., 2005), and we were interested to explore how these mitotic kinases interfere with HURP spindle localization and function.

4.3.1 Structure-function analysis of HURP domains

As described before, HURP specifically stabilizes K-fibers (Sillje et al., 2006). K-fibers consist of 20-40 KMTs, which are cross-linked to form stable MT bundles. Other known MT stabilizers, like Clip170 and XMAP215 interact with the growing MT plus ends and carry out their function either by homodimerization, as in the case of Clip170, a +TIP that binds to MTs via tandem repeats in its basic N-terminus and stabilizes MTs through dimerization of its long central coiled coil domains (Pierre et al., 1994; Pierre et al., 1992); or they contain separate MT and tubulin binding sites, like TOGp, the human homolog of XMAP215 (Spittle et al., 2000). In contrast, the long coiled coil protein NuMA interacts with the MT minus ends and stabilizes MT as a divalent crosslinker by oligomerization of its C-terminal tail, thereby focusing MTs at the spindle pole (Haren and Merdes, 2002). We considered that HURP could function in a similar manner to these proteins. Thus, HURP may need to dimerize, or to have multiple MT binding sites to carry out its MT stabilization function. To explore these two possibilities, we first analyzed the HURP N- and C-terminus by co-immunoprecipitation from in vitro-translated N- and C-terminal fragments. Under the conditions tested, we did not observe HURP dimerization, however we cannot rule out that importin β present in the reticulocyte lysate interfered with HURP self-association. Nevertheless, the displacement of different HURP fragments to the spindle pole, in contrast to the full-length protein that localizes to the KMT plus ends, also argues against HURP dimerization.

To identify the potential MT binding sites of HURP, we focused on the conserved N-terminal coiled coil domains, identified by bioinformatics analysis, that typically play important roles in intermolecular interactions (Burkhard et al., 2001). We investigated the function of these domains in spindle targeting and MT stabilization by transient overexpression, MT co-sedimentation and MT bundling assays, using HURP constructs, which contained either both coiled coil domains (1-201, 1-150), or lacked the first (60-150, ΔCC1), or else part of the second coiled coil domain (1-116, ΔCC2), respectively. Strikingly, all N-terminal recombinant HURP fragments tested (1-404, 1-201, 1-116, 60-150), bound to MTs *in vitro*, which suggests that HURP may have at least two MT binding sites, presumably overlapping with the coiled coil domains. However, when the coiled coil regions were overexpressed in cells separately, some of these fragments did not bind to

DISCUSSION

spindle MTs *in vivo*. Thus, we observed that the HURP fragments lacking the second coiled coil domain (1-60, 1-116 and ΔCC2) did not localize to the spindle anymore. In contrast, the fragment comprising only this domain (60-150) still localized to the spindle pole caps, indicating that this protein region is important for the initial loading of HURP to the spindle MTs *in vivo*. Furthermore, while *in vitro* the coiled coil regions were able to directly bind MTs individually, both domains were necessary to stabilize MTs *in vitro* and *in vivo*. This was an interesting result, since coiled coil domains have long been known to be involved in oligomerization (Burkhard et al., 2001). However, the N-terminus of HURP, including the coiled coil domains, has many basic clusters and is therefore likely to interact with the negatively charged MT lattice (Woehlke et al., 1997) (1-150 pI: 10.2). Interestingly, it has been reported for the *S. pombe* spindle protein Fin1 that its two C-terminal coiled coil domains both contribute to MT affinity and are important for spindle MT binding (Woodbury and Morgan, 2007), demonstrating that coiled coil domains can indeed be involved in MT interactions.

In summary, our analysis shows that the N-terminus of HURP that contains two coiled coil domains is involved in MT stabilization and important for the initial spindle loading of HURP. In contrast, the C-terminus, including a Guanylate kinase-associated protein (GKAP) domain is necessary for the specific recruitment of HURP to the KMT plus end. GKAP domains interact with proteins containing Gyanylate kinase (GK) domains. Guanylate kinases are enzymes that convert GMP to GDP via ATP hydrolysis (Kim et al., 1997). However, the ATP-binding site is not conserved in the GK domains and hence they exhibit no enzymatic activity, though they do bind GMP (Kistner et al., 1995). In the absence of enzymatic activity it has been proposed that the GK domains have instead evolved into protein binding sites. However, the physiological role of this HURP domain was unclear. Our data now demonstrate that this domain is required to concentrate HURP at the plus end region of the MTs and furthermore, contains a regulatory Cdk1 phosphorylation site that may be important to specifically restrict HURP to the K-fibers (see below). K-fiber formation at least partially depends on high RanGTP concentrations, which ensures GTP-tubulin addition and results in MT polymerization (see Introduction). In addition to the overall RanGTP gradient from chromosomes to the spindle poles, proteins involved in the regeneration of GTP may hence play an important role,

promoting K-fiber stabilization at specific sites of the mitotic apparatus. Furthermore, mitotic progression requires the precise positioning of Ran network components and it is interesting to speculate that HURP could maintain local K-fiber stability during mitosis by recruiting proteins involved in the regeneration of GTP.

In interphase cells, the overexpression of the different HURP fragments demonstrated that the N-terminus accumulated in the nucleus, but the C-terminus localized to the cytoplasm (see HURP map, Figure 42). From these results we propose that the C-terminus of HURP has an NES, whereas the N-terminus contains an NLS. However, HURP does not possess NES or NLS consensus motifs (Chook and Blobel, 2001; Lee et al., 2006). Therefore, the exact positions of the potential NES and NLS were not predictable by bioinformatics analysis (la Cour et al., 2004), or single point mutations of conserved sites. Nevertheless, we identified the importin β binding site in the first 60 amino acids, within the N-terminus of HURP. The HURP fragment (60-846) lacking this region did not bind to importin β in immunoprecipitations and was insensitive to nuclear export inhibition by LMB. In contrast, the corresponding HURP fragment, containing only the area aa 1-60 (CC1) colocalized with importin β on the nuclear envelope in interphase cells.

Strikingly, in addition to the effect on the importin β binding by mutations in the far N-terminus of HURP, the spindle localization of the protein was also affected, emphasizing the essential role of this region for the mitotic function of HURP. One possible explanation for the aberrant spindle localization of the HURP NLS-mutant may be that the importin β and MT binding sites partially overlap. In this case, microtubules and importin β would compete for HURP binding. However, by MT co-sedimentation we observed that HURP still binds to MTs in the presence of importin β, although it could not bundle MTs anymore. This data is consistent with the recent observation that HURP and importin β can be co-sedimented with mitotic MTs (Tedeschi et al., 2007). This indicates that HURP might be able to interact with MTs in concert with importin β, although its MT stabilization capability is impaired. The same has been proposed before for TPX2 and NuMA. In the case of these proteins, MT aster formation but not MT binding is inhibited by importin α/β *in vitro,* although NuMA also contains the NLS within the C-terminal MT binding site (Haren and Merdes, 2002; Saredi et al., 1996; Schatz et al., 2003).

DISCUSSION

In our study, the mutual interaction of HURP with importin β and MTs could be explained by the observation that HURP seems to have at least two MT binding sites linked to the coiled coil regions, which can interact with MTs separately, but are both essential for MT bundling. In the presence of importin β, HURP can therefore still interact with MTs, although one of the binding sites is shared with the importin β binding site. Since HURP has to bind to more than one MT in order to crosslink and bundle them, the competition with importin β binding to one of these domains would thereby inhibit the MT stabilization function of HURP. Once this inhibitory complex faces the high RanGTP levels generated by chromatin-bound RCC1 (Carazo-Salas et al., 2001), HURP would be released from importin β in the vicinity of the chromosomes, in order to specifically stabilize the K-fibers (see above, Model Figure 41), a prerequisite for proper KMT attachment and chromosome congression (Sillje et al., 2006; Wong and Fang, 2006).
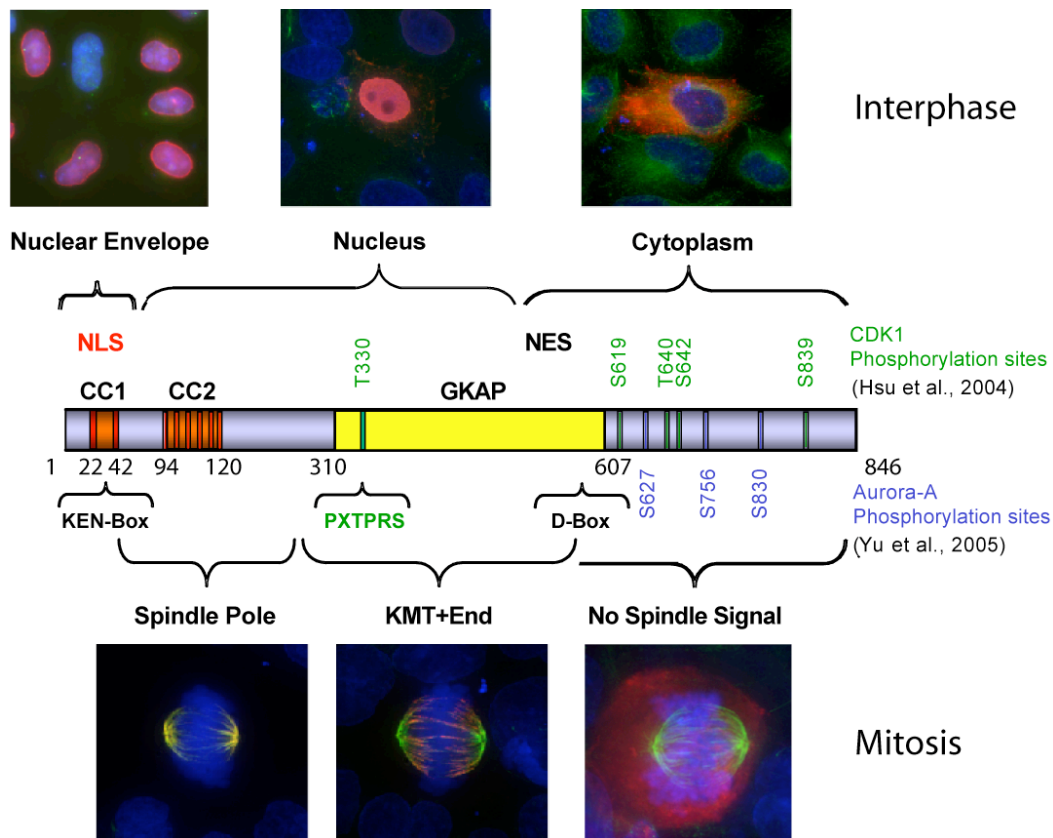
Figure 42. Structure-function HURP domain map
Primary structure of HURP including the predicted N-terminal coiled coil domains (orange), the GKAP domain (yellow), the reported conserved Cdk1 (green), and Aurora-A (blue) phosphorylation sites, as well as the mitosis-specific PXT^{330}PRS phosphorylation site identified by MS, and the presumed NLS (aa 1-60) and NES (aa 400-550) regions. Representative IF pictures show the subcellular localization of the different HURP fragments in interphase and mitotic cells.

4.3.2 Regulation of HURP by phosphorylation

Most spindle proteins are controlled by phosphorylation, with Cdk1 being the key regulator of mitotic progression (Nigg, 2001). HURP has also been reported to be regulated by phosphorylation and several Cdk1 and Aurora-A phosphorylation sites have been identified *in vitro* by MS analysis (Hsu et al., 2004; Yu et al., 2005). However, only some of these sites are conserved and the function of specific phosporylation sites was not revealed so far.

We identified a conserved mitosis-specific Cdk1 phosphorylation site (T330) by MS analysis of a large-scale immunoprecipitation of HURP from a spindle preparation. In addition to eight other predicted Cdk1 sites, this site has previously been reported to be involved in HURP degradation (Hsu et al., 2004). However, in this study, the function of the individual sites was not defined and an effect on HURP degradation was only observed when all nine phosphorylation sites were mutated simultaneously (Hsu et al., 2004). Interestingly, the phosphorylation site (T330) we identified here was located within the GKAP domain that is required to target HURP to the microtubule plus ends (see above). Mutation of this site lead to a spreading of HURP over the entire spindle MTs and, in agreement with the bundling activity of HURP, caused MT-hyperstabilization. Furthermore, cells that overexpressed the HURP phosphorylation site mutants (HURP-T330A, HURP-T330D) had problems to progress through the cell cycle an approximately half of these cells died after cytokinesis, as seen by live-cell imaging.

A similar mislocalization of HURP, together with MT hyperstabilization and chromosome congression defects was reported, as a result of RanBP1 depletion (Tedeschi et al., 2007). RanBP1 is a non-catalytical partner of Ran that regulates the nucleotide turnover on Ran by stimulating GTP hydrolysis through RanGAP1 and inhibits the RanGEF, RCC1 (Bischoff et al., 1995). Hence, the depletion of RanBP1 disrupts the Ran gradient, which leads to the displacement of HURP along the spindle (Tedeschi et al., 2007), reminiscent to the HURP localization in cells transfected with RanQ69L (non-hydrolysable RanGTP mutant) (Sillje et al., 2006). Whether the displacement of HURP due to the perturbed Ran gradient is a direct or indirect effect is still unclear. However, these observations confirm that HURP needs to be firmly restricted to the K-fibers, to avoid deleterious effects on the spindle architecture and hence chromosome misalignment (Ciciarello et al., 2007).

Apart from stabilizing MTs*,* HURP has also been reported to polymerize MTs and induce formation of additional tubulin sheets around MTs *in vitro* (Davis and Wordeman, 2007; Santarella et al., 2007). The existence of these sheets *in vivo* is not clear, and the relevance of this potential function of HURP to spindle assembly remains to be clarified. However, these observations again demonstrate that HURP protein levels and spindle localization need to be tightly regulated.

Our results show that, aside from the Ran gradient, the localization of HURP to the K-fibers is influenced by Cdk1-phosphorylation. Hence, the RanGTP gradient and Cdk1 phosphorylation may cooperate in the exclusion of HURP from the poles and its accumulation at the KMTs in the vicinity of the chromosomes. Aurora-A, a mitotic kinase localizing to polar MTs (Bischoff et al., 1998; Kufer et al., 2003) has also been reported to phosphorylate HURP (Yu et al., 2005), and is thought to be a component of the Ran-dependent HURP complex identified in *Xenopus* (Koffa et al., 2006). Whether this kinase is involved in excluding HURP from the poles was not investigated in detail. However, by immunoprecipitation analysis of HURP, under importin β-reduced conditions, we confirmed Aurora-A as a potential HURP interaction partner in somatic cells (see below).

4.3.3   Search for new HURP interaction partners

Importin β is the main interaction partner of HURP, forming an inhibitory complex that is resolved upon high RanGTP concentrations around the chromatin or the addition of excess RanQ69L (Sillje et al., 2006). Therefore, it has been difficult to investigate more transient interaction partners of HURP. Nevertheless, HURP has been isolated in a complex with XMAP215, Eg5, TPX2 and Aurora-A, in a gel filtration analysis of *Xenopus* egg extracts, (Koffa et al., 2006). Since Eg5 is a plus end-directed motor (Kapoor et al., 2000; Mayer et al., 1999), and the Aurora-A kinase is another indirect Ran target (Kufer et al., 2002; Tsai et al., 2003), both are promising candidates for regulating the spindle localization of HURP. We were therefore interested in investigating whether this complex also exists in human somatic cells. Although we did not observe a significant interdependency between HURP and Eg5 by immunofluorescence, we detected a weak mitosis-specific interaction with Eg5 in HURP immunoprecipitates. To increase the potential for these interactions, we separated HURP from importin β by size exclusion

chromatography, which allowed us to analyze transient HURP interactors under importin β-reduced conditions. The analysis of this mitosis-specific HURP complex through immunoprecipitations of HURP and Eg5 finally enabled us to confirm the interactions of HURP with Eg5 and Aurora-A, which probably occurs once HURP is released from importin β during mitosis.

In conclusion, we confirmed that HURP forms different complexes in interphase and mitotic cells. We isolated a large mitosis-specific HURP complex that includes Eg5 and Aurora-A from human somatic cells, which may resemble the reported Ran-regulated HURP complex from *Xenopus* (Koffa et al., 2006). Furthermore, MS analysis of this HURP complex enabled us to identify new mitosis-specific HURP interactors. Among them were spindle-associated proteins, like NuMA, which organizes the MTs at the spindle pole (Ban et al., 2007; Merdes et al., 2000) (see below), spindle checkpoint proteins, including Cdc20 and Bub3, and proteins which play a role in RanGTP turnover, like MgcRacGAP1 and finally, Nup153, a nucleoporin that functions in membrane trafficking, regulated by Ran-importin (Ball and Ullman, 2005). Nup153 was previously identified in a large-scale immunoprecipitation of HURP from a spindle preparation, and thus represents an interesting HURP binding partner. Interestingly, some nucleoporins have been reported to localize to kinetochores (Orjalo et al., 2006), and may be involved in spindle assembly as part of the recycling of proteins from the nuclear import/export pathway, during mitosis (Zuccolo et al., 2007).

Altogether, the isolation of the mitosis-specific HURP complex with reduced amounts of importin β allowed us to analyze additional HURP interactions, which may otherwise be prevented by the inhibitory HURP/importin β complex. Although thorough investigations will be necessary to confirm these potential interactors, the results from this approach may be useful in the future, to study the relationship between HURP and other mitotic spindle proteins, in order to further elucidate the function of HURP in K-fiber stabilization and chromosome congression.

5 Material and Methods

5.1 Chemicals and materials

All chemicals were ordered from Sigma-Aldrich Chemical Company (Sigma, St Louis, MO), Fluka-Biochemika, Switzerland, Roth or Merck, unless otherwise stated. Components of growth media for *E. coli* and yeast were purchased from Difco Laboratories or Merck. The Minigel system was from Bio-Rad and the Hoefer SemiPHor Blotting system from Pharmacia-Biotech. Tabletop centrifuges were from Eppendorf.

5.2 Plasmid preparation and site directed mutagenesis

All cloning procedures were performed according to standard techniques, as described in Current Protocols in Molecular Biology, Wiley, 1999 Current Protocols in Molecular Biology, Wiley, 1999 and Molecular Cloning, A Laboratory Manual, 2nd Edition, Sambrook, J., Fritsch, E.F., Maniatis, Cold Spring Harbor Laboratory Press, 1989. Restriction enzymes were used as specified by the suppliers (NEB, Ipswich, MA) and ligation reactions were carried out using T4 DNA Ligase or a Rapid Ligation Kit (Roche Diagnostics, Indianapolis, IN). DNA extraction from agarose gels and plasmid DNA preparation were performed with Qiagen (Qiagen GmbH, Germany) Kits, as recommended by the manufacturer. PCR reactions were carried out in a RoboCycler Gradient 96 by using Pfu DNA polymerase, according to the manufacturer's instructions (Stratagene, La Jolla, CA). Primers used for PCR reactions are listed in Table 10.2 (Appendix). All constructs were verified by the in-house sequencing service.

For cloning, the following cDNAs were obtained from the "Deutsches Ressourcenzentrum für Genomforschung" (RZPD):

HURP / KIAA0008 (IRAKp961M1813), CHICA / C20Orf129 (IMAGp958M1212), importin α (IRAKp961J1471Q2) and importin β (IMAGp958F07162Q2).

All coding DNA sequences were amplified by PCR with specific primers and cloned into a pRCMV vector in-frame with a sequence encoding an amino-terminal FLAG, EGFP, Cherry or triple myc-tag. The Cherry-tagged vector was a kind gift from Sabine Elowe and Ran protein expression plasmids were a kind gift from Oliver Gruss (RZPD, Heidelberg).

5.3 Recombinant protein expression and purification

The HURP cDNA was subcloned into pVL1393 expression vectors (BD Biosciences Pharmingen, San Diego, CA), in frame with either a polyhistidine or a GST encoding sequence. Recombinant baculoviruses, encoding human His6- and GST-tagged HURP, respectively, were produced in Sf9 cells with the BaculoGold kit according to the manufacturer (BD Biosciences Pharmingen). For isolation of GST-tagged HURP, infected Sf9 cells were lysed in GST-lysis buffer (10mM HEPES, pH 7.7, 1% NP-40, 5 mM EGTA, 150 mM NaCl), which contained phosphatase inhibitors and protease inhibitors. GST-HURP was isolated from the cleared lysate with glutathione-Sepharose 4B beads (GE Healthcare, Buckinghamshire, UK), and the GST-tag was removed by over night incubation at 4°C with PreScission protease (Amersham Biosciences). For isolation of His6-tagged HURP, infected cells were resuspended in His6-lysis buffer (50 mM NaPhosphate buffer, pH 8.0, 10 mM imidazole, 150 mM NaCl, 0.5% NP-40), which contained protease and phosphates inhibitors. His6-tagged HURP was isolated from cleared cell lysates with NiNTA agarose (Qiagen) and eluted from the beads with 50 mM NaPhosphate buffer (pH 8.0), which contained 250 mM imidazole and 150 mM NaCl and dialyzed against PBS.

Full-length CHICA, tagged with MBP (maltose-binding protein) (MBP-CHICA, aa 1-585) was expressed and purified from *E. coli.* Recombinant His6-tagged Ran and importin proteins were expressed in *E. coli* and purified essentially, as described previously (Gorlich et al., 1994). The His-tagged Ran proteins (RanWT, RanT24N and RanQ69L) were expressed in *E.coli* at 37°C for 4 hr, after induction with 1 mM IPTG. Following centrifugation, the cells were resuspended in lysis buffer (300 mM NaCl, 8 mM Imidazole, 3 mM β-Mercaptoethanol, 2 mM $MgCl_2$) and lysed with a cell cracker. His6-tagged Ran proteins were then isolated from cleared cell lysates with NiNTA agarose (Qiagen), and eluted from the beads with elution buffer (20 mM Hepes, 100 mM KCl, 2 mM $MgCl_2$ 5% Glycerin, 1 mM DTT, pH 7.7), including 100 mM imidazole, followed by gel filtration on a superose 6 in elution buffer (including 10 mM EDTA for nucleotide exchange on RanQ69L) and dialysis of the clean peak fractions against PBS including 1 mM GTP in the case of RanQ69L, for 16 hr at 4°C. Recombinant proteins were shock-frozen in liquid nitrogen and stored at -80°C as 100 μl aliquots containing 5% glycerol.

5.4 Antibody production and testing

To produce the CHICA-specific antibody, a C-terminal fragment (residues 383-585) was fused to a N-terminal polyhistidine tag, by means of the bacterial expression vector pQE30 (Qiagen, Hilden, Germany). To produce a HURP-specific antibody, a N-terminal fragment (residues 1–401) was fused to a N-terminal polyhistidine tag, using pQE30. The fragments were expressed in *Escherichia coli* and purified from the pellet under denaturing conditions. First the pellet was dissolved in 6 M guanidium buffer (6 M guanidium, 0.1 M NaH_2PO_4, 0.01 M Tris-HCL, pH 8.0) and incubated with Ni-NTA agarose beads, as described by the manufacturer (Qiagen). Then the beads were washed with 6 M guanidium and 8 M urea buffer (8 M urea, 0.1 M NaH_2PO_4, 0.01 M Tris-HCL, pH 8.0) and boiled in sample buffer. After further purification on a preparative 10% SDS-PAGE gel, 250 µg of the protein was injected several times into New Zealand white rabbits (Charles River Laboratories, Romans, France). Anti-HURP and anti-CHICA antibodies were purified by applying 2 ml immune serum onto nitrocellulose filters (Schleicher & Schuell, Keene, NH), which contained 400 mg bound HURP- or CHICA fusion protein, respectively, and were blocked with 5% BSA in PBST (PBS + 0.05% Tween20). After 2 hr incubation, the filters were extensively washed with PBST, and anti-HURP or anti-CHICA antibodies, respectively were subsequently eluted from the filters with glycine buffer (100 mM, pH 2.8) and dialyzed against PBST.

The specificity of the polyclonal antibodies was tested by dot blotting. To this end, 1 µl of recombinant antigen or molecular weight marker (MW) as negative control were spotted on a membrane stripe blocked with PBST 5% milk for 30 min and incubated with pre-immune, 1st, 2nd or 3rd serum (1:500), respectively, for 1 hr on the shaker at room temperature. After washing with PBST, the stripes were incubated with anti-rabbit alkaline phosphatase (AP, 1:750) conjugated antibody for another hour on the shaker. The signal was detected with a fresh mix of 66 µl 4-nitro blue tetrazolium chloride (NBT) and 33 µl 5-bromo-4-chloro-3-indolyl-phosphate (BCIP) disodiumsalt, in 10 ml AP-buffer (100 mM NaCl, 5 mM $MgCl_2$, 100 mM Tris HCL, pH 9.5).

5.5 Cell culture and synchronization

HeLa S3, HEK293T, COS-7, and tsBN2 cells were maintained in DMEM (Invitrogen, Carlsbad, CA), supplemented with 10% heat-inactivated fetal calf serum (FCS) and penicillin/streptomycin (100 IU/ml and 100 mg/ml, respectively) and cultured in a 5% CO_2 atmosphere in humidified incubator. Cells were grown at 37°C, except for tsBN2 cells, which were cultured at 32°C. To arrest exponentially growing HeLa S3 cells at prometaphase, these cells were presynchronized at the G1/S phase boundary with 1.6 mg/ml aphidicolin for 14 hr. Subsequently, these cells were released for 6 hr in fresh pre-warmed medium, before 50 ng/ml nocodazole was added, and culturing was continued for an additional 6 hr. Mitotic cells were collected by mitotic shake-off, washed twice with PBS, and incubated in fresh pre-warmed medium. Cell samples were taken after release for various time intervals.

5.6 Transient transfections and siRNA

Plasmid transfections were performed with FUGENE6 reagent (Roche, Diagnostics, Indianapolis, IN), according to the manufacturer's instructions. SiRNAs were transfected with oligofectamine (Invitrogen, Carlsbad, CA), as described (Elbashir et al., 2001). Proteins were depleted with siRNA duplex oligonucleotides (Darmacon RNA Technologies, Lafayette, CO, and Qiagen), which targeted the following cDNA sequences: HURP duplex 1: AATGACTCGATCAGCTACTCA, HURP duplex 2: GGTGGCAAGTCAATAATAA, and CHICA duplex 1: CCAGGATAGCAAGCTCTCAAA. A siRNA duplex (GL2) targeting luciferase (Elbashir et al., 2001), was used as a siRNA control.

5.7 Cell extracts, Western blots, and immunoprecipitations

For cell extracts of HeLa S3 or HEK293(T) cells, the cells were washed once with ice-cold PBS, including 1 mM PMSF, scraped or shaked off the plate and resuspended in ice-cold RIPA lysis buffer (50 mM Tris, pH 7.4, 150 mM NaCl, 1% NP-40, 0.5% Na-Desoxycholate), which contained 1 mM DTT, 30 μg/ml RNase, 30 μg/ml DNase and protease and phosphatase inhibitors. For immunoprecipitations, cell extracts were generated in HEPES lysis buffer (50 mM HEPES, pH 7.4, 150 mM NaCl, 0.5% Triton-X100), including RNase, DNase and protease and phosphatase inhibitors. After 15 min on ice, lysed cells were centrifuged at 13000 rpm for 15 min

at 4°C. Protein concentrations in the cleared lysate were determined with the Dc protein assay (Bio-Rad Laboratories, Hercules, CA). For immunoprecipitation of endogenous HURP, affinity-purified anti-HURP antibody and pre-immune IgGs, respectively, were covalently coupled to Affi-prep Protein A beads (Bio-Rad Laboratories, Hercules, CA). Equal amounts of cleared HeLa S3 cell lysates from nocodazole arrested and released (30 min) mitotic cells were then incubated with these beads for 14 hr. Incubations were performed in a rotating wheel, at 4°C. Immune complexes were spun down and washed four times with the same lysis buffer and then boiled in SDS-PAGE sample buffer. For immunoprecipitation of transiently expressed myc-tagged proteins, anti-myc 9E10 antibodies, bound to protein G-Sepharose (GE Healthcare, Buckingham, UK) were used. Western blot membranes were probed with the following antibodies: pre-immune rabbit serum (1:200), anti-HURP serum (1:200), affinity purified polyclonal anti-HURP antibody (2 mg/ml), mouse anti-myc 9E10 mAb (1:10, culture supernatant), mouse anti-α-tubulin mAb (1:3000, Sigma, St. Louis, MO), mouse anti-importin β mAb (1:1000, Abcam, Cambridge, UK), and goat polyclonal anti-importin α antibody (1:1000, Abcam). Signals were detected by ECL Supersignal (Pierce Biotechnology, Rockford, IL), with a digital Fujifilm LAS-1000 camera, which was attached to an Intelligent Darkbox II (Raytest GmbH, Straubenhardt, Germany).

5.8 Immunofluorescence microscopy

Cells were either fixed with paraformaldehyde for 10 min at RT, followed by a 5 min permeabilization with 0.5% Triton-X100 at 4°C, fixed in -20°C methanol for 10 min, or simultaneously fixed and permeabilized for 10 min at RT in PTEMF buffer (20 mM PIPES, pH 6.8, 4% formaldehyde, 0.2% Triton-X100, 10 mM EGTA, 1 mM MgCl$_2$). Primary antibodies used in this study were: purified rabbit anti-HURP antibody (2 mg/ml), mouse anti-myc 9E10 mAb (1:10, culture supernatant), mouse anti-α-tubulin mAb (1:1000, Sigma), goat polyclonal anti-α-tubulin antibody (Cytoskeleton Inc., Denver, CO), and mouse anti-Hec1 mAb (1:1000, Abcam). Secondary antibodies conjugated either to Alexa 488, Alexa 555, Alexa 568, or Alexa 647 were used to visualize antibody staining (1:1000, Molecular Probes, Eugene, OR). DNA was stained with 4',6-diamidino-2-phenylindole (DAPI, 2 mg/ml). Immunofluorescence microscopy was performed with a Zeiss Axioplan II

microscope with a Plan Apochromat 633/1.40 oil immersion objective (Zeiss, Jena, Germany). Photographs were taken with a Micromax CCD camera (model CCD-1300-Y, Princeton Instruments, Trenton, NJ) and Metaview software (Vistrion Systems GmbH, Puchheim, Germany). For high-resolution images, a microscope (Deltavision; Applied Precision, Issaquah, WA) on a base (Olympus IX71; Applied Precision) that was equipped with PlanApo 603/1.40 oil and UplanApo 1003/1.35 oil immersion objectives (Olympus) and a camera (CoolSNAP HQ; Photometrics) was used for collecting 0.15 mm distanced optical sections in the z-axis. For deltavision figures, images at single focal planes were processed.

5.9 Live-cell imaging

For live-cell imaging, a HeLa S3 cell line, stably expressing histone H2B-GFP was used. Cells were treated with aphidicolin (1.6 mg/ml) for 14 hr, to arrest the cells at the G1/S phase boundary. Upon release from this block, cells were treated with siRNAs and 10 hr later, aphidicolin was added again for an additional 14 hr, to synchronize cells at the G1/S phase boundary. 8 hr after release from this second block, the medium was changed into CO_2-independent medium and the culture dish was placed onto a heated sample stage (37°C). Live-cell imaging was performed with a Zeiss Axiovert-2 microscope and a Plan Neofluar 40x objective. Metaview software (Visitron Systems GmbH) was used to collect, and process data. Images were captured with 50 ms exposure times with 2 min intervals for 16 hr.

5.10 In-vitro microtubule co-sedimentation and bundling assays

Rhodamine-labeled and unlabeled porcine tubulin was a kind gift from Thomas Mayer. For MT polymerization, 100 μM tubulin was incubated for 40 min at 37°C with 20 mM GTP in BRB80 buffer (80 mM K-pipes, 1 mM EGTA, 1 mM $MgCl_2$, pH 6.8) containing 50% glycerol. Subsequently, 35 μM paclitaxel (taxol) was added to stabilize the formed MTs and incubation was continued for an additional 40 min. The reaction mixture was then centrifuged at 68000 rpm for 30 min at 35°C. The pellet was resuspended in BRB80, which contained 5 μM taxol, to a final concentration of 5 mg/ml MTs (50 μM tubulin) and stored at room temperature. For *in vitro* MT co-sedimentation assays, 2 μg of recombinant human HURP or human CHICA (MBP- tagged full-length CHICA) respectively were incubated in BRB80 buffer for 15 min at 25°C, with and without 15 μg MTs, in a total volume of 30 μl. In parallel, the

same was done with 2 μg BSA as a negative control. Samples were then centrifuged through a 40% glycerol-BRB80-cushion at 55000 rpm for 20 min at 25°C. Proteins in the pellet and supernatant fractions were separated by SDS-PAGE and visualized by Coomassie blue staining. *In vitro* MT bundling was analyzed with rhodamine-labeled MTs. MTs were mixed with HURP or BSA, as described above. After 5 min incubation at RT, these samples were analyzed by immunofluorescence microscopy. To study the effect of importin proteins on the MT bundling activity of HURP, these recombinant proteins were added in a 16-fold excess over HURP. Recombinant RanQ69L and RanT24N were added at a final concentration of 12 μM.

5.11 Yeast two-hybrid analysis

Yeast two-hybrid screens were performed by Anja Wehner with a system described previously (James et al., 1996). A HURP cDNA fragment, encoding residues 1–550, was cloned into a pFBT9 Gal4 DNA binding domain vector. A human HEK293 two-hybrid library (BD Clontech, Mountain View, CA) was screened, and clones able to activate both the Ade2 and His3 selection markers, specifically in the presence of the bait, were selected.

5.12 In vitro coupled transcription translation

The respective 3xmyc- and FLAG-tagged proteins were generated by *in vitro* coupled transcription translation (IVT) with the TNT T7 Quick coupled Transcription/Translation System (Promega, Madison, WI). For immunoprecipitation, these reactions were diluted in HB buffer (25 mM HEPES, pH 7.4, 0.5% NP40, 150 mM NaCl, 2 mM EGTA, 2 mM MgCl$_2$), which contained 1 mM DTT, RNase, DNase and protease and phosphatase inhibitors, and incubated with anti-myc (9E10) antibody coated Protein G beads (Pierce Biotechnology) or anti-FLAG®M2 Affinity gel (Sigma), for 90 min at 4°C, on a rotating wheel. After washing, samples were boiled in sample buffer and equal amounts of protein from input and IP were separated by SDS-PAGE and probed by Western blotting with anti-myc (9E10) monoclonal and anti-FLAG polyclonal rabbit antibodies, respectively.

5.13 Gel filtration of cell extracts

Interphase and mitotic extracts were produced from several triple flasks of HeLa S3 cells, presynchronized with 4 mM thymidine for 14 hr and released in thymidine or nocodazole (50 ng/ml) block over night. After a 50 min release, cells were harvested

by scraping or shake off, respectively. Cells were then washed in ice cold PBS, including 1 mM PMSF and lysed in detergent-free HB buffer (25 mM HEPES, pH 7.4, 150 mM NaCl, 2 mM EGTA, 2 mM $MgCl_2$), which contained 1 mM DTT, 30 μg/ml RNase, 30 μg/ml DNase and protease and phosphatase inhibitors by mechanical sheering with a 7 ml Tenbroek Tissue Grinder (Wheaton, USA) for 30 min at 4°C. The lysates were then cleared by centrifugation at 13000 for 15 min and protein concentration was measured. Gelfiltration was performed with an Aekta-Prime® LC-Device (Amersham). 500 μl of cell extract (6 mg/ml) were filtered with a 0.2 μm filter (Millex GV, Millipore) and loaded on a previously PBS-equilibrated Superose 12 10/300 GL Tricorn column (Amersham-Pharmacia). The separation was carried out at a flow rate of 0.3 ml/min and 1 ml fractions were collected. Proteins in the elution were detected by an UV-spectrometer and blotted on a chromatogram. Peak fractions were analyzed by SDS-PAGE and Western blotting. The calibration was done with a standard curve from the elution profile of Ferritin (440 kDa), Aldolase (158 kDa), Ovalbumin (43 kDa) and Ribonuclease A (13.7 kDa) in PBS.

5.14 Mass spectrometry

The sample preparation and MS analysis was done by René Lenobel. Coomassie-stained protein bands were in-gel digested with modified trypsin (sequencing grade; Promega) (Shevchenko et al., 1996) and desalted by using homemade mini-reverse phase columns (Gobom et al., 1999). Matrix-assisted laser desorption/ionization time-of-flight (MALDI-TOF) mass spectra were acquired on a Reflex III instrument (Bruker Daltonik, Bremen, Germany), in both positive and negative reflector modes. A 2,5-dihydroxybenzoic acid matrix (Bruker Daltonik, Bremen) was used. Phosphoproteins were isolated by immobilized metal (Fe3+) affinity chromatography (IMAC) (Andersson and Porath, 1986). For the search of new phosphorylation sites, mass spectra were scanned for peptides, which showed a difference of 80 mass units. Candidate phosphopeptides were submitted to post-source decay fragment ion analysis (Hoffmann et al., 1999). Peptides with the typical losses of 98 mass units (phosphoric acid) and 80 mass units (phosphate) were accepted as phosphopeptides. To sequence peptides by tandem mass spectrometry, samples were dissolved in H_2O/Methanol (1/1, v/v) with 2% formic acid, filled into nanospray needles (Protana), and analyzed on a Q-TOF Ultima mass spectrometer.

6 Appendix

6.1 Abbreviations

All units are abbreviated according to the International Unit System.

aa	Amino acid(s)
AD	Activator domain
AIDA	Advanced Data Image Analyzer
AMP-PNP	Adenosine 5'-monophosphate
AMT	Astral microtubule
AP	Alkaline phosphatase
APC	Anaphase promoting complex
ATP	Adenosine 5'-triphosphate
BCIP	5-bromo-4-chloro-3-indolyl-phosphate
BD	Binding domain
BLAST	Basic Local Alignment Search Tool
BSA	Bovine serum albumin
CC	Coiled coil
Cdk	Cyclin-dependent kinase
CID	Collision-induced dissociation
C-terminus	Carboxyl terminus
DAPI	4´,6-diamidino-2-phenylindole
DNA	Deoxyribonucleic Acid
dNTP	Deoxynucleosidtriphosphate
DTT	Dithiothreitol
DUF	Domain of unknown function
ECL	enhanced chemiluminescence
E. coli	*Escherichia coli*
EDTA	ethylenediaminetetraacetic acid
EGFP	enhanced green fluorescent protein
EGTA	ethylene glycol-bis(2-aminoethylether)-N,N,N',N'-tetraacetic acid
Fbx7	F-box protein 7
FCS	Fetal calf serum

FSM	Fluorescence speckle microscopy
γTuRC	Gamma tubulin ring complex
GEF	Guanosine exchange factor
GFP	green fluorescent protein
GKAP	Guanylate kinase-associated protein homology domain
GTP	Guanosine 5'-triphosphate
H2B	Histone 2B
HC	heavy chain
HCl	hydrochloric acid
HEPES	N-2-Hydroxyethylpiperazine-N'-2-ethane sulfonic acid
Hs	*Homo sapiens*
hr	hours
IF	Immunofluorescence
IgG	Immunoglobulin G
IMAC	immobilized metal (Fe3+) affinity chromatography
IMT	Interpolar microtubule
IP	Immunoprecipitation
IPTG	Isopropyl-beta-D-thiogalactopyranoside
IU	International units
IVT	*in vitro* coupled transcription translation
K-fibers	Kinetochore fibers
kDa	kilo Daltons
KMT	Kinetochore microtubule
KRM	Kinesin related motor protein
LB	Luria broth
LC	light chain
LMB	Leptomycin B
mAb	monoclonal antibody
MALDI	Matrix-assisted laser desorption/ionization
MAP	Microtubule-associated protein
MS	Mass spectrometry
MT	Microtubule
MTOC	Microtubule organizing centre

APPENDIX

MW	Molecular weight
NBT	4-nitro blue tetrazolium chloride
n.d.	not determined
NE	Nuclear envelope
NES	Nuclear export sequence
Ni-NTA	Nickel-nitriloacetic acid
NLS	Nuclear localization sequence
N-terminus	Amino terminus
OD	optical density
PBS	Phosphate-buffered saline
PCM	Pericentriolar matrix
PCR	Polymerase chain reaction
PDB	Protein Data Bank
Pfam	Protein family database
Pfu	*Pyrococcus furiosus*
PIPES	1,4-Piperazinediethansulfonic acid
PMSF	Phenylmethylsulfonyl fluoride
PreI.	pre-immune
Q-Tof	quadrupole time-of-flight
Rb	Rabbit
RNA	Ribonucleic Acid
rpm	Rounds per minute
RT	Room temperature
SAC	Spindle assembly checkpoint
SDS-PAGE	Sodium dodecylsulfate polyacrylamid gelelectrophoresis
siRNA	small interfering RNA
SMART	Simple Modular Architecture Research Tool
Sup	Supernatant
Tris	Tris(hydroxymethyl)-aminomethan
WB	Western blot
WT	Wild-type
X. laevis	*Xenopus laevis*

6.2   List of primers

name	Sequence (5' – 3')	purpose
M1565	TGAGGATCCATGTCTTCATCACATTTTGCCAGTCGACAC	full length HURP-WT
M1566	CCGCTCGAGTACAAATTCTCCTGGTTGTAGAGGTGAAAAAG	full length HURP-WT
M3282	GGCGGATCCATGGAGCTGATCACCATTCTCG	Importin β from cDNA
M3283	CTTGCGGCCGCTCAAGCTTGGTTCTTCAGTTTCCTC	Importin β from cDNA
M3284	GGCGGATCCATGTCCACCAACGAGAATGCTAATAC	Importin α from cDNA
M3285	GGCCTCGAGCTAAAAGTTAAAGGTCCCAGGAG	Importin α from cDNA
M3336	GATCCATGTCTTCATCACATTTTGCCAGTGCACACGCTGCAGATATAAGT	HURP-NLSIA (R9A/R11A/K12A)
M3337	ACTTATATCTGCAGCGTGTGCACTGGCAAAATGTGATGAAGACATG	HURP-NLSIA (R9A/R11A/K12A)
M3338	ATAAGTACTGAAATGATTGCAACTGCAATTGCTCATGCTGCATCACTGTCTCAGAAAG	HURP-NLSIB (R20A/K22A/R26A/K27A)
M3787	GGTGATCAAGCAGCACAGATGCTCC	HURP-NLSIIA (R90A/K91A)
M3788	CTGTGCTGCTTGATCACCTAGAATAG	HURP-NLSIIA (R90A/K91A)
M3789	GAGAGAGGCAGCTGCAGGAATATTTAAAGTG	HURP-NLSIIB (K112A/K114A/R115A)
M3705	ACCTAGAATAGTTTTCATTGCCCTTGGC	HURP-ΔCC2
M3706	GGGCAATGAAAACTATTCTAGGTCGTTATAGACCTGATATGCCTTGTTTTCTTTTATC	HURP-ΔCC2
M3707	ACACCTATGGCCCCCAGAAGTGCCAATGC	HURP-T330A
M3708	GGCACTTCTGGGGGGCCATAGGTGTTACTTG	HURP-T330A
M4332	ACACCTATGGACCCCAGAAGTGCCAATGC	HURP-T330D
M4333	GGCACTTCTGGGGTCCATAGGTGTTACTTG	HURP-T330D
M4620	GGAAGGATATAGCTACTGAAATGATTAGAAC	HURP-S15A
M4621	TCATTTCAGTAGCTATATCCTTCCTGTGTCG	HURP-S15A
M4624	GCTTTTTTGGCACCCAGTTACACCTGGACTCC	HURP-T338A
M4625	CCAGGTGTAACTGGGTGCCAAAAAAGCATTGG	HURP-T338A
M4628	TAAAGGAGACTGCCTGTACAGATCTGGATGG	HURP-T502A
M4629	CCAGATCTGTACAGGCAGTCTCCTTTATACC	HURP-T502A

6.3   Table of plasmids

Name	Tag	Gene	Insert	Vector
HS342	myc	C20orf129	WT - full length	pcDNA3.1/3xmyc-C
HS343	GST	C20orf129	WT - full length	pGEX-6P-3
HS344	GFP	C20orf129	WT - full length	pEGFP-T7/C1
HS345	myc	C20orf129	WT - N-term.	pcDNA3.1/3xmyc-B
HS346	myc	C20orf129	WT - C-term.	pcDNA3.1/3xmyc-B
HS348	AD	C20orf129	WT - full length	pGAD-C1
HS350	myc	C20orf129	WT - full length	pcDNA3.1/3xmyc-C
HS351	myc	C20orf129	WOS - full length	pcDNA3.1/3xmyc-C
HS352	GST	C20orf129	WT - C-term.	pGEX-6P-3
HS374	BD	C20Orf129	WT - full length	pFBT9'
SN1	C-term. HIS	C20Orf129	WOS - full length	pET-28b-HS1
SN2	FLAG	C20Orf129	WOS - full length	pcDNA3.1-CFLAG
SN3	N-term. HIS	C20Orf129	WT - N-term. (aa 1-383)	pET-28b-HS2
SN4	C-term. HIS	C20Orf129	WOS - N-term. (aa 1-383)	pET-28b-HS1
SN5	N-term. HIS	C20Orf129	WT - C-term. (aa 383-585)	pET-28b-HS2
SN6	C-term. HIS	C20Orf129	WOS - C-term. (a.a 380-585)	pET-28b-HS1
SN7	N-term. HIS	C20Orf129	WT - C-term. (aa 471-585)	pET-28b-HS2
HS268	myc	KIAA0008	WT - full length	pcDNA3.1/3xmyc-C
HS274	HIS	KIAA0008	WT - full length	pQE-30
HS275	HIS	KIAA0008	WT - N-term. (aa 1-404)	pQE-30
HS276	HIS	KIAA0008	WT - C-term. (aa 405-846)	pQE-30
HS277	EGFP	KIAA0008	WT - full length	pEGFP-T7/C1
HS278	HIS-preScission	KIAA0008	WT - full length	pVL1393
HS279	GST-preScission	KIAA0008	WT - full length	pVL1393
HS290	myc	KIAA0008	WT - C-term. (aa 405-846)	pcDNA3.1/3xmyc-A
HS291	myc	KIAA0008	WT - N-term. (aa1-404)	pcDNA3.1/3xmyc-C
HS292	Flag	KIAA0008	WT - full length	pcDNA3.1/Flag-C
HS293	Flag	KIAA0008	WT - N-term. (aa 1-404)	pcDNA3.1/Flag-C
HS294	Flag	KIAA0008	WT - C-term. (aa 405-846)	pcDNA3.1/Flag-A
HS295	myc	KIAA0008	WT - N2-term. (aa 1-201)	pcDNA3.1/3xmyc-C
HS296	myc	KIAA0008	WT - C2-term. (aa 202-846)	pcDNA3.1/3xmyc-A
HS304	myc	KIAA0008	WT - N3-term. (aa 1-115)	pcDNA3.1/3xmyc-C
HS305	myc	KIAA0008	WT - C3-term. (aa 116-846)	pcDNA3.1/3xmyc-A
HS307	myc	KIAA0008	WT - N5-term. (aa 0-150)	pcDNA3.1/3xmyc-C
HS308	myc	KIAA0008	WT - N6-term. (aa 0-550)	pcDNA3.1/3xmyc-C
HS309	myc	KIAA0008	WT - N7-term. (aa 60-150)	pcDNA3.1/3xmyc-C
HS310	myc	KIAA0008	WT - N8-term. (aa 60-200)	pcDNA3.1/3xmyc-C
HS311	myc	KIAA0008	WT - N9-term. (aa 60-550)	pcDNA3.1/3xmyc-C
HS333	myc	KIAA0008	WT - N10-term. (aa 1-150)	pcDNA3.1/3xmyc-C
HS334		KIAA0008	WT - N11-term (aa 568-846)	pCR4-TOPO
HS335	myc	KIAA0008	WT - N12-term (aa 1-622)	pcDNA3.1/3xmyc-C
HS336	myc	KIAA0008	WT - N13-term (aa 1-700)	pcDNA3.1/3xmyc-C

Name	Tag	Gene	Insert	Vector
HS339	GST	KIAA0008	WT - C-term. (aa 405-846)	pGEX-6P-3
HS340	GST	KIAA0008	WT - N2-term. (aa 1-201)	pGEX-6P-3
HS341	GST	KIAA0008	WT - N7-term. (aa 60-150)	pGEX-6P-3
SN8		Importin α	Importin α 1A (IRAKp961J1471Q2)	pOTB7
SN9		Importin α	Importin α 1B (IRAKp961G1613Q2)	pOTB7
SN10		Importin β	Importin β (IMAGp958F07162Q2)	pOTB7
SN11	myc	Importin α	Importin α 1A / WT - full length	pcDNA3.1/3xmyc-C
SN12	myc	Importin α	Importin α 1B / WT - full length	pcDNA3.1/3xmyc-C
SN13	myc	Importin β	Importin β / WT - full length	pcDNA3.1/3xmyc-C
SN14	HIS	Ran	WT - full length	pQE-32
SN15	HIS	Ran	RanQ69L - full length	pQE-32
SN16	HIS	Ran	RanT24L - full length	pQE-32
SN17	myc	Ran	WT - full length	pcDNA3.1/3xmyc-A
SN18	myc	Ran	RanQ69L - full length	pcDNA3.1/3xmyc-A
SN19	myc	Ran	RanT24L - full length	pcDNA3.1/3xmyc-A
SN20	myc	HURP	ΔCC1 (aa 60-846)	pcDNA3.1/3xmyc-A
SN21	myc	HURP	NLSIA (R9A/R11A/K12A)	pcDNA3.1/3xmyc-A
SN22	myc	HURP	NLSIB (R20A/K22A/R26A/K27A)	pcDNA3.1/3xmyc-A
SN23	myc	HURP	NLSIIA (R90A/K91A)	pcDNA3.1/3xmyc-A
SN24	myc	HURP	NLSIIB (K112A/K114A/R115A)	pcDNA3.1/3xmyc-A
SN25	myc	HURP	CC1 (aa 1-60)	pcDNA3.1/3xmyc-A
SN26	myc	HURP	ΔCC2 = 88-120 (aa 1-88 + 120-846)	pcDNA3.1/3xmyc-A
SN27	myc	HURP	NLSIA + ΔCC2 (SN21 + ΔCC2)	pcDNA3.1/3xmyc-A
SN28	HIS	HURP	CC2 (aa 60-150) (HS309)	pQE-30
SN29	HIS	HURP	CC1 + CC2 (aa 1-150) (HS307)	pQE-30
SN30	HIS	HURP	CC1 + 1/2 CC2 (aa 1-116) (HS304)	pQE-30
SN31	HIS	HURP	CC1 + CC2 (aa 1-201) (HS295)	pQE-30
SN32	FLAG	HURP	CC2 (aa 60-150) (HS309)	pcDNA3.1/Flag-C
SN33	myc	HURP	T330A - full length	pcDNA3.1/3xmyc-A
SN34	myc	HURP	T330D - full length	pcDNA3.1/3xmyc-A
SN35	myc	HURP	T330D (aa 1-404)	pcDNA3.1/3xmyc-A
SN36	myc	HURP	T330A (aa 1-404)	pcDNA3.1/3xmyc-A
SN37	MBP-HIS	HURP	WT - full length	pMAL-tFNHis
SN38	MBP-HIS	HURP	ΔCC1 (aa 60-846)	pMAL-tFNHis
SN39	myc	HURP	S15A full-length	pcDNA3.1/3xmyc-A
SN40	myc	HURP	T338A full-length	pcDNA3.1/3xmyc-A
SN41	myc	HURP	T502A full-length	pcDNA3.1/3xmyc-A
SN42	myc	HURP	T330A/T338A full-length	pcDNA3.1/3xmyc-A
SN43	Cherry	HURP	WT - full length	pcDNA3.1/Cherry
SN44	Cherry	HURP	T330A - full length	pcDNA3.1/Cherry
SN45	Cherry	HURP	T330D - full length	pcDNA3.1/Cherry
SN46	GFP	HURP	T330A - full length	pEGFP T7/C1
SN47	GFP	HURP	T330D - full length	pEGFP T7/C1

6.4   Alignments

A: Coiled coil domains and potential NLS-mutations in conserved basic residues

```
            1               *   * *                    **              42
Hs-HURP    MSSSHFASRHRKDISTEMIRTKIAHRKSLSQKENRHKEYERN
Mm-HURP    MLVSRFASRFRKDSSTEMVRTNLAHRKSLSQKENRHRVYERN
Gg-HURP    AATSQFTSRYKKDLSTETIRTKVAHRKSMLQKENRHKMFEKG
Xt-HURP    ETRTQFTGRYKKDLSTENLRAKVAHRKSITQKENRHNEFKKC
                                        Coiled coil domain 1 (CC1)

            88  * *                       *  * *          120
Hs-HURP    DQRKQMLQKYKEEKQLQKLKEQREKAKRGIFKV
Mm-HURP    DQRKQLLQKYKEEKQLQKLKEQREKAKRGVFKV
Gg-HURP    NERREMLQRYKEEKELRKLKEQREKAKKGVFKV
Xt-HURP    KQRRDMLQRFKEEKELRKLKEQREKAAKGVFKC
                      Coiled coil domain 2 (CC2)
```

B: GKAP domain with conserved leucin residues (potential NES)

```
            432                                                       484
Hs-HURP    YFRNILQSETEKLTSHCFEWDRKLELDIPDDAKDLIRTAVGQTRLLMKERFKQ
Mm-HURP    YFRKILQSETDRLTSHCQEWEGKLDLDIPDEAKGLIRTTVGQTRLLIKERFKQ
Gg-HURP    YFRNILQSETERLMSQCLQWDGKLELGIPEDAEDLICTTVGQTRLLIAERFKQ
Xt-HURP    YFRDTLKSEIARLKQLCCEWDKRIELDIPEDAKDLIRTTVGQTRLLMCERFKQ

                                                                     537
Hs-HURP    FEGLVDDCEYKRGIKETTCTDLDGFWDMVSFQIEDVIHKFNNLIKLEESGWQV
Mm-HURP    FEGLVDNCEYKRGEKETTCTDLDGFWDMVSFQVDDVNQKFNNLIKLEASGWKD
Gg-HURP    FEGLVDNCEFKRGEKETTCTDLDGFWDMINFQIEDVNKKFDDLQKLQDNKWQP
Xt-HURP    FEGLVDNCEFKRGEKETTCTDLDGFWDMIYFQIEDVGKKFINLGKMEENSWQQ

                                                        GH1 domain
```

C: Prediction of the NES of HURP by NetNES
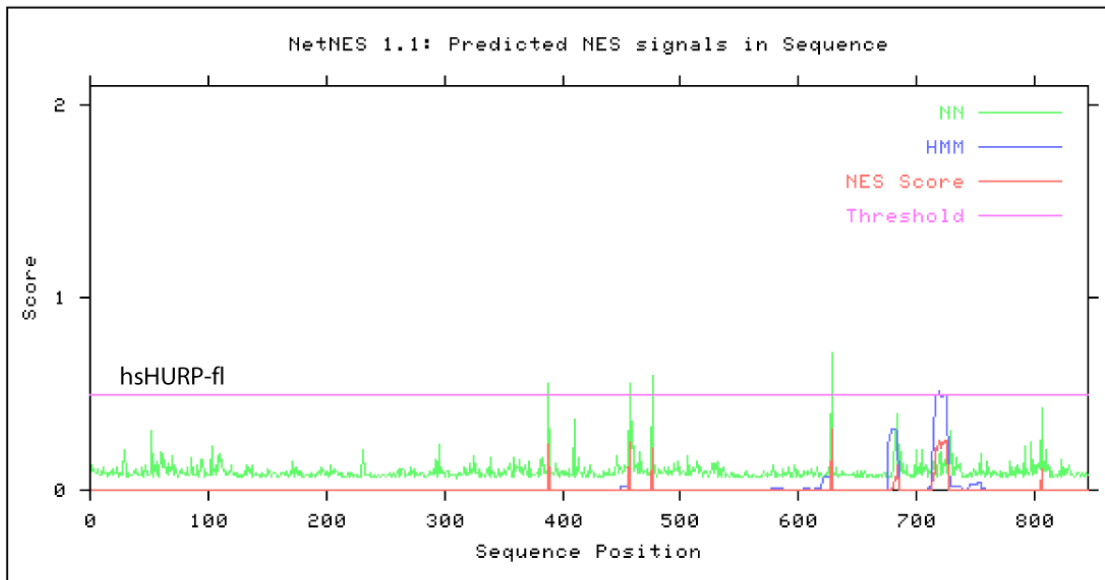
D: HURP phosphorylation site (T330), predicted by MS

```
                    330
                     *
    Hs-HURP    ----PMTPRSANAFL----
    Mm-HURP    ----PLSPRSANAFL----
    Gg-HURP    ----PMTPSRANAFL----
    Xt-HURP    ----PMTPSRANAFL----
```

6.5 Gel filtration Chromatograms on Superose 12
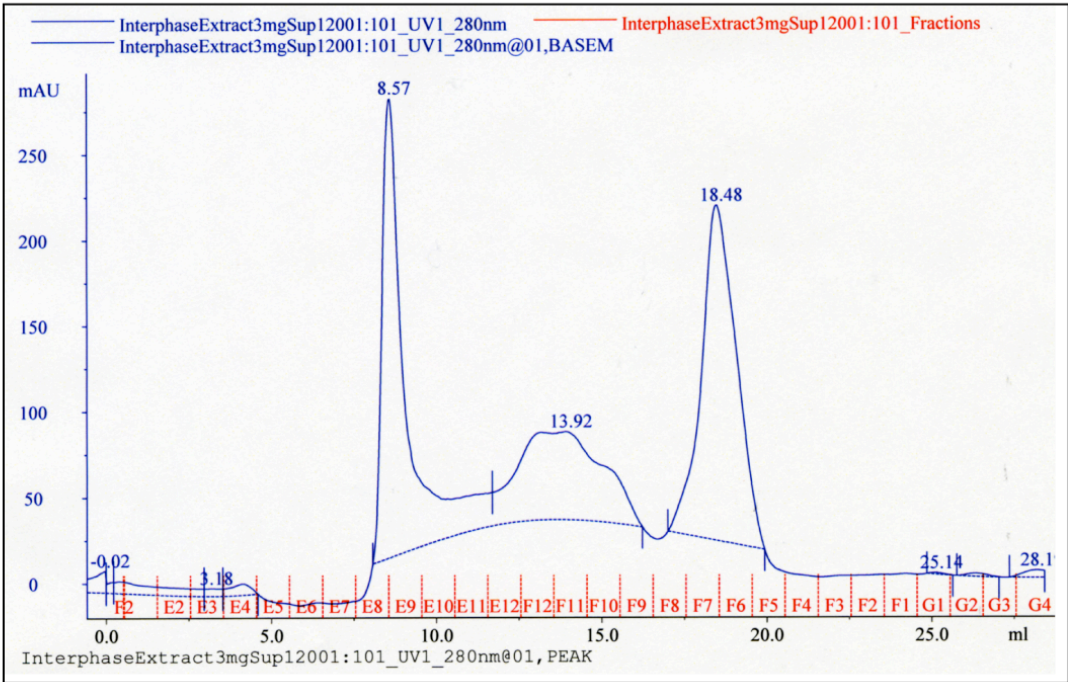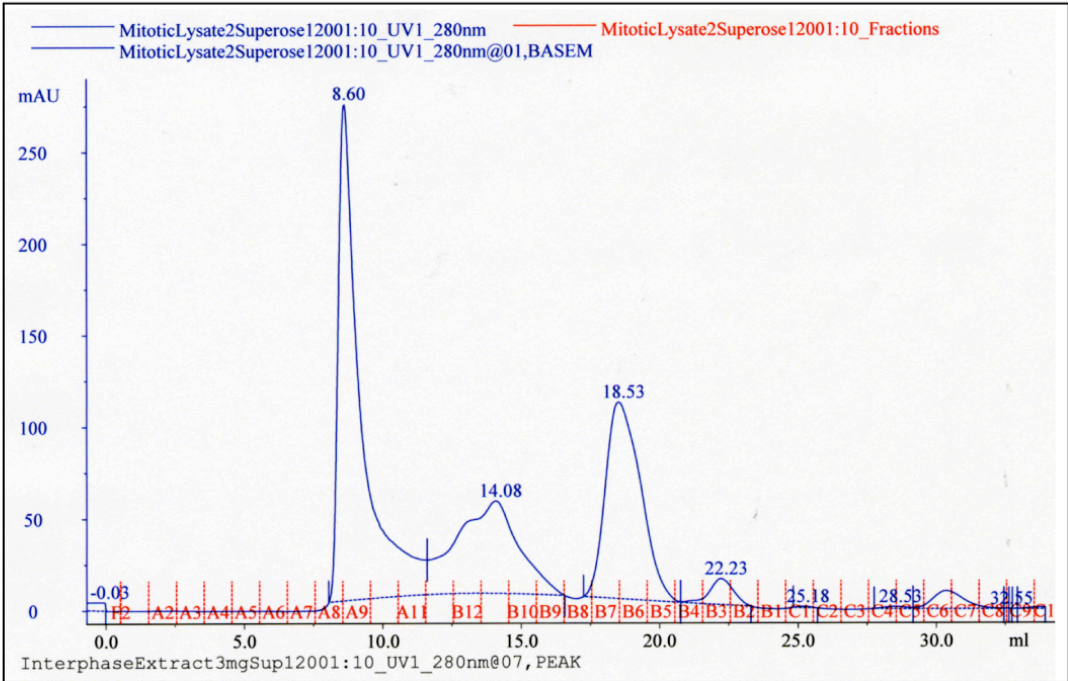
Figure 43. Size exclusion chromatography of mitotic and interphase cell extracts
(A) An interphase cell extract was produced from several triple flasks of HeLa S3 cells that were previously synchronized by a double thymidine-block. 3 mg of lysate in detergent-free HB-buffer were then loaded on a superose 12 column and separated by gel filtration.
(B) A mitotic cell extract was produced by shake-off from several triple flasks of HeLa S3 cells that were previously synchronized with thymidine-, followed by nocodazole block. 3 mg of lysate in detergent-free HB-buffer were then loaded on a superose 12 column and separated by gel filtration.

Danksagungen

Zunächst möchte ich mich bei Herrn Prof. Erich Nigg dafür bedanken, dass er mir die Chance gegeben hat in einem so professionellen und internationalen Umfeld meine Doktorarbeit zu machen. Es hat mir sehr viel bedeutet hier am Max-Planck Institut in seiner Abteilung forschen zu können. Als nächstes möchte ich mich bei Herman Silljé, meinem Supervisor dafür bedanken, dass ich sein hochinteressantes Projekt übernehmen durfte und zu dessen erfolgreichem Gelingen beitragen konnte. Sowohl fachlich wie auch menschlich stand mir Herman stets mit Rat und Tat zur Seite und hat mich mit seinem Enthusiasmus stets inspiriert.

Als nächstes möchte ich mich bei allen "Angels" bedanken: Anja H., Eunice, Anna und Anja W. Sie alle waren an dem HURP Projekt beteiligt und ich möchte mich hier in aller Form für ihre Unterstützung bedanken. Insbesondere gilt mein Dank Anja W., die durch Klonierungen, Y2H Screens und Protein Aufreinigungen einen wesentlichen Beitrag zu meinen Ergebnissen geleistet hat. Anja H. und Eunice waren für mich Vorbilder in Bezug auf Perfektionismus und kreatives Chaos. Als nächstes möchte ich mich bei Anna bedanken. Ich bin froh, dass wir unser Projekt gemeinsam zu Ende führen konnten und darüber zu Freunden geworden sind. Ich bin sicher sie wird eine hervorragende Gruppenleiterin und wünsche Ihr mit allen verbleibenden Laborkollegen alles Gute für die Zukunft in Basel oder anderswo. Außerdem bin ich Anna, Tom und Sabine sehr dankbar, dass sie sich die Zeit genommen haben meine Doktorarbeit sowohl inhaltlich als auch sprachlich Korrektur zu lesen und die Geduld hatten alle meine Fragen zu diskutieren. Bei Sabine möchte ich mich außerdem für Reagenzien und Diskussionen sowie nützliche Ratschläge bezüglich meines Projektes bedanken. Bei Tom möchte ich mich für seinen guten Musikgeschmack bedanken, und dass er und Luca wesentlich zur guten Atmosphäre in unserem Labor beigetragen haben. Außerdem danke für die Kicker-Sessions in den Bergen und gute Ratschläge wie man auch ohne Baggy-Pants zu einem coolen Snowboarder werden kann. Bei Stefan Hümmer möchte ich mich besonders für seine Hilfe und Geduld mit dem Live-cell Mikroskop, sowie Reagenzien und Unterstützung beim Erlernen des Umgangs mit Mikrotubuli bedanken. Weiter, danke ich der ganzen Mayer-Gruppe für wichtige Anregungen bezüglich meines Projektes. Weitere Kollegen, die mich unterstützt haben sind

Susanne B., Kerstin und Christoph und ich möchte mich insbesondere bei Christoph bedanken, der mir gezeigt hat, dass man für seine Sache kämpfen muss und trotz Ruhm und Glory mit beiden Füßen auf dem Boden bleiben bzw. auf den Bierbänken tanzen kann. Auch im Centrosomenlabor arbeiten nette Menschen und so möchte ich mich vor allem bei Thorsten und Jens bedanken, dass sie mit ins kalte Wasser gesprungen sind. Last but not least möchte ich mich bei Albert und Rainer für (bio)informatischen Beistand und Alison für ihr besonderes Verständnis für meine persönliche Situation bedanken.

Mein ganz besonderer Dank gilt meiner Familie, zu allererst meiner Mutter, die mich auch in schweren Zeiten in allem gefördert hat und immer für mich da war, sowie meinen Schwiegereltern, die uns gerade in den letzten Jahren sehr geholfen haben. Außerdem möchte ich mich bei meinen Großeltern für Ihre Unterstützung bedanken, insbesondere meinem Opa und meiner Omi, da sie schon früh mein Interesse für die Biologie geweckt haben. Außerdem möchte ich mich bei meinen Freundinnen, Dani, Sabine, Daniela, Anna, Uschi, Vera und Vivi bedanken. Sie hatten immer ein offenes Ohr für mich und ich konnte mit ihnen die schönen Dinge des Lebens genießen. Als nächstes möchte ich mich bei Katha und Doffa bedanken, die nicht nur gute Freunde sondern auch Teil unserer Familie geworden sind und immer da waren, wenn man sie brauchte. Weiter gebührt mein ausdrücklicher Dank Vicky, unserer Kinderfrau, ohne deren unermüdlichen Einsatz diese Arbeit nicht möglich gewesen wäre. Die Anstellung von Vicky wurde uns von der Christiane Nüsslein-Volhard Stiftung ermöglicht. Es bleibt zu hoffen dass weitere diesem Beispiel folgen, damit Kinder endlich kein Hinderungsgrund mehr für eine Promotion sind! In diesem Zusammenhang möchte ich mich auch bei Conchi, Gisela, Michaela, Mirjam, Margit und natürlich der Köchin des Kinderhauses bedanken, die meine Mädchen so wunderbar begleitet haben, so dass ich in Ruhe meiner Arbeit nachgehen konnte. Außerdem möchte ich mich bei allen Kinderhauseltern bedanken, die spontan bereit waren einzuspringen, wenn meine Experimente mal wieder länger dauerten.

Letztlich bleibt mir nur noch mich bei Sarah und Lisa zu bedanken. Danke, dass ihr mich ertragen habt und mir gezeigt habt was wirklich wichtig ist im Leben. Alexander, ohne Dich wäre das alles nicht möglich gewesen und ich danke Dir, dass Du an meiner Seite warst in guten und in schlechten Zeiten. Danke für alles, für alles was war und was noch kommen wird.

References

Andersson, L., and Porath, J. (1986). Isolation of phosphoproteins by immobilized metal (Fe3+) affinity chromatography. Anal Biochem *154*, 250-254.

Antonio, C., Ferby, I., Wilhelm, H., Jones, M., Karsenti, E., Nebreda, A. R., and Vernos, I. (2000). Xkid, a Chromokinesin Required for Chromosome Alignment on the Metaphase Plate. Cell *102*, 425-435.

Arnaoutov, A., Azuma, Y., Ribbeck, K., Joseph, J., Boyarchuk, Y., Karpova, T., McNally, J., and Dasso, M. (2005). Crm1 is a mitotic effector of Ran-GTP in somatic cells. Nat Cell Biol *7*, 626-632.

Ball, J. R., and Ullman, K. S. (2005). Versatility at the nuclear pore complex: lessons learned from the nucleoporin Nup153. Chromosoma *114*, 319-330.

Ban, K. H., Torres, J. Z., Miller, J. J., Mikhailov, A., Nachury, M. V., Tung, J. J., Rieder, C. L., and Jackson, P. K. (2007). The END network couples spindle pole assembly to inhibition of the anaphase-promoting complex/cyclosome in early mitosis. Dev Cell *13*, 29-42.

Barr, F. A., Sillje, H. H., and Nigg, E. A. (2004). Polo-like kinases and the orchestration of cell division. Nat Rev Mol Cell Biol *5*, 429-440.

Bastiaens, P., Caudron, M., Niethammer, P., and Karsenti, E. (2006). Gradients in the self-organization of the mitotic spindle. Trends in Cell Biology *16*, 125-134.

Basto, R., Lau, J., Vinogradova, T., Gardiol, A., Woods, C. G., Khodjakov, A., and Raff, J. W. (2006). Flies without centrioles. Cell *125*, 1375-1386.

Bayliss, R., Sardon, T., Vernos, I., and Conti, E. (2003). Structural basis of Aurora-A activation by TPX2 at the mitotic spindle. Mol Cell *12*, 851-862.

REFERENCES

Belmont, L. D., and Mitchison, T. J. (1996). Identification of a protein that interacts with tubulin dimers and increases the catastrophe rate of microtubules. Cell *84*, 623-631.

Bischoff, F., Klebe, C., Kretschmer, J., Wittinghofer, A., and Ponstingl, H. (1994). RanGAP1 Induces GTPase Activity of Nuclear Ras-Related Ran. Proceedings of the National Academy of Sciences *91*, 2587-2591.

Bischoff, F. R., Krebber, H., Smirnova, E., Dong, W., and Ponstingl, H. (1995). Co-activation of RanGTPase and inhibition of GTP dissociation by Ran-GTP binding protein RanBP1. Embo J *14*, 705-715.

Bischoff, J. R., Anderson, L., Zhu, Y., Mossie, K., Ng, L., Souza, B., Schryver, B., Flanagan, P., Clairvoyant, F., Ginther, C.*, et al.* (1998). A homologue of Drosophila aurora kinase is oncogenic and amplified in human colorectal cancers. Embo J *17*, 3052-3065.

Blangy, A., Lane, H. A., d'Herin, P., Harper, M., Kress, M., and Nigg, E. A. (1995). Phosphorylation by p34cdc2 regulates spindle association of human Eg5, a kinesin-related motor essential for bipolar spindle formation in vivo. Cell *83*, 1159-1169.

Blower, M. D., Nachury, M., Heald, R., and Weis, K. (2005). A Rae1-Containing Ribonucleoprotein Complex Is Required for Mitotic Spindle Assembly. Cell *121*, 223-234.

Bonaccorsi, S., Giansanti, M. G., and Gatti, M. (1998). Spindle Self-organization and Cytokinesis During Male Meiosis in asterless Mutants of Drosophila melanogaster. J Cell Biol *142*, 751-761.

Brouhard, G. J., and Hunt, A. J. (2005). Microtubule movements on the arms of mitotic chromosomes: polar ejection forces quantified in vitro. Proc Natl Acad Sci U S A *102*, 13903-13908.

Burkhard, P., Stetefeld, J., and Strelkov, S. V. (2001). Coiled coils: a highly versatile protein folding motif. Trends in Cell Biology *11*, 82-88.

Carazo-Salas, R. E., Gruss, O. J., Mattaj, I. W., and Karsenti, E. (2001). Ran-GTP coordinates regulation of microtubule nucleation and dynamics during mitotic-spindle assembly. Nat Cell Biol *3*, 228-234.

Carazo-Salas, R. E., Guarguaglini, G., Gruss, O. J., Segref, A., Karsenti, E., and Mattaj, I. W. (1999). Generation of GTP-bound Ran by RCC1 is required for chromatin-induced mitotic spindle formation. Nature *400*, 178-181.

Carvalho, P., Tirnauer, J. S., and Pellman, D. (2003). Surfing on microtubule ends. Trends in Cell Biology *13*, 229-237.

Castoldi, M., and Vernos, I. (2006). Chromokinesin Xklp1 contributes to the regulation of microtubule density and organization during spindle assembly. Mol Biol Cell *17*, 1451-1460.

Caudron, M., Bunt, G., Bastiaens, P., and Karsenti, E. (2005). Spatial Coordination of Spindle Assembly by Chromosome-Mediated Signaling Gradients. Science *309*, 1373-1376.

Chan, E. H., Nousiainen, M., Chalamalasetty, R. B., Schafer, A., Nigg, E. A., and Sillje, H. H. (2005). The Ste20-like kinase Mst2 activates the human large tumor suppressor kinase Lats1. Oncogene *24*, 2076-2086.

Chook, Y. M., and Blobel, G. (2001). Karyopherins and nuclear import. Curr Opin Struct Biol *11*, 703-715.

Ciciarello, M., Mangiacasale, R., and Lavia, P. (2007). Spatial control of mitosis by the GTPase Ran. Cell Mol Life Sci *64*, 1891-1914.

REFERENCES

Cochran, J. C., Sontag, C. A., Maliga, Z., Kapoor, T. M., Correia, J. J., and Gilbert, S. P. (2004). Mechanistic analysis of the mitotic kinesin Eg5. J Biol Chem *279*, 38861-38870.

Compton, D. A. (2000). Spindle assembly in animal cells. Annu Rev Biochem *69*, 95-114.

Dasso, M. (2002). The Ran GTPase: Theme and Variations. Current Biology *12*, R502-R508.

Dasso, M., Seki, T., Azuma, Y., Ohba, T., and Nishimoto, T. (1994). A mutant form of the Ran/TC4 protein disrupts nuclear function in Xenopus laevis egg extracts by inhibiting the RCC1 protein, a regulator of chromosome condensation. Embo J *13*, 5732-5744.

Davis, T. N., and Wordeman, L. (2007). Rings, bracelets, sleeves, and chevrons: new structures of kinetochore proteins. Trends Cell Biol *17*, 377-382.

Desai, A., Maddox, P. S., Mitchison, T. J., and Salmon, E. D. (1998). Anaphase A Chromosome Movement and Poleward Spindle Microtubule Flux Occur At Similar Rates in Xenopus Extract Spindles. J Cell Biol *141*, 703-713.

Desai, A., and Mitchison, T. J. (1997). Microtubule polymerization dynamics. Annu Rev Cell Dev Biol *13*, 83-117.

Desai, A., Verma, S., Mitchison, T. J., and Walczak, C. E. (1999). Kin I kinesins are microtubule-destabilizing enzymes. Cell *96*, 69-78.

Elbashir, S. M., Harborth, J., Lendeckel, W., Yalcin, A., Weber, K., and Tuschl, T. (2001). Duplexes of 21-nucleotide RNAs mediate RNA interference in cultured mammalian cells. Nature *411*, 494-498.

Elia, A. E., Rellos, P., Haire, L. F., Chao, J. W., Ivins, F. J., Hoepker, K., Mohammad, D., Cantley, L. C., Smerdon, S. J., and Yaffe, M. B. (2003). The molecular basis for phosphodependent substrate targeting and regulation of Plks by the Polo-box domain. Cell *115*, 83-95.

Elowe, S., Hummer, S., Uldschmid, A., Li, X., and Nigg, E. A. (2007). Tension-sensitive Plk1 phosphorylation on BubR1 regulates the stability of kinetochore microtubule interactions. Genes Dev *21*, 2205-2219.

Ems-McClung, S. C., Zheng, Y., and Walczak, C. E. (2004). Importin {alpha}/{beta} and Ran-GTP Regulate XCTK2 Microtubule Binding through a Bipartite Nuclear Localization Signal. Mol Biol Cell *15*, 46-57.

Finn, R. D., Mistry, J., Schuster-Bockler, B., Griffiths-Jones, S., Hollich, V., Lassmann, T., Moxon, S., Marshall, M., Khanna, A., Durbin, R.*, et al.* (2006). Pfam: clans, web tools and services. Nucleic Acids Res *34*, D247-251.

Funabiki, H., and Murray, A. W. (2000). The Xenopus Chromokinesin Xkid Is Essential for Metaphase Chromosome Alignment and Must Be Degraded to Allow Anaphase Chromosome Movement. Cell *102*, 411-424.

Gadde, S., and Heald, R. (2004). Mechanisms and molecules of the mitotic spindle. Curr Biol *14*, R797-805.

Galjart, N. (2005). CLIPs and CLASPs and cellular dynamics. Nat Rev Mol Cell Biol *6*, 487-498.

Gard, D. L., and Kirschner, M. W. (1987). A microtubule-associated protein from Xenopus eggs that specifically promotes assembly at the plus-end. J Cell Biol *105*, 2203-2215.

Glover, D. M. (2005). Polo kinase and progression through M phase in Drosophila: a perspective from the spindle poles. Oncogene *24*, 230-237.

REFERENCES

Glover, D. M., Leibowitz, M. H., McLean, D. A., and Parry, H. (1995). Mutations in aurora prevent centrosome separation leading to the formation of monopolar spindles. Cell *81*, 95-105.

Gobom, J., Nordhoff, E., Mirgorodskaya, E., Ekman, R., and Roepstorff, P. (1999). Sample purification and preparation technique based on nano-scale reversed-phase columns for the sensitive analysis of complex peptide mixtures by matrix-assisted laser desorption/ionization mass spectrometry. J Mass Spectrom *34*, 105-116.

Golsteyn, R. M., Mundt, K. E., Fry, A. M., and Nigg, E. A. (1995). Cell cycle regulation of the activity and subcellular localization of Plk1, a human protein kinase implicated in mitotic spindle function. J Cell Biol *129*, 1617-1628.

Gorbsky, G. J., Sammak, P. J., and Borisy, G. G. (1988). Microtubule dynamics and chromosome motion visualized in living anaphase cells. J Cell Biol *106*, 1185-1192.

Gorlich, D., Prehn, S., Laskey, R. A., and Hartmann, E. (1994). Isolation of a protein that is essential for the first step of nuclear protein import. Cell *79*, 767-778.

Gorlich, D., Seewald, M. J., and Ribbeck, K. (2003). Characterization of Ran-driven cargo transport and the RanGTPase system by kinetic measurements and computer simulation. Embo J *22*, 1088-1100.

Groen, A. C., Cameron, L. A., Coughlin, M., Miyamoto, D. T., Mitchison, T. J., and Ohi, R. (2004). XRHAMM functions in ran-dependent microtubule nucleation and pole formation during anastral spindle assembly. Curr Biol *14*, 1801-1811.

Gruss, O. J., Carazo-Salas, R. E., Schatz, C. A., Guarguaglini, G., Kast, J., Wilm, M., Le Bot, N., Vernos, I., Karsenti, E., and Mattaj, I. W. (2001). Ran induces spindle assembly by reversing the inhibitory effect of importin alpha on TPX2 activity. Cell *104*, 83-93.

Gruss, O. J., and Vernos, I. (2004). The mechanism of spindle assembly: functions of Ran and its target TPX2. J Cell Biol *166*, 949-955.

Gruss, O. J., Wittmann, M., Yokoyama, H., Pepperkok, R., Kufer, T., Sillje, H., Karsenti, E., Mattaj, I. W., and Vernos, I. (2002). Chromosome-induced microtubule assembly mediated by TPX2 is required for spindle formation in HeLa cells. Nat Cell Biol *4*, 871-879.

Hanisch, A., Sillje, H. H., and Nigg, E. A. (2006). Timely anaphase onset requires a novel spindle and kinetochore complex comprising Ska1 and Ska2. Embo J *25*, 5504-5515.

Haren, L., and Merdes, A. (2002). Direct binding of NuMA to tubulin is mediated by a novel sequence motif in the tail domain that bundles and stabilizes microtubules. J Cell Sci *115*, 1815-1824.

Hayden, J. H., Bowser, S. S., and Rieder, C. L. (1990). Kinetochores capture astral microtubules during chromosome attachment to the mitotic spindle: direct visualization in live newt lung cells. J Cell Biol *111*, 1039-1045.

Heald, R. (2000). Motor function in the mitotic spindle. Cell *102*, 399-402.

Heald, R., Tournebize, R., Blank, T., Sandaltzopoulos, R., Becker, P., Hyman, A., and Karsenti, E. (1996). Self-organization of microtubules into bipolar spindles around artificial chromosomes in Xenopus egg extracts. Nature *382*, 420-425.

Heald, R., Tournebize, R., Habermann, A., Karsenti, E., and Hyman, A. (1997). Spindle Assembly in Xenopus Egg Extracts: Respective Roles of Centrosomes and Microtubule Self-Organization. J Cell Biol *138*, 615-628.

Heald, R., and Weis, K. (2000). Spindles get the Ran around. Trends in Cell Biology *10*, 1-4.

REFERENCES

Hinchcliffe, E. H., Miller, F. J., Cham, M., Khodjakov, A., and Sluder, G. (2001). Requirement of a centrosomal activity for cell cycle progression through G1 into S phase. Science *291*, 1547-1550.

Hoffmann, R., Metzger, S., Spengler, B., and Otvos, L., Jr. (1999). Sequencing of peptides phosphorylated on serines and threonines by post-source decay in matrix-assisted laser desorption/ionization time-of-flight mass spectrometry. J Mass Spectrom *34*, 1195-1204.

Howard, J., and Hyman, A. A. (2003). Dynamics and mechanics of the microtubule plus end. Nature *422*, 753-758.

Hsu, J. M., Lee, Y. C., Yu, C. T., and Huang, C. Y. (2004). Fbx7 functions in the SCF complex regulating Cdk1-cyclin B-phosphorylated hepatoma up-regulated protein (HURP) proteolysis by a proline-rich region. J Biol Chem *279,* 32592-32602.

James, P., Halladay, J., and Craig, E. A. (1996). Genomic libraries and a host strain designed for highly efficient two-hybrid selection in yeast. Genetics *144*, 1425-1436.

Kalab, P., Pralle, A., Isacoff, E. Y., Heald, R., and Weis, K. (2006). Analysis of a RanGTP-regulated gradient in mitotic somatic cells. Nature *440*, 697-701.

Kalab, P., Weis, K., and Heald, R. (2002). Visualization of a Ran-GTP Gradient in Interphase and Mitotic Xenopus Egg Extracts. Science *295*, 2452-2456.

Kapitein, L. C., Peterman, E. J., Kwok, B. H., Kim, J. H., Kapoor, T. M., and Schmidt, C. F. (2005). The bipolar mitotic kinesin Eg5 moves on both microtubules that it crosslinks. Nature *435*, 114-118.

Kapoor, T. M., and Compton, D. A. (2002). Searching for the middle ground: mechanisms of chromosome alignment during mitosis. J Cell Biol *157*, 551-556.

Kapoor, T. M., Lampson, M. A., Hergert, P., Cameron, L., Cimini, D., Salmon, E. D., McEwen, B. F., and Khodjakov, A. (2006). Chromosomes can congress to the metaphase plate before biorientation. Science *311*, 388-391.

Kapoor, T. M., Mayer, T. U., Coughlin, M. L., and Mitchison, T. J. (2000). Probing spindle assembly mechanisms with monastrol, a small molecule inhibitor of the mitotic kinesin, Eg5. J Cell Biol *150*, 975-988.

Karsenti, E., and Vernos, I. (2001). The mitotic spindle: a self-made machine. Science *294*, 543-547.

Khodjakov, A., Cole, R. W., Oakley, B. R., and Rieder, C. L. (2000). Centrosome-independent mitotic spindle formation in vertebrates. Current Biology *10*, 59-67.

Khodjakov, A., Copenagle, L., Gordon, M. B., Compton, D. A., and Kapoor, T. M. (2003). Minus-end capture of preformed kinetochore fibers contributes to spindle morphogenesis. J Cell Biol *160*, 671-683.

Kim, E., Naisbitt, S., Hsueh, Y. P., Rao, A., Rothschild, A., Craig, A. M., and Sheng, M. (1997). GKAP, a novel synaptic protein that interacts with the guanylate kinase-like domain of the PSD-95/SAP90 family of channel clustering molecules. J Cell Biol *136*, 669-678.

Kimura, K., Hirano, M., Kobayashi, R., and Hirano, T. (1998). Phosphorylation and activation of 13S condensin by Cdc2 in vitro. Science *282*, 487-490.

Kirschner, M., and Mitchison, T. (1986). Beyond self-assembly: From microtubules to morphogenesis. Cell *45*, 329-342.

Kistner, U., Garner, C. C., and Linial, M. (1995). Nucleotide binding by the synapse associated protein SAP90. FEBS Lett *359*, 159-163.

REFERENCES

Klebe, C., Bischoff, F. R., Ponstingl, H., and Wittinghofer, A. (1995). Interaction of the Nuclear GTP-Binding Protein Ran with Its Regulatory Proteins RCC1 and RanGAP1. Biochemistry *34*, 639-647.

Koffa, M. D., Casanova, C. M., Santarella, R., Kocher, T., Wilm, M., and Mattaj, I. W. (2006). HURP is part of a Ran-dependent complex involved in spindle formation. Curr Biol *16*, 743-754.

Kufer, T. A., Nigg, E. A., and Silljé, H. H. W. (2003). Regulation of Aurora-A kinase on the mitotic spindle. Chromosoma *112*, 159-163.

Kufer, T. A., Sillje, H. H., Korner, R., Gruss, O. J., Meraldi, P., and Nigg, E. A. (2002). Human TPX2 is required for targeting Aurora-A kinase to the spindle. J Cell Biol *158*, 617-623.

Kwok, B. H., and Kapoor, T. M. (2007). Microtubule flux: drivers wanted. Current Opinion in Cell Biology. Cell structure and dynamics *19*, 36-42.

la Cour, T., Kiemer, L., Molgaard, A., Gupta, R., Skriver, K., and Brunak, S. (2004). Analysis and prediction of leucine-rich nuclear export signals. Protein Eng Des Sel *17*, 527-536.

Lee, B. J., Cansizoglu, A. E., Suel, K. E., Louis, T. H., Zhang, Z., and Chook, Y. M. (2006). Rules for nuclear localization sequence recognition by karyopherin beta 2. Cell *126*, 543-558.

Levesque, A. A., and Compton, D. A. (2001). The chromokinesin Kid is necessary for chromosome arm orientation and oscillation, but not congression, on mitotic spindles. J Cell Biol *154*, 1135-1146.

Li, H.-Y., and Zheng, Y. (2004). Phosphorylation of RCC1 in mitosis is essential for producing a high RanGTP concentration on chromosomes and for spindle assembly in mammalian cells. Genes Dev *18*, 512-527.

Li, J. J., and Li, S. A. (2006). Mitotic kinases: the key to duplication, segregation, and cytokinesis errors, chromosomal instability, and oncogenesis. Pharmacol Ther *111*, 974-984.

Littlepage, L. E., Wu, H., Andresson, T., Deanehan, J. K., Amundadottir, L. T., and Ruderman, J. V. (2002). Identification of phosphorylated residues that affect the activity of the mitotic kinase Aurora-A. Proc Natl Acad Sci U S A *99*, 15440-15445.

Maddox, P., Straight, A., Coughlin, P., Mitchison, T. J., and Salmon, E. D. (2003). Direct observation of microtubule dynamics at kinetochores in Xenopus extract spindles: implications for spindle mechanics. J Cell Biol *162*, 377-382.

Maiato, H., Fairley, E. A. L., Rieder, C. L., Swedlow, J. R., Sunkel, C. E., and Earnshaw, W. C. (2003). Human CLASP1 Is an Outer Kinetochore Component that Regulates Spindle Microtubule Dynamics. Cell *113*, 891-904.

Maiato, H., Rieder, C. L., and Khodjakov, A. (2004). Kinetochore-driven formation of kinetochore fibers contributes to spindle assembly during animal mitosis. J Cell Biol *167*, 831-840.

Maiato, H., Sampaio, P., Lemos, C. L., Findlay, J., Carmena, M., Earnshaw, W. C., and Sunkel, C. E. (2002). MAST/Orbit has a role in microtubule-kinetochore attachment and is essential for chromosome alignment and maintenance of spindle bipolarity. J Cell Biol *157*, 749-760.

Maresca, T. J., Niederstrasser, H., Weis, K., and Heald, R. (2005). Xnf7 Contributes to Spindle Integrity through Its Microtubule-Bundling Activity. Current Biology *15*, 1755-1761.

Margolis, R. L., and Wilson, L. (1981). Microtubule treadmills--possible molecular machinery. Nature *293*, 705-711.

REFERENCES

Mayer, T. U., Kapoor, T. M., Haggarty, S. J., King, R. W., Schreiber, S. L., and Mitchison, T. J. (1999). Small molecule inhibitor of mitotic spindle bipolarity identified in a phenotype-based screen. Science *286*, 971-974.

McEwen, B. F., Heagle, A. B., Cassels, G. O., Buttle, K. F., and Rieder, C. L. (1997). Kinetochore Fiber Maturation in PtK1 Cells and Its Implications for the Mechanisms of Chromosome Congression and Anaphase Onset. J Cell Biol *137*, 1567-1580.

Megraw, T. L., Kao, L.-R., and Kaufman, T. C. (2001). Zygotic development without functional mitotic centrosomes. Current Biology *11*, 116-120.

Merdes, A., Heald, R., Samejima, K., Earnshaw, W. C., and Cleveland, D. W. (2000). Formation of spindle poles by dynein/dynactin-dependent transport of NuMA. J Cell Biol *149*, 851-862.

Mitchison, T., and Kirschner, M. (1984). Dynamic instability of microtubule growth. Nature *312*, 237-242.

Mitchison, T. J., and Salmon, E. D. (2001). Mitosis: a history of division. Nat Cell Biol *3*, E17-21.

Miyamoto, D. T., Perlman, Z. E., Burbank, K. S., Groen, A. C., and Mitchison, T. J. (2004). The kinesin Eg5 drives poleward microtubule flux in Xenopus laevis egg extract spindles. J Cell Biol *167*, 813-818.

Morgan, D. O. (1997). Cyclin-dependent kinases: engines, clocks, and microprocessors. Annu Rev Cell Dev Biol *13*, 261-291.

Morgan, D. O. (2006). The Cell Cycle: Principles of Control, Vol 1: Oxford University Press).

Mountain, V., Simerly, C., Howard, L., Ando, A., Schatten, G., and Compton, D. A. (1999). The kinesin-related protein, HSET, opposes the activity of Eg5 and cross-links microtubules in the mammalian mitotic spindle. J Cell Biol *147*, 351-366.

Nachury, M. V., Maresca, T. J., Salmon, W. C., Waterman-Storer, C. M., Heald, R., and Weis, K. (2001). Importin-beta Is a Mitotic Target of the Small GTPase Ran in Spindle Assembly. Cell *104*, 95-106.

Neef, R., Preisinger, C., Sutcliffe, J., Kopajtich, R., Nigg, E. A., Mayer, T. U., and Barr, F. A. (2003). Phosphorylation of mitotic kinesin-like protein 2 by polo-like kinase 1 is required for cytokinesis. J Cell Biol *162*, 863-875.

Nigg, E. A. (2001). Mitotic kinases as regulators of cell division and its checkpoints. Nat Rev Mol Cell Biol *2*, 21-32.

Nigg, E. A. (2002). Centrosome aberrations: cause or consequence of cancer progression? Nat Rev Cancer *2*, 815-825.

Nishi, K., Yoshida, M., Fujiwara, D., Nishikawa, M., Horinouchi, S., and Beppu, T. (1994). Leptomycin B targets a regulatory cascade of crm1, a fission yeast nuclear protein, involved in control of higher order chromosome structure and gene expression. J Biol Chem *269*, 6320-6324.

Nishitani, H., Ohtsubo, M., Yamashita, K., Iida, H., Pines, J., Yasudo, H., Shibata, Y., Hunter, T., and Nishimoto, T. (1991). Loss of RCC1, a nuclear DNA-binding protein, uncouples the completion of DNA replication from the activation of cdc2 protein kinase and mitosis. Embo J *10*, 1555-1564.

O'Connell, C. B., and Khodjakov, A. L. (2007). Cooperative mechanisms of mitotic spindle formation. J Cell Sci *120*, 1717-1722.

REFERENCES

Orjalo, A. V., Arnaoutov, A., Shen, Z., Boyarchuk, Y., Zeitlin, S. G., Fontoura, B., Briggs, S., Dasso, M., and Forbes, D. J. (2006). The Nup107-160 nucleoporin complex is required for correct bipolar spindle assembly. Mol Biol Cell *17*, 3806-3818.

Peter, M., Heitlinger, E., Haner, M., Aebi, U., and Nigg, E. A. (1991). Disassembly of in vitro formed lamin head-to-tail polymers by CDC2 kinase. Embo J *10*, 1535-1544.

Pfleger, C. M., and Kirschner, M. W. (2000). The KEN box: an APC recognition signal distinct from the D box targeted by Cdh1. Genes Dev *14*, 655-665.

Pierre, P., Pepperkok, R., and Kreis, T. (1994). Molecular characterization of two functional domains of CLIP-170 in vivo. J Cell Sci *107*, 1909-1920.

Pierre, P., Scheel, J., Rickard, J. E., and Kreis, T. E. (1992). CLIP-170 links endocytic vesicles to microtubules. Cell *70*, 887-900.

Pines, J., and Rieder, C. L. (2001). Re-staging mitosis: a contemporary view of mitotic progression. Nat Cell Biol *3*, E3-6.

Ponting, C. P., and Kerr, I. D. (1996). A novel family of phospholipase D homologues that includes phospholipid synthases and putative endonucleases: identification of duplicated repeats and potential active site residues. Protein Sci *5*, 914-922.

Raemaekers, T., Ribbeck, K., Beaudouin, J., Annaert, W., Van Camp, M., Stockmans, I., Smets, N., Bouillon, R., Ellenberg, J., and Carmeliet, G. (2003). NuSAP, a novel microtubule-associated protein involved in mitotic spindle organization. J Cell Biol *162*, 1017-1029.

Ren, M., Drivas, G., D'Eustachio, P., and Rush, M. (1993). Ran/TC4: a small nuclear GTP-binding protein that regulates DNA synthesis. J Cell Biol *120*, 313-323.

Ribbeck, K., Groen, A. C., Santarella, R., Bohnsack, M. T., Raemaekers, T., Kocher, T., Gentzel, M., Gorlich, D., Wilm, M., Carmeliet, G.*, et al.* (2006). NuSAP, a mitotic RanGTP target that stabilizes and cross-links microtubules. Mol Biol Cell *17*, 2646-2660.

Ribbeck, K., Raemaekers, T., Carmeliet, G., and Mattaj, I. W. (2007). A role for NuSAP in linking microtubules to mitotic chromosomes. Curr Biol *17*, 230-236.

Rieder, C., and Alexander, S. (1990). Kinetochores are transported poleward along a single astral microtubule during chromosome attachment to the spindle in newt lung cells. J Cell Biol *110*, 81-95.

Rieder, C. L. (1981). The structure of the cold-stable kinetochore fiber in metaphase PtK1 cells. Chromosoma *84*, 145-158.

Rieder, C. L. (2005). Kinetochore fiber formation in animal somatic cells: dueling mechanisms come to a draw. Chromosoma *114*, 310-318.

Rieder, C. L., and Salmon, E. D. (1994). Motile kinetochores and polar ejection forces dictate chromosome position on the vertebrate mitotic spindle. J Cell Biol *124*, 223-233.

Roghi, C., Giet, R., Uzbekov, R., Morin, N., Chartrain, I., Le Guellec, R., Couturier, A., Doree, M., Philippe, M., and Prigent, C. (1998). The Xenopus protein kinase pEg2 associates with the centrosome in a cell cycle-dependent manner, binds to the spindle microtubules and is involved in bipolar mitotic spindle assembly. J Cell Sci *111 (Pt 5)*, 557-572.

Salina, D., Enarson, P., Rattner, J. B., and Burke, B. (2003). Nup358 integrates nuclear envelope breakdown with kinetochore assembly. J Cell Biol *162*, 991-1001.

Sanderson, H. S., and Clarke, P. R. (2006). Cell biology: Ran, mitosis and the cancer connection. Curr Biol *16*, R466-468.

REFERENCES

Santarella, R. A., Koffa, M. D., Tittmann, P., Gross, H., and Hoenger, A. (2007). HURP wraps microtubule ends with an additional tubulin sheet that has a novel conformation of tubulin. J Mol Biol *365*, 1587-1595.

Saredi, A., Howard, L., and Compton, D. A. (1996). NuMA assembles into an extensive filamentous structure when expressed in the cell cytoplasm. J Cell Sci *109 (Pt 3)*, 619-630.

Sauer, G., Korner, R., Hanisch, A., Ries, A., Nigg, E. A., and Sillje, H. H. (2005). Proteome analysis of the human mitotic spindle. Mol Cell Proteomics *4*, 35-43.

Savoian, M. S., Goldberg, M. L., and Rieder, C. L. (2000). The rate of poleward chromosome motion is attenuated in Drosophila zw10 and rod mutants. Nat Cell Biol *2*, 948-952.

Schatz, C. A., Santarella, R., Hoenger, A., Karsenti, E., Mattaj, I. W., Gruss, O. J., and Carazo-Salas, R. E. (2003). Importin alpha-regulated nucleation of microtubules by TPX2. Embo J *22*, 2060-2070.

Schuyler, S. C., and Pellman, D. (2001). Microtubule "plus-end-tracking proteins": The end is just the beginning. Cell *105*, 421-424.

Sharp, D. J., Rogers, G. C., and Scholey, J. M. (2000). Microtubule motors in mitosis. Nature *407*, 41-47.

Shevchenko, A., Wilm, M., Vorm, O., and Mann, M. (1996). Mass spectrometric sequencing of proteins silver-stained polyacrylamide gels. Anal Chem *68*, 850-858.

Sillje, H. H., Nagel, S., Korner, R., and Nigg, E. A. (2006). HURP is a Ran-importin beta-regulated protein that stabilizes kinetochore microtubules in the vicinity of chromosomes. Curr Biol *16*, 731-742.

Spittle, C., Charrasse, S., Larroque, C., and Cassimeris, L. (2000). The interaction of TOGp with microtubules and tubulin. J Biol Chem *275*, 20748-20753.

Sullivan, M., and Morgan, D. O. (2007). Finishing mitosis, one step at a time. Nat Rev Mol Cell Biol *8*, 894-903.

Sumara, I., Gimenez-Abian, J. F., Gerlich, D., Hirota, T., Kraft, C., de la Torre, C., Ellenberg, J., and Peters, J. M. (2004). Roles of polo-like kinase 1 in the assembly of functional mitotic spindles. Curr Biol *14*, 1712-1722.

Sun, Q. Y., and Schatten, H. (2006). Role of NuMA in vertebrate cells: review of an intriguing multifunctional protein. Front Biosci *11*, 1137-1146.

Tahara, K., Takagi, M., Ohsugi, M., Sone, T., Nishiumi, F., Maeshima, K., Horiuchi, Y., Tokai-Nishizumi, N., Imamoto, F., Yamamoto, T.*, et al.* (2008). Importin-beta and the small guanosine triphosphatase Ran mediate chromosome loading of the human chromokinesin Kid. J Cell Biol *180*, 493-506.

Tan, D., Asenjo, A. B., Mennella, V., Sharp, D. J., and Sosa, H. (2006). Kinesin-13s form rings around microtubules. J Cell Biol *175*, 25-31.

Tanaka, K., Mukae, N., Dewar, H., van Breugel, M., James, E. K., Prescott, A. R., Antony, C., and Tanaka, T. U. (2005). Molecular mechanisms of kinetochore capture by spindle microtubules. Nature *434*, 987-994.

Tedeschi, A., Ciciarello, M., Mangiacasale, R., Roscioli, E., Rensen, W. M., and Lavia, P. (2007). RANBP1 localizes a subset of mitotic regulatory factors on spindle microtubules and regulates chromosome segregation in human cells. J Cell Sci *120*, 3748-3761.

Tokai, N., Fujimoto-Nishiyama, A., Toyoshima, Y., Yonemura, S., Tsukita, S., Inoue, J., and Yamamota, T. (1996). Kid, a novel kinesin-like DNA binding protein, is localized to chromosomes and the mitotic spindle. EMBO J *15*, 457-467.

REFERENCES

Tournebize, R., Popov, A., Kinoshita, K., Ashford, A. J., Rybina, S., Pozniakovsky, A., Mayer, T. U., Walczak, C. E., Karsenti, E., and Hyman, A. A. (2000). Control of microtubule dynamics by the antagonistic activities of XMAP215 and XKCM1 in Xenopus egg extracts. Nat Cell Biol *2*, 13-19.

Trieselmann, N., Armstrong, S., Rauw, J., and Wilde, A. (2003). Ran modulates spindle assembly by regulating a subset of TPX2 and Kid activities including Aurora A activation. J Cell Sci *116*, 4791-4798.

Tsai, M. Y., Wiese, C., Cao, K., Martin, O., Donovan, P., Ruderman, J., Prigent, C., and Zheng, Y. (2003). A Ran signalling pathway mediated by the mitotic kinase Aurora A in spindle assembly. Nat Cell Biol *5*, 242-248.

Tsou, A. P., Yang, C. W., Huang, C. Y., Yu, R. C., Lee, Y. C., Chang, C. W., Chen, B. R., Chung, Y. F., Fann, M. J., Chi, C. W.*, et al.* (2003). Identification of a novel cell cycle regulated gene, HURP, overexpressed in human hepatocellular carcinoma. Oncogene *22*, 298-307.

Uhlmann, F. (2004). The mechanism of sister chromatid cohesion. Exp Cell Res *296*, 80-85.

Vernos, I., and Karsenti, E. (1995). Chromosomes take the lead in spindle assembly. Trends Cell Biol *5*, 297-301.

Vernos, I., Raats, J., Hirano, T., Heasman, J., Karsenti, E., and Wylie, C. (1995). Xklp1, a chromosomal Xenopus kinesin-like protein essential for spindle organization and chromosome positioning. Cell *81*, 117-127.

Wadsworth, P., and Khodjakov, A. (2004). E pluribus unum: towards a universal mechanism for spindle assembly. Trends in Cell Biology *14*, 413-419.

Watanabe, Y. (2005). Shugoshin: guardian spirit at the centromere. Curr Opin Cell Biol *17*, 590-595.

114

Westermann, S., Avila-Sakar, A., Wang, H. W., Niederstrasser, H., Wong, J., Drubin, D. G., Nogales, E., and Barnes, G. (2005). Formation of a dynamic kinetochore-microtubule interface through assembly of the Dam1 ring complex. Mol Cell *17*, 277-290.

Wiese, C., Wilde, A., Moore, M. S., Adam, S. A., Merdes, A., and Zheng, Y. (2001). Role of Importin-beta in Coupling Ran to Downstream Targets in Microtubule Assembly. Science *291*, 653-656.

Wilde, A. (2006). "HURP on" we're off to the kinetochore! J Cell Biol *173*, 829-831.

Wilde, A., Lizarraga, S. B., Zhang, L., Wiese, C., Gliksman, N. R., Walczak, C. E., and Zheng, Y. (2001). Ran stimulates spindle assembly by altering microtubule dynamics and the balance of motor activities. Nat Cell Biol *3*, 221-227.

Wilde, A., and Zheng, Y. (1999). Stimulation of microtubule aster formation and spindle assembly by the small GTPase Ran. Science *284*, 1359-1362.

Wittmann, T., Hyman, A., and Desai, A. (2001). The spindle: a dynamic assembly of microtubules and motors. Nat Cell Biol *3*, E28-34.

Wittmann, T., Wilm, M., Karsenti, E., and Vernos, I. (2000). TPX2, A Novel Xenopus MAP Involved in Spindle Pole Organization. J Cell Biol *149*, 1405-1418.

Woehlke, G., Ruby, A. K., Hart, C. L., Ly, B., Hom-Booher, N., and Vale, R. D. (1997). Microtubule interaction site of the kinesin motor. Cell *90*, 207-216.

Wollman, R., Cytrynbaum, E. N., Jones, J. T., Meyer, T., Scholey, J. M., and Mogilner, A. (2005). Efficient chromosome capture requires a bias in the 'search-and-capture' process during mitotic-spindle assembly. Curr Biol *15*, 828-832.

Wong, J., and Fang, G. (2006). HURP controls spindle dynamics to promote proper interkinetochore tension and efficient kinetochore capture. J Cell Biol *173*, 879-891.

REFERENCES

Woodbury, E. L., and Morgan, D. O. (2007). The role of self-association in Fin1 function on the mitotic spindle. J Biol Chem *282*, 32138-32143.

Xie, Z., Ho, W. T., and Exton, J. H. (1998). Association of N- and C-terminal domains of phospholipase D is required for catalytic activity. J Biol Chem *273*, 34679-34682.

Yajima, J., Edamatsu, M., Watai-Nishii, J., Tokai-Nishizumi, N., Yamamoto, T., and Toyoshima, Y. (2003). The human chromokinesin Kid is a plus end-directed microtubule-based motor. EMBO J *22*, 1067-1074.

Yu, C. T., Hsu, J. M., Lee, Y. C., Tsou, A. P., Chou, C. K., and Huang, C. Y. (2005). Phosphorylation and stabilization of HURP by Aurora-A: implication of HURP as a transforming target of Aurora-A. Mol Cell Biol *25*, 5789-5800.

Zuccolo, M., Alves, A., Galy, V., Bolhy, S., Formstecher, E., Racine, V., Sibarita, J. B., Fukagawa, T., Shiekhattar, R., Yen, T., and Doye, V. (2007). The human Nup107-160 nuclear pore subcomplex contributes to proper kinetochore functions. Embo J *26*, 1853-1864.

Publications

Parts of this work are published in:

1. Silljé, H. H. W.,* <u>Nagel, S.</u>,* Körner, R., and Nigg, E. A. (2006). HURP is a Ran-Importin β-regulated Protein that stabilizes Kinetochore Microtubules in the Vicinity of Chromosomes. Curr. Biol. 16, 731-42.
   *These authors contributed equally to the experimental part of this study.

2. Santamaria, A., <u>Nagel, S.</u>, Anja, W., Silljé, H. H. W., and Nigg, E. A. (2008). CHICA, a partner of the chromokinesin Kid, is required for Kid loading onto the mitotic spindle (Curr. Biol., in press).

Curriculum Vitae

SUSANNA NAGEL (nee Heilmeier)

Date of birth: 03.09.1977

Place of birth: Rotenburg an der Wümme (Germany)

Marital status: married (two kids)

Tertiary Education

Since November 2004

Degree PhD

Major Biochemistry and Cell Biology

Institution Max Planck Institute of Biochemistry, Munich

Thesis Title Initial characterization of two novel spindle proteins, CHICA and HURP: focus on the role of the Ran-importin β-regulated HURP protein in kinetochore-fiber stabilization.

Supervisors Prof. Erich A. Nigg and Dr. Hermann H. W. Silljé

June 2002 – April 2003

Degree Diploma (1.0)

Major Biochemistry, Structural Biology and Molecular Biology

Institution Gene Center, Institute of Biochemistry, University of Munich

Thesis Title The CTD-Phosphatase Fcp1 from *S. cerevisiae* /

A structural and biochemical characterization.

Supervisor Prof. P. Cramer

February 2000 – August 2003

Degree Diploma (1.2)

Major Microbiology, Genetics and Biochemistry

Institution Ludwig Maximilian University of Munich

October 1997 – July 1999

Degree Vordiplom (1.5)

Major Microbiology and Genetics

Institution University of Vienna (Austria)

Publications

1) Kamenski, T., <u>Heilmeier, S.</u>, Meinhart, A., Cramer, P. (2004). Structure and Mechanism of RNA-Polymerase II CTD Phosphatases. Mol. Cell 15, 399-407.

2) Silljé, H. H. W.,* <u>Nagel, S.</u>,* Körner, R., and Nigg, E. A. (2006). HURP is a Ran-Importin β-regulated Protein that stabilizes Kinetochore Microtubules in the Vicinity of Chromosomes. Curr. Biol. 16, 731-42.
*These authors contributed equally to the experimental part of this study.

3) Santamaria, A., <u>Nagel, S.</u>, Anja, W., Silljé, H. H. W., and Nigg, E. A. (2008). CHICA, a partner of the chromokinesin Kid, is required for Kid loading onto the mitotic spindle (Curr. Biol., in press).

Awards and Funding

- Nature Poster Price at the SEB Cell Cycle Meeting 2006 (Southampton, UK)
- Christiane Nüsslein-Volhard scholarship since August 2006
- Project funding since Mai 2007 by the DFG through the SFB646:
  "Regulatory Networks in Genome Expression and Maintenance"

Research Presentations

SEB Cell Cycle Meeting 2006, Southampton (UK)

Poster: HURP is a Ran-importin β-regulated protein that stabilizes kinetochore microtubules in the vicinity of chromosomes

CNV-Meeting (Max-Planck Institute for Developmental Biology, Tübingen)

Talk: Regulation of mitotic spindle assembly factors in mammalian cells

ELSO Meeting 2007, Dresden

Poster: How is Ran-regulated HURP specifically localized to K-fibers?

Second International Gene Center SFB 646 Symposium, (University of Munich)

Talk: HURP – a target of the Ran-regulated spindle assembly pathway

INTERACT – Munich PhD Symposium 2007 (MPI of Biochemistry, Munich)

Poster: Regulation of mitotic spindle assembly factors in mammalian cells.